INVESTIGATING THE ROLE OF THE ESSENTIAL GTPASE RBGA IN THE ASSEMBLY OF THE LARGE RIBOSOMAL SUBUNIT IN *BACILLUS SUBTILIS*

By

Megha Gulati

A DISSERTATION

Submitted to
Michigan State University
in partial fulfillment of the requirements
for the degree of

Genetics - Doctor of Philosophy

2014

ABSTRACT

INVESTIGATING THE ROLE OF THE ESSENTIAL GTPASE RBGA IN THE ASSEMBLY OF THE LARGE RIBOSOMAL SUBUNIT IN *BACILLUS SUBTILIS*

By

Megha Gulati

Ribosomes are large ribonucleoprotein complexes required for synthesis of proteins and are a major target of several types of antibiotics. Ribosome assembly defects have been linked to several diseases, most notably Diamond-Blackfan anemia and Schwachman-Diamond syndrome. Although ribosome assembly has been studied extensively through *in vitro* reconstitution analysis, relatively little is known about the steps involved *in vivo*. Assembly factors such as GTPases are a crucial universal requirement for ribosome assembly yet their precise role has remained elusive. This thesis focuses on characterization of RbgA (ribosome biogenesis GTPase A), an essential GTPase in *Bacillus subtilis*, and its role in the assembly of the large ribosomal subunit. RbgA is widely distributed evolutionarily and its homologs have been functionally implicated in ribosome assembly in yeast (Lsg1p, Nog2p and Nug1p) as well as mammalian cells (Mtg1). Analysis of the ribosome assembly intermediate isolated from RbgA-depleted cells indicated that the GTPase plays a crucial role at a late stage in maturation of the 50S subunit and in recruitment of r-proteins L16, L27 and L36 during the assembly process. To elucidate the role of RbgA in 50S assembly, first, we performed extensive biochemical analysis to determine the kinetic parameters of RbgA and its interaction with the 50S subunit and ribosomal intermediates (Chapter 2). These studies revealed that RbgA requires K^+ ion for optimal GTPase activity and this activity is enhanced ~60 fold only in the presence of mature 50S subunit, and laid the groundwork for developing a model for the role of RbgA in the 50S assembly process. Next, we

generated a library of loss-of-function mutant RbgA proteins through site-directed mutagenesis and performed kinetic analyses and biochemical characterization to delineate the critical functional sites of the enzyme (Chapter 3). To analyze the mutations *in vivo,* we engineered *B. subtilis* strains to express mutated RbgA protein(s) and analyzed the ribosomal intermediates formed in the cells. These studies identified a potential catalytic residue of RbgA and provided insight into its catalytic mechanism when complexed with its ribosomal substrate. Further, we identified and characterized an RNA-binding domain required for RbgA function. Lastly, we designed a genetic suppressor screen, and isolated, and characterized six independent extragenic suppressor mutations that partially alleviated the growth defect in the RbgA-defective *B. subtilis* strain (Chapter 4). These studies revealed a novel *in vivo* ribosomal intermediate and determined a functional interaction between RbgA and r-protein L6. Together, these studies provide a model for the molecular mechanism of RbgA interaction with the 50S ribosomal subunit and the role of the enzyme in the assembly process.

I dedicate this thesis to my loving family, my father, Pankaj, my mother, Anjali, and my best friend and sister, Neha, who have supported me and encouraged me to follow my dreams across the oceans, and to my husband Shiven, whose unconditional love and support provided me with the strength and perseverance I needed to achieve my goals.

ACKNOWLEDGEMENTS

First and foremost I express my gratitude to my mentor, Dr. Robert Britton, for his support and guidance on my projects and my maturation through graduate school. He has been a wonderful supervisor, mentor and friend who taught me innumerable scientific and life lessons. He encouraged me to think critically, be the toughest critic of my own work and helped me hone my skills as a scientist. His sound advice, insightful criticisms and thoughtful guidance are invaluable and deeply appreciated. My experience of working under his guidance is one I will always remember and cherish.

I would also like to thank my committee members: Dr. Lee Kroos, Dr. Robert Hausinger, Dr. Donna Koslowsky and Dr. Ronald Patterson for their continued advice and support throughout my projects and scientific career. My acknowledgement also goes to Dr. Lee Kroos for the discussions during our joint group meetings and I am grateful for the ideas and suggestions that contributed to the work presented in this thesis. A special thanks for allowing me to use the chemiluminescence imager. In addition, my thanks to Dr. Barb Sears for her support and guidance and Jeannine Lee for her tremendous help in solving the administrative issues I came across and helping me assimilate to a new university system.

My appreciation for all the past and present members of Dr. Britton's laboratory, for numerous stimulating discussions and all their camaraderie. They made the lab a fun place to work, and were a large part of my academic and personal life. My wonderful labmates and friends at MSU; Caleb, Amy, Hirosha, Nicole, Denise and Anthony; our frequent outings as a group were most

enjoyable and made me feel at home, far away from, India, my home country. They provided me ceaseless support, necessary ‘distractions’ and lots of laughs.

Lastly, I would like to thank my family, my parents Anjali and Pankaj, for always encouraging me to pursue my interests and passion, for waking up at *odd* hours in India so we could talk according to US time, for moving heaven and earth to plan my dream wedding in Michigan as I couldn’t travel home and for lots of gift and ‘care packages’ sent through anyone who was traveling from Delhi to *anywhere* in the US. Also, I could not have done any of this without the love and support of my sister Neha, who kept me grounded by reminding me that there exists a world that doesn’t revolve around me and *wisely* did not follow in my footsteps choosing instead to complete her MBA. We shared a room for 19 years, sharing secrets and whispering late into the night and it was most painful to leave you behind to follow my dreams of research and pursuit of doctoral work.

My new family, Preeti and Navin Kapur receive my sincere love and gratitude for accepting me as a second daughter and for loving me unconditionally. I would especially like to acknowledge Shivani Kapur, who provided me a shoulder to lean on and for being a sister-in-arms in our shared experience in navigating life and family.

Finally, I would like to thank my loving husband Shiven, for encouraging me to shoot for the stars, for sharing my passion of science as a fellow scientist and for numerous late night discussions and troubleshooting problems, for always being there for *me* and for never letting geographical distance be a factor in our relationship. Without you all none of this would have been possible.

TABLE OF CONTENTS

LIST OF TABLES

LIST OF FIGURES

CHAPTER 1

Literature Review

Introduction

Ribosomes are large ribonucleoprotein machines that are essential for decoding mRNA to synthesize proteins [1,2]. Extensive structural and biochemical studies over the last several decades have provided insights about the function of ribosome and the translational machinery that regulates [3-6]. In contrast relatively little is known about the *in vivo* assembly of this complex. Though functionally active ribosomal subunits can be reconstituted *in vitro* from its purified components this process requires extreme non-physiological conditions [7-14]. In addition, the slow kinetics and low efficiency of *in vitro* reconstitution strongly suggests that ribosomal assembly factors are required for *in vivo* assembly. While more than 200 assembly factors have been indentified in eukaryotes relatively fewer are known in prokaryotic ribosome assembly [15-17]. These assembly factors include rRNA modification enzymes, RNA helicases, chaperone proteins and GTPases [18-23]. In bacteria GTPases comprise the largest class of essential ribosome assembly factors [22,23]. Several GTPases have been implicated in assembly of the 50S as well as the 30S subunit [22,23]. Most of these GTPases are widely conserved and in most instances the homologs of these proteins have also been implicated in ribosome assembly. In this chapter a general overview of ribosome assembly is discussed with an emphasis on the assembly factors implicated in ribosome assembly *in vivo*. Also highlighted are several GTPases that are involved in the assembly of the 50S and 30S subunits and the unique features of these enzymes.

Bacterial Ribosome

Ribosomes are essential macromolecular machines that catalyze the fundamental cellular process of protein synthesis [1-3,6]. In *Escherichia coli* 40% of the cells energy output is channeled

towards ribosome assembly and protein synthesis [18]. Ribosomes are also the targets of most antibiotics that bind to specific sites on the ribosome and inhibit protein synthesis [24-28]. The bacterial ribosome is a 70S complex that comprises of two individual subunits, the large subunit 50S and the small subunit 30S [6,29]. The 50S subunit is composed of 23S rRNA, 5S rRNA and 33 ribosomal proteins (r-proteins) designated as L1-L36 and contains the peptidyl transferase center, the site of peptide bond formation [3,6]. The 16S rRNA and 21 ribosomal proteins designated as S1-S21 form the 30S subunit which is responsible for binding to the mRNA during translation and contributes to the fidelity of translation by monitoring base pairing between codon and anticodon in the decoding process [3,6].

The availability of high resolution crystal structures of the ribosome bound to various antibiotics have provided a clear picture of the catalytic sites that lie within the rRNA and contributed to a detailed understanding of the mechanism of translation [3-6]. Each subunit has three binding sites for tRNA, the A-site (aminoacyl) that accepts the aminoacyl tRNA, the P-site (peptidyl) that is bound to the tRNA with a nascent peptide chain and the E-site (exit) which holds the deacylated tRNA before it exits the ribosome [2,30]. These sites are crucial to the function of the ribosome and are the target of most antibiotics that bind to the ribosome and inhibit protein synthesis [24,31]. However the details of how these complex structures are assembled *in vivo* via the precise and coordinated binding of >50 r-proteins and rRNA into a functional multicomponent complex is lacking.

Ribosome Assembly in Bacteria

Ribosome assembly is a complex and tightly regulated process that involves the coordinated assembly of >50 r-proteins and 3 rRNA molecules to form functional subunits [1]. In actively

growing bacteria 40% of total energy production is consumed by ribosome assembly and thus successful and efficient ribosome assembly is critical for the cells [9]. Ribosome assembly defects have been linked to several diseases including cancer and diabetes [32]. Several cancers show a deregulation of the ribosome assembly and function most notably Diamond-Blackfan anemia (DBA), Schwachman-Diamond syndrome and tuberous sclerosis [33,34]. DBA is a congenital bone marrow failure syndrome characterized by red blood cell aplasia, macrocytic anemia and increased risk of malagnancy and mutations in four r-proteins S19, S24, S17 and S35a is seen in 30% of DBA patients [34]. In addition mutations in r-proteins L5 and L11 are associated with cleft palate and physical abnormalities including thumb and heart anomalies [35]. While it is clear that mutations in r-proteins disrupt ribosome biogenesis and cause specific clinical phenotypes how these mutations lead to the disease state is unknown. R-proteins are some of the most conserved proteins across all kingdoms of life and their relative position and structure in the ribosomes is similar in prokaryotic and eukaryotic cells [6,29]. Understanding the role of r-proteins in ribosome assembly *in vivo* in bacterial cells would provide insight into the role of their homologs in eukaryotic cells and help elucidate the principles underlying these ribosomopathies and may also lead to new therapeutic strategies [34,36].

Ribosome assembly is an intricate process and the basic steps involve a) the transcription, processing and modification of rRNA; b) the proper folding of rRNA into distinct domains; c) the translation and modification of r-proteins; d) the binding of r-proteins to rRNA in a precise manner and e) the binding and release of various assembly factors involved at different steps in the process. Many of these steps are coupled and occur in parallel in the cell.

In the late 1960s Nomura and coworkers demonstrated the assembly of an active 30S subunit from free rRNA and r-proteins without any additional factors [11,37]. Successful *in vitro*

reconstitution of the 50S subunit was soon achieved by Nierhaus and Dohme [38]. This pioneering work highlighted the fact that all the information necessary for ribosome assembly is encoded within the rRNA and r-proteins themselves [9]. The ability to reconstitute active ribosomal subunits represented a major breakthrough as it became possible to dissect ribosome assembly by altering the various components involved in the process. These crucial experiments led to the construction of assembly maps for both the 30S and the 50S subunits [39,40].

Assembly of the 50S subunit

In vitro assembly of the 50S subunit in *Escherichia coli* is a four step process that involves three intermediates [7,38,41]. The first intermediate $RI_{50}(I)$ migrates at 33S and contains the 23S rRNA, 5S rRNA and 22 r-proteins. Conversion of $RI_{50}(I)$ to the second intermediate $RI_{50}^{*}(I)$ that migrates at 41S-43S requires an extended incubation at high temperature. This is followed by the addition of the remaining 11 r-proteins to form the final intermediate $RI_{50}(2)$ which migrates at 48S and contains all the components of an active 50S subunit. However, a further incubation step at high temperature and under high ionic conditions is required to form the mature 50S subunit.

Reconstitution of 50S subunits in *Bacillus stearothermophilus* reveals that *in vitro* assembly is distinct from that seen in *E. coli* resulting in a different intermediate during the assembly process [13,42]. The major intermediate in *B. stearothermophilus* is RI_{50} which lacks only three r-proteins, the identities of which were not determined. Addition of the missing proteins and a long incubation at high temperatures yields a functional 50S subunit.

Aside from a few studies in *B. stearothermophilus* and recent studies in *Bacillus subtilis* the bulk of our knowledge on ribosome assembly stems from research in *E. coli* [22]. The prevailing idea was that a single pathway or regulatory mechanism for ribosome synthesis and assembly existed and *E. coli* was the chosen representative of bacteria. However, mounting evidence now indicates that the majority of bacteria likely utilize different mechanism and regulatory systems for ribosome synthesis compared to *E. coli* [18,22,41]. This underscores the need to investigate the ribosome assembly pathways and regulatory apparatus in other systems such as *B. subtilis* that have largely been ignored.

Factors implicated in Ribosome Assembly

While *in vitro* reconstitution of ribosomal subunits requires 90 minutes ribosomes are assembled in the cell at 37°C in two minutes [43]. The harsh non-physiological conditions such as long incubation times, high ionic concentrations and high temperature required for *in vitro* ribosome assembly suggested that additional factors must be involved in the assembly process *in vivo*. In the past decade there has been a large increase in the identification of assembly factors in bacteria as well as eukaryotes [41,43,44]. While more than 200 assembly factors have been identified in eukaryotes relatively few proteins in bacteria have been shown to be involved in ribosome assembly [15,45]. These factors include GTPases, RNA helicases, chaperone proteins and rRNA modification factors [18,44]. Characterization of assembly factors in bacteria will elucidate the mechanistic details of how these proteins assist in ribosome assembly. In addition these assembly factors represent novel targets for modern antibacterial drug discovery and could be part of a solution to multi-drug resistance in bacteria [46,47].

RNA Modification Enzymes

Ribosome assembly begins with the transcription of rRNA in a single primary transcript which is processed by a number of endonucleases [48,49]. Modification of rRNA occurs post-transcriptionally and consists of two main types, methylation and pseudo-uridinylation. While modification of rRNA is conserved in all organisms the site of modifications and the number of modifications varies. Mapping of all methylations and pseudouridinylations onto the ribosome reveal that they cluster around active sites of the ribosome such as the tRNA-mRNA binding site and peptidyltransferase center [18]. However, the functional role of these modifications remains a mystery [18]. Some rRNA modifications have been linked to antibiotic resistance indicating that these studies could result in findings relevant to study and design of drug targets [24]. While several pseudouridine synthases and methyltransferases have been identified by deletion analysis only rluD has been shown to play a role in ribosome assembly [21]. RluD is a pseudouridine synthase required for ribosome assembly in *E. coli* [21]. This enzyme acts on the 23S rRNA and loss of RluD results in immature 50S subunits and a breakdown of unstable 70S subunits [21].

RNA Helicases

rRNA is prone to the formation of unfavorable secondary structures and thus RNA helicases play an important role in ribosome assembly [50,51]. A large subfamily of RNA helicases are termed DEAD box helicases as they contain conserved motif Asp-Glu-Ala-Asp (DEAD) [19,52]. They are conserved from bacteria to viruses to humans and these proteins are ATP-dependant [19,52,53]. These proteins are believed to play multiple roles in ribosome assembly as they are needed for helicase activity, unwinding of local RNA secondary structure, act as RNA chaperones by assisting with proper RNA folding and modulate RNA-protein interactions [41].

While DEAD box proteins are essential for eukaryotic ribosome assembly they are dispensable for assembly in bacteria under normal growth conditions [20]. Only three DEAD box helicases SrmB, CsdA and DbpA have been implicated in assembly of *the 50S subunit in E. coli* [19,20,54]. CsdA is induced by cold shock suggesting that the enzyme may be important under stress conditions [20]. Deletion of wither csdA or srmB leads to a temperature sensitive phenotype likely due to rRNA misfolding at low temperatures [19]. Deletion of csdA results in an immature 50S complex that lacks late assembly proteins. In contrast the deletion of srmB results in accumulation of a pre-50S complex that lacks the early assembly r-protein L13. Studies have shown that the deletion of csdA and srmB suppress temperature sensitive mutations in genes encoding for r-proteins S2 and L24 respectively [19,20].

DbpA differs from CsdA and SrmB in that it requires a specific sequence present in helix 92 of 23S rRNA for its helicase activity [20,54]. Studies of DbpA homolog in *B. subtilis* YxiN indicate that the region responsible for specificity is located in the C-terminal of the protein [55]. Interestingly the deletion of *dbpA* does not result in a growth defect [20]. However, the expression of a DbpA mutant yields a dominant slow growth phenotype and results in defects in ribosome assembly [54]. In this mutant the maturation of 50S subunits is affected resulting in accumulation of immature particles. This suggests that the presence of an inactive or partially active DbpA disrupts assembly of the 50S subunit while complete absence of the protein does not affect assembly. Taken together these studies suggest that helicases play a role in ribosome assembly under stress conditions such as low temperature however the mechanistic details of their role in assembly process is unknown.

Chaperone Proteins

Another set of protein factors that have been implicated in ribosome assembly are chaperone proteins [56,57]. While RNA helicases seem to be needed at low temperatures for proper ribosome assembly, chaperone proteins play an important role in biogenesis at high temparatures. The chaperones DnaJ and DnaK are part of heat shock protein 70 (HSP70) chaperone machine DnaK-DnaJ-GrpE and have been implicated in ribosome assembly [56]. DnaK has been shown to stably associate with pre-30S complex and it has been proposed that DnaK overcomes the high temperature activation step required for the *in vitro* reconstitution of 30S subunits. Strains with a deletion in dnaK gene show no assembly defects at lower temperatures (30°C) but at temperature above 42°C ribosome assembly comes to a halt resulting in accumulation of immature complexes in both the 30S and 50S assembly. Reconstitution experiments with the 30S have been reported in the presence and absence of DnaK and in both conditions a heat activation step was still required for complete assembly. The mechanism by which DnaK facilitates ribosome assembly is undetermined although a direct affect on 30S subunits has been suggested and debated [56-58]. These conflicting results regarding the role of DnaK underscore the difficulty of correlating *in vivo* and *in vitro* ribosome assembly and elucidating the precise function of assembly factors.

Bacterial GTPases implicated in Ribosome Assembly

GTPases occur in all domains of life and regulate key cellular processes [59,60]. The extent of GTPase control of ribosome function is evident during translation where all steps, namely, initiation, elongation and termination require GTPases [30,61-63]. In addition to regulating ribosome function GTPases are also implicated in ribosome assembly. Nearly all bacterial

GTPases involved in ribosome assembly are essential for the cells and have been studied in multiple bacterial species [22,23]. In addition these GTPases are conserved throughout evolution and have eukaryotic homologs, several of which have also been implicated in eukaryotic ribosome assembly in mitochondria and chloroplast [64,65]. Biochemical and genetic studies have provided valuable functional insights into these GTPases [60,66]. However, their role in the ribosome assembly process remains a mystery. Understanding the function of these GTPases in ribosome assembly will uncover general principles of ribosome assembly *in vivo* and also provide insights into how other multi-component complexes are regulated through GTPases.

GTPases implicated in the Assembly of the 50S subunit

RbgA

RbgA (ribosome biogenesis GTPase A) is an essential GTPase in *B. subtilis* that is required for assembly of the 50S subunit. Cells depleted of RbgA are defective in ribosome assembly with a drastic reduction in 70S ribosomes and an absence of the 50S subunit. Instead they accumulate a complex that migrates at 45S and lacks three key r-proteins present in the mature 50S subunit [67,68]. This is strikingly similar to the reconstitution intermediate RI_{50} seen in *B. stearothermophilus* that is formed upon incubation of individual components at 30 °C and was also found to be lacking in three ribosomal proteins indicating that the 45S complex seen in RbgA depleted cells may be an *in vivo* intermediate in 50S assembly. The three r-proteins not present in 45S are L16, L27 and L36 and all three proteins are located at key functional sites on the mature 50S subunit [61]. R-proteins L16 and L27 are crucial to the formation of the A-site and the P-site in the 50S subunit and are proposed to directly participate in the binding of the A-site tRNA and the P-site tRNA respectively [62,69]. *E. coli* deletion mutants of L27 and L36

show a severe growth defect while a deletion mutant of L16 has not been reported [69]. Assembly maps indicate that binding of L16 to the growing 50S subunit is a late step in the assembly process [39].

RbgA can interact directly with the 45S complex and the mature 50S subunit though the latter is strongest in the presence of a non-hydrolysable form of GTP [70,71]. Foot-printing assays have indicated that RbgA protects nucleotides in the 23S rRNA near the A-site and the P-site [71]. These results together have suggested a model in which RbgA recruits r-proteins L16, L27 and L36 to the 45S complex at a late stage in 50S assembly. The mechanism by which RbgA participates in assembly of the 50S subunit is unknown. RbgA could either directly recruit one or more of the r-proteins to the 45S complex or it could alter the conformation of the intermediate leading to the incorporation of the r-proteins. Another key unanswered question is whether this 45S complex that is formed in the absence of RbgA is a true intermediate that can be matured to a 50S subunit or is this a dead end complex that forms in absence of functional RbgA.

RbgA is a widely conserved protein and eukaryotic homologs of RbgA have been implicated in ribosome assembly in chloroplast and mitochondria. Three homologs of RbgA in yeast Nog2, Nug1 and Lsg1 are involved in maturation of 60S, the large ribosomal subunit in eukaryotes [72,73]. Interestingly, Lsg1 is implicated to play a role in loading of r-protein Rpl10, the eukaryotic homolog of L16, onto the pre-60S complex indicating that this may be an evolutionarily conserved role of the RbgA protein family [74].

The eukaryotic protein that bears the most similarity to RbgA is the human Mtg1 protein that is implicated in ribosome assembly in the mitochondria [75]. Mutations of mtg1 in yeast are defective in mitochondrial protein synthesis leading to defective respiratory competence and suppressors of mtg1 mutations map to the rRNA in large ribosomal subunit. Interestingly, the

human homolog of Mtg1 can partially rescue the respiratory deficiency of mutant *mtg1* in yeast indicating the conserved function of this protein across different organisms.

B. subtilis is an ideal system for investigating the function of RbgA in order to gain insight into the role of essential GTPases in ribosome assembly. In eukaryotic systems defects in ribosome assembly usually result in degradation of the intermediates or dead end complexes making it difficult to elucidate the pathway of ribosome assembly. The accumulation of a stable 45S complex in *B. subtilis* upon depletion of RbgA offers a unique opportunity to study ribosome assembly *in vivo* and tease apart the role of RbgA in this process. This would also further our understanding of the function of RbgA homologs in eukaryotic ribosome assembly.

ObgE

ObgE is an essential GTPase that is conserved from bacteria to humans and is involved in several processes including ribosome assembly, modulation of the general stress response, sporulation and chromosomal segregation and replication [22]. Several studies show that ObgE is involved in assembly of the 50S subunit and ribosome function. Mutation or depletion of ObgE results in a reduction of 70S ribosomes and an accumulation of individual subunits 50S and 30S [76]. The 50S subunits that accumulate in these strains are unstable and under conditions of high ionic strength and low Mg^{2+} concentration they dissociate into a 40S complex. Proteomic analysis of this subunit indicated reduced amounts of L16, L33 and L34 and increased amounts of two assembly factors RrmJ, a rRNA methyltransferase and RluC, a pseudouridine synthase [77]. In addition overexpression of ObgE suppressed a temperature sensitive mutation in rrmJ. ObgE has also been shown to specifically interact with r-protein L13. Recent evidence also indicates that ObgE also interacts with SpoT, a bifunctional protein that both synthesizes and degrades the

second messenger (p)ppGpp [76]. These results suggest that ObgE could provide a link between ribosome assembly and the synthesis of new rRNA and r-proteins.

YsxC

YsxC is a universally conserved protein that is essential for growth. Studies in *E. coli* indicate that YsxC plays a role in cell division and the progression of the cell cycle. Subsequently studies in *B. subtilis* showed that YsxC is involved in the assembly of the large ribosomal subunit [68]. Cells depleted of YsxC are defective in assembly of the 50S subunit and accumulate a complex similar to RbgA depleted cells that migrates slightly slower at 44.5S and lacks three r-proteins L16, L27 and L36. YsxC has also been shown to specifically bind to the 50S subunit in a GTP dependant manner and can interact with r-proteins L1, L10 and L7/L12 [78]. Studies from Staphylococcus aureus show that YsxC copurifies with the 50S subunit. The crystal structure of YsxC from *B. subtilis* shows a patch of basic residues on the protein in the GTP-bound form but not in the GDP bound form and this region could potentially be involved in interaction with the ribosome [79]. However, the precise mechanism of interaction of YsxC with the ribosomes has not been determined.

YphC

YphC is another widely conserved GTPase that is essential for growth and implicated in the assembly of 50S subunits [68]. It is a unique protein which contains two GTP binding domains. Studies on YphC from both *E. coli* as well as *B. subtilis* show that depletion of this protein results in the reduction of 70S ribosomes and accumulation of individual subunits indicating disruption of ribosome assembly and maturation [22]. However, the products of ribosome

assembly differ in each case. In *B. subtilis* YphC depletion leads to the accumulation of a complex that migrates at 45S and also lacks proteins L16, L27 and L36 [68]. In contrast, depletion in *E. coli* results in accumulation of the 50S subunit that are unstable compared with mature 50S subunits seen in wild type cells [80]. Incubation of these 50S subunits in reduced levels of Mg^{2+} leads them to dissociate and result in a 40S complex that lacks r-proteins L9 and L18. The differences between the *E. coli* and *B. subtilis* phenotypes further exemplifies the importance of studying ribosome assembly in different bacterial systems.

Structural analysis of YphC provided further insight into guanine nucleotide control of the interaction of the protein with the ribosome. The structure of YphC shows the presence of a KH-domain (a RNA binding domain) between the two GTP binding domains [81]. When the N-terminal domain is bound to GTP the KH domain is solvent exposed. However, when both G domains are bound to GDP the KH domain is buried. This raises intriguing possibilities of guanine nucleotide control of RNA binding to YphC. This is further supported by evidence that GTP is required for association of YphC with the ribosome.

Era

Era is an essential GTPase shown play a role in assembly of 30S subunits and is known to bind to 16S rRNA [82]. The protein binds directly to 30S subunits and crystal structures of Era with the 30S subunit provide further insight into RNA-protein interaction. Era binds to the 30S subunit at the interface that interacts with 50S subunit [82]. Mutations in Era result in reduction of 70S subunits and accumulation of individual subunits. Together these results suggest that Era plays a role in the association of the 30S subunit to the 50S subunit. However the precise role of Era in maturation of the 30S subunit is unknown.

The immature 30S subunits that accumulate in Era mutants contain unprocessed 17S rRNA instead of processed 16S rRNA which has led to a model that suggests that Era is involved in processing of rRNA. However the appearance of 17S rRNA in 30S subunits is not limited to Era mutants and has been observed in strains with mutations in genes that play a role in maturation of the large subunit or inhibit translation.

RsgA

RsgA is implicated in the assembly of the 30S subunit and association of 30S and 50S subunits [83]. However RsgA is different from other GTPases in that it is not essential for cell growth. Studies from *E. coli* and *B. subtilis* show that RsgA interacts with the 30S subunit directly and null mutants show a reduction in 70S ribosomes though the 30S and 50S subunits appear normal. RsgA interacts with the 30S subunit close to the A-site and the P-site via its N-terminal domain and deletion mutants of this domain cannot interact with the ribosome. The GTPase activity of RsgA is stimulated ~160 fold upon interaction with the ribosome. Mutations in RsgA can be suppressed by overexpression of Era and initiation factor IF-2.

YqeH

YqeH is found in a diverse group of bacteria and plants [84]. Depletion of YqeH causes a complete loss of 30S subunits and a reduction in levels of 16S rRNA. Studies show that premature 16S rRNA and breakdown products of 16S rRNA are seen indicating small subunit assembly defects [85]. However there is a complete lack of immature 30S subunits making it difficult to assess the function of the protein. The intrinsic GTPase activity of YqeH is not enhanced by the 30S as seen in Era and RsgA [86]. Unlike other GTPases YqeH does not

directly interact with the ribosome. The YqeH homolog in Arabidopsis thaliana is involved in the assembly of mitochondrial ribosomes as well as chloroplast ribosomes. The crystal structure of YqeH from *B. stearothermophilus* indicates that C-terminal domain of the protein interacts with rRNA.

Unique features of Ribosome Assembly GTPases

All GTPases are believed to have evolved from a common ancestor and this is reflected in the conservation of the three dimensional fold as well as the sequence motifs of the G-domain. Five conserved motifs G1-G5 form the G-domain that is responsible for binding and hydrolysis of GTP. The G1 motif or P-loop is characterized by GXXXXGKS/T and interacts with the β and γ phosphates of GTP. The G2 motif is characterized by a single conserved T residue that coordinates the Mg^{2+} ion. The G3 motif, characterized by DXXG of which residue D also coordinates the Mg^{2+} ion and residue G interacts with the γ phosphate of GTP. Motifs G2 and G3 are also called switch I and switch II and acquire distinct conformations in GTP and GDP bound forms. The G4 motif, characterized by NKXD is responsible for specificity of binding to guanine nucleotide. The G5 motif, characterized by SAK/L is not universally present in all GTPases. Although all GTPases share these conserved structural features there are some characteristics that are specific to ribosome assembly GTPases.

The GTPase activity of these enzymes can be stimulated by a GTPase activating protein (GAP) that is thought to provide the arginine residue in order to neutralize the negative charge buildup on the β-and γ-phosphate. Hence, GAPs stabilize the transition state of the GTPase reaction [87]. In several ribosome assembly GTPases the ribosomal subunits stimulates GTPase activity suggesting that a rRNA residue(s) could also act as a GAP.

HAS-GTPases

All GTPases that are implicated in ribosome assembly are members of the HAS (hydrophobic amino acid substituted) family of GTPases [88]. In classical GTPases the catalytic residue Q follows the G3 motif. This residue activates the nucleophilic water molecule to attack the γ-phosphate bond. In HAS-GTPases a hydrophobic amino acid is found in place of this catalytic Q and thus the mechanism of GTP hydrolysis in ribosome assembly GTPases is not known. It has been proposed that the catalytic residue could be provided in cis by another part of the protein or in trans by another factor. The structure of RbgA shows that the isoleucine residue found in place of the catalytic glutamine is retracted from the active site which leaves a void for a residue from another protein or factor or an rRNA residue could facilitate GTP hydrolysis.

Circularly permuted GTPases

Some ribosome assembly GTPases such as RbgA, RsgA and YqeH are part of the circularly permuted GTPase family (cpGTPases) [89]. In this family the G4 motif preceeds the G1 motif resulting in a unique circular permutation of the G-domain. While there are subtle structural differences between cpGTPases and classical GTPases the structure of the GTP binding pocket remains relatively unaltered. All of the cpGTPases for which a function has been described or predicted either interact with RNA or are involved in ribosome assembly.

Another feature of these ribosome assembly cpGTPases is that the G3 motif (switch II) is no longer anchored to the G4 motif. Instead switch II is linked to a C-terminal domain which is necessary to stabilize the switch II region. This arrangement in ribosome assembly GTPases would allow for guanine nucleotide occupancy to control the conformation and/or movement of the C-terminal domain of the protein. How this circular permutation of the G-domain allows the

proteins to interact with the ribosome remains unanswered. Another relevant question in this context concerns the role of the C-terminal domain in GTPase function in these enzymes.

Affinity for guanine nucleotides

Classical GTPases of the Ras superfamily bind guanine nucleotides in the nanomolar to picomolar range. Such a high affinity for GTP and GDP indicates that guanine nucleotide exchange factors (GEFs) are necessary for catalytic turnover. However this is not the case for the ribosome assembly GTPases that have been characterized so far. The ribosome assembly GTPases bind to guanine nucleotide in the micromolar range approximating the physiological guanine nucleotide concentration in the cells during stress conditions with RbgA and RsgA displaying the weakest binding affinities. Further, studies have shown that both Era and ObgE have fast nucleotide exchange rates. Together, these data suggest that ribosome assembly GTPases may not require GEFs and are likely regulated directly by the GTP/GDP ratio in the cells. Such a system would allow ribosome assembly to be directly coupled to the energy status of the cell. Further biochemical characterization of ribosome assembly GTPases is required in light of these observations.

Possible mechanisms by which GTPases could participate in Ribosome Assembly

There is much evidence of the crucial role of GTPases in ribosome assembly. However the mechanisms by which these GTPases regulate ribosome assembly remains a mystery. Two possible mechanisms have been suggested based on the available data.

Ribosome GTPases could play a role in directly recruiting r-proteins or other assembly factors to the ribosome during assembly. Such a function has been shown for yeast GTPase Bms1 which

directly recruits assembly factor Rcl1 to the pre-40S complex. Rcl1 is an essential enzyme required for processing of pre-rRNA during ribosome maturation. This was the first demonstration of direct recruitment of an assembly? factor by ribosome assembly GTPase. To date no such function has been demonstrated in bacterial GTPases.

It is possible that ribosome assembly GTPases could regulate the activity of RNA helicases and thus control rRNA structure. In the regulation of spliceosome in yeast GTPase Snu114p stimulates the RNA helicase activity of DEAD box helicase Brr2p and thus controls the assembly and disassembly of the spliceosome. A similar interplay between ribosome assembly GTPases and RNA helicases could be possible during the assembly process.

Research over the past decade has shown that GTPases play a crucial role in assembly of bacterial, mitochondrial and chloroplast ribosomes. The fact that GTPases are required for ribosome assembly in all three kingdoms of life underscores their critical importance for the biogenesis process. What remains to be addressed is how these GTPases participate in ribosome assembly on a molecular level.

REFERENCES

REFERENCES

1. Nomura, M. (1970) Bacterial Ribosome. *Bacteriological Reviews* 34: 228-77.

2. Nierhaus, K.H., Wilson, D.N. (2006) Peptidyl Transfer on the Ribosome. *eLS*.

3. Ogle, J.M., Carter, A.P., Ramakrishnan, V. (2003) Insights into the decoding mechanism from recent ribosome structures. *Trends Biochem Sci* 28: 259-66.

4. Puglisi, J.D. (2009) Resolving the elegant architecture of the ribosome. *Mol Cell* 36: 720-3.

5. Wekselman, I*., et al.* (2009) Ribosome's mode of function: myths, facts and recent results. *J Pept Sci* 15: 122-30.

6. Steitz, T.A. (2008) A structural understanding of the dynamic ribosome machine. *Nat Rev Mol Cell Biol* 9: 242-53.

7. Amils, R., Matthews, E.A., Cantor, C.R. (1978) An efficient *in vitro* total reconstitution of the Escherichia coli 50S ribosomal subunit. *Nucleic Acids Res* 5: 2455-70.

8. Ballesta, J.P., Vazquez, D. (1972) Reconstitution of the 50S ribosome subunit. Role of proteins L 7 and L 12 in the GTPase activities. Site of action of thiostrepton. *FEBS Lett* 28: 337-42.

9. Nierhaus, K.H. (1991) The assembly of prokaryotic ribosomes. *Biochimie* 73: 739-55.

10. Kischa, K., Moller, W., Stoffler, G. (1971) Reconstitution of a GTPase activity by a 50S ribosomal protein and *E. coli*. *Nat New Biol* 233: 62-3.

11. Fahnestock, S., Erdmann, V., Nomura, M. (1973) Reconstitution of 50S ribosomal subunits from protein-free ribonucleic acid. *Biochemistry* 12: 220-4.

12. Nomura, M., Erdmann, V.A. (1970) Reconstitution of 50S ribosomal subunits from dissociated molecular components. *Nature* 228: 744-8.

13. Green, R., Noller, H.F. (1999) Reconstitution of functional 50S ribosomes from *in vitro* transcripts of Bacillus stearothermophilus 23S rRNA. *Biochemistry* 38: 1772-9.

14. Nomura, M., Fahnestock, S. (1973) Reconstitution of 50S ribosomal subunits and the role of 5S RNA. *Basic Life Sci* 1: 241-50.

15. Granneman, S., Baserga, S.J. (2004) Ribosome biogenesis: of knobs and RNA processing. *Exp Cell Res* 296: 43-50.

16. Panse, V.G., Johnson, A.W. (2010) Maturation of eukaryotic ribosomes: acquisition of functionality. *Trends Biochem Sci* 35: 260-6.

17. Dez, C., Tollervey, D. (2004) Ribosome synthesis meets the cell cycle. *Curr Opin Microbiol* 7: 631-7.

18. Wilson, D.N., Nierhaus, K.H. (2007) The weird and wonderful world of bacterial ribosome regulation. *Crit Rev Biochem Mol Biol* 42: 187-219.

19. Charollais, J., Pflieger, D., Vinh, J., Dreyfus, M., Iost, I. (2003) The DEAD-box RNA helicase SrmB is involved in the assembly of 50S ribosomal subunits in Escherichia coli. *Mol Microbiol* 48: 1253-65.

20. Peil, L., Virumae, K., Remme, J. (2008) Ribosome assembly in Escherichia coli strains lacking the RNA helicase DeaD/CsdA or DbpA. *FEBS J* 275: 3772-82.

21. Gutgsell, N.S., Deutscher, M.P., Ofengand, J. (2005) The pseudouridine synthase RluD is required for normal ribosome assembly and function in Escherichia coli. *Rna* 11: 1141-52.

22. Britton, R.A. (2009) Role of GTPases in bacterial ribosome assembly. *Annu Rev Microbiol* 63: 155-76.

23. Karbstein, K. (2007) Role of GTPases in ribosome assembly. *Biopolymers* 87: 1-11.

24. Poehlsgaard, J., Douthwaite, S. (2005) The bacterial ribosome as a target for antibiotics. *Nat Rev Microbiol* 3: 870-81.

25. Sohmen, D., Harms, J.M., Schlunzen, F., Wilson, D.N. (2009) SnapShot: Antibiotic inhibition of protein synthesis I. *Cell* 138: 1248 e1.

26. Tenson, T., Mankin, A. (2006) Antibiotics and the ribosome. *Mol Microbiol* 59: 1664-77.

27. Wilson, D.N. (2011) On the specificity of antibiotics targeting the large ribosomal subunit. *Ann N Y Acad Sci* 1241: 1-16.

28. Yonath, A. (2005) Antibiotics targeting ribosomes: resistance, selectivity, synergism and cellular regulation. *Annu Rev Biochem* 74: 649-79.

29. Ban, N. (2000) The Complete Atomic Structure of the Large Ribosomal Subunit at 2.4 A Resolution. *Science* 289: 905-20.

30. Youngman, E.M., Mcdonald, M.E., Green, R. (2008) Peptide release on the ribosome: mechanism and implications for translational control. *Annu Rev Microbiol* 62: 353-73.

31. Wilson, D.N. (2009) The A-Z of bacterial translation inhibitors. *Crit Rev Biochem Mol Biol* 44: 393-433.

32. Ruggero D, P.P., P. (2003) Does the ribosome translate cancer? *Nat Rev Cancer* 3: 179-92.

33. Kozma S. C., G., T. (2002) Regulation of cell size in growth, development and human disease: PI3K, PKB and S6K. *Bioessays* 24: 65-71.

34. Narla A., B.L., E. (2010) Ribosomopathies: human disorders of ribosome dysfunction. *Blood* 115: 3196-205.

35. H.T, G. (2008) Ribosomal Protein L5 and L11 MutationsAre Associated with Cleft Palate and Abnormal Thumbsin Diamond-Blackfan Anemia Patients. *Am J Hum Genet* 83: 769-80.

36. Freed, E.F., Bleichert, F., Dutca, L.M., Baserga, S.J. (2010) When ribosomes go bad: diseases of ribosome biogenesis. *Mol Biosyst* 6: 481-93.

37. Culver, G.M. (2003) Assembly of the 30S ribosomal subunit. *Biopolymers* 68: 234-49.

38. Nierhaus, K.H., Dohme, F. (1974) Total reconstitution of functionally active 50S ribosomal subunits from Escherichia coli. *Proc Natl Acad Sci U S A* 71: 4713-7.

39. Rohl, R., Nierhaus, K. (1982) Assembly map of the large subunit (50S) of *Escherichia coli* ribosomes. *Proc Natl Acad Sci U S A* 79: 729-33.

40. Grondek, J.F., Culver, G.M. (2004) Assembly of the 30S ribosomal subunit: positioning ribosomal protein S13 in the S7 assembly branch. *Rna* 10: 1861-6.

41. Shajani, Z., Sykes, M.T., Williamson, J.R. (2011) Assembly of bacterial ribosomes. *Annu Rev Biochem* 80: 501-26.

42. Raue, H.A., Lorenz, S., Erdmann, V.A., Planta, R.J. (1981) Reconstitution of biologically active 50S ribosomal subunits with artificial 5S RNA molecules carrying disturbances in the base pairing within the molecular stalk. *Nucleic Acids Res* 9: 1263-9.

43. Connolly, K., Culver, G. (2009) Deconstructing ribosome construction. *Trends Biochem Sci* 34: 256-63.

44. Kressler, D., Hurt, E., Bassler, J. (2010) Driving ribosome assembly. *Biochim Biophys Acta* 1803: 673-83.

45. Fromont-Racine, M., Senger, B., Saveanu, C., Fasiolo, F. (2003) Ribosome assembly in eukaryotes. *Gene* 313: 17-42.

46. Maguire, B.A. (2009) Inhibition of bacterial ribosome assembly: a suitable drug target? *Microbiol Mol Biol Rev* 73: 22-35.

47. Comartin, D.J., Brown, E.D. (2006) Non-ribosomal factors in ribosome subunit assembly are emerging targets for new antibacterial drugs. *Curr Opin Pharmacol* 6: 453-8.

48. Mathy, N.*, et al.* (2007) 5'-to-3' exoribonuclease activity in bacteria: role of RNase J1 in rRNA maturation and 5' stability of mRNA. *Cell* 129: 681-92.

49. Britton, R.A.*, et al.* (2007) Maturation of the 5' end of *Bacillus subtilis* 16S rRNA by the essential ribonuclease YkqC/RNase J1. *Mol Microbiol* 63: 127-38.

50. Remme, J. (2011) How to avoid undesirable interactions during ribosome assembly? *Mol Microbiol* 82: 269-71.

51. Bleichert, F., Baserga, S.J. (2007) The long unwinding road of RNA helicases. *Mol Cell* 27: 339-52.

52. Srivastava, L., Lapik, Y.R., Wang, M., Pestov, D.G. (2010) Mammalian DEAD box protein Ddx51 acts in 3' end maturation of 28S rRNA by promoting the release of U8 snoRNA. *Mol Cell Biol* 30: 2947-56.

53. Small, E.C., Leggett, S.R., Winans, A.A., Staley, J.P. (2006) The EF-G-like GTPase Snu114p regulates spliceosome dynamics mediated by Brr2p, a DExD/H box ATPase. *Mol Cell* 23: 389-99.

54. Sharpe Elles, L.M., Sykes, M.T., Williamson, J.R., Uhlenbeck, O.C. (2009) A dominant negative mutant of the *E. coli* RNA helicase DbpA blocks assembly of the 50S ribosomal subunit. *Nucleic Acids Res* 37: 6503-14.

55. Kossen, K., Karginov, F.V., Uhlenbeck, O.C. (2002) The carboxy-terminal domain of the DExDH protein YxiN is sufficient to confer specificity for 23S rRNA. *J Mol Biol* 324: 625-36.

56. Maki, J.A., Southworth, D.R., Culver, G.M. (2003) Demonstration of the role of the DnaK chaperone system in assembly of 30S ribosomal subunits using a purified *in vitro* system. *Rna* 9: 1418-21.

57. Rene, O., Alix, J.H. (2011) Late steps of ribosome assembly in *E. coli* are sensitive to a severe heat stress but are assisted by the HSP70 chaperone machine. *Nucleic Acids Res* 39: 1855-67.

58. Alix, J.H. (2003) DnaK-facilitated ribosome assembly in Escherichia coli revisited. *Rna* 9: 787-93.

59. Verstraeten, N., Fauvart, M., Versees, W., Michiels, J. (2011) The universally conserved prokaryotic GTPases. *Microbiol Mol Biol Rev* 75: 507-42, second and third pages of table of contents.

60. Bourne H.R, Sanders D.A., Mccormick F. (1990) The GTPase superfamily: a conserved switch for diverse cell functions. *Nature* 348: 125-32.

61. Ramakrishnan, V. (2002) Ribosome structure and the mechanism of translation. *Cell* 108: 557-72.

62. Schmeing, T.M., Ramakrishnan, V. (2009) What recent ribosome structures have revealed about the mechanism of translation. *Nature* 461: 1234-42.

63. Leung, E.K., Suslov, N., Tuttle, N., Sengupta, R., Piccirilli, J.A. (2011) The mechanism of peptidyl transfer catalysis by the ribosome. *Annu Rev Biochem* 80: 527-55.

64. Kotani, T., Akabane, S., Takeyasu, K., Ueda, T., Takeuchi, N. (2013) Human G-proteins, ObgH1 and Mtg1, associate with the large mitochondrial ribosome subunit and are involved in translation and assembly of respiratory complexes. *Nucleic Acids Res* 41: 3713-22.

65. Jeon, Y.*, et al.* (2014) DER containing two consecutive GTP-binding domains plays an essential role in chloroplast ribosomal RNA processing and ribosome biogenesis in higher plants. *J Exp Bot* 65: 117-30.

66. Sprang, S.R. (1997) G protein mechanisms: insights from structural analysis. *Annu Rev Biochem* 66: 639-78.

67. Uicker, W.C., Schaefer, L., Britton, R.A. (2006) The essential GTPase RbgA (YlqF) is required for 50S ribosome assembly in *Bacillus subtilis*. *Mol Microbiol* 59: 528-40.

68. Schaefer, L.*, et al.* (2006) Multiple GTPases participate in the assembly of the large ribosomal subunit in *Bacillus subtilis*. *J Bacteriol* 188: 8252-8.

69. Trobro, S., Åqvist, J. (2008) Role of Ribosomal Protein L27 in Peptidyl Transfer. *Biochemistry* 47: 4898-906.

70. Achila, D., Gulati, M., Jain, N., Britton, R.A. (2012) Biochemical characterization of ribosome assembly GTPase RbgA in *Bacillus subtilis*. *J Biol Chem* 287: 8417-23.

71. Matsuo, Y.*, et al.* (2006) The GTP-binding protein YlqF participates in the late step of 50 S ribosomal subunit assembly in *Bacillus subtilis*. *J Biol Chem* 281: 8110-7.

72. Kallstrom, G., Hedges, J., Johnson, A. (2003) The Putative GTPases Nog1p and Lsg1p Are Required for 60S Ribosomal Subunit Biogenesis and Are Localized to the Nucleus and Cytoplasm, Respectively. *Mol Cell Biol* 23: 4344-55.

73. Bassler, J., Kallas, M., Hurt, E. (2006) The NUG1 GTPase reveals and N-terminal RNA-binding domain that is essential for association with 60 S pre-ribosomal particles. *J Biol Chem* 281: 24737-44.

74. Hedges, J., West, M., Johnson, A.W. (2005) Release of the export adapter, Nmd3p, from the 60S ribosomal subunit requires Rpl10p and the cytoplasmic GTPase Lsg1p. *EMBO J* 24: 567-79.

75. Barrientos, A.*, et al.* (2003) MTG1 codes for a conserved protein required for mitochondrial translation. *Mol Biol Cell* 14: 2292-302.

76. Wout, P.*, et al.* (2004) The Escherichia coli GTPase CgtAE cofractionates with the 50S ribosomal subunit and interacts with SpoT, a ppGpp synthetase/hydrolase. *J Bacteriol* 186: 5249-57.

77. Jiang, M.*, et al.* (2006) The Escherichia coli GTPase CgtAE is involved in late steps of large ribosome assembly. *J Bacteriol* 188: 6757-70.

78. Wicker-Planquart, C., Foucher, A.E., Louwagie, M., Britton, R.A., Jault, J.M. (2008) Interactions of an essential *Bacillus subtilis* GTPase, YsxC, with ribosomes. *J Bacteriol* 190: 681-90.

79. Ruzheinikov, S.N.*, et al.* (2004) Analysis of the open and closed conformations of the GTP-binding protein YsxC from *Bacillus subtilis*. *J Mol Biol* 339: 265-78.

80. Bharat, A., Jiang, M., Sullivan, S.M., Maddock, J.R., Brown, E.D. (2006) Cooperative and critical roles for both G domains in the GTPase activity and cellular function of ribosome-associated Escherichia coli EngA. *J Bacteriol* 188: 7992-6.

81. Muench, S.P., Xu, L., Sedelnikova, S.E., Rice, D.W. (2006) The essential GTPase YphC displays a major domain rearrangement associated with nucleotide binding. *Proc Natl Acad Sci U S A* 103: 12359-64.

82. Sharma, M.R.*, et al.* (2005) Interaction of Era with the 30S ribosomal subunit implications for 30S subunit assembly. *Mol Cell* 18: 319-29.

83. Goto, S., Kato, S., Kimura, T., Muto, A., Himeno, H. (2011) RsgA releases RbfA from 30S ribosome during a late stage of ribosome biosynthesis. *EMBO J* 30: 104-14.

84. Uicker, W.C., Schaefer, L., Koenigsknecht, M., Britton, R.A. (2007) The essential GTPase YqeH is required for proper ribosome assembly in *Bacillus subtilis*. *J Bacteriol* 189: 2926-9.

85. Anand, B., Surana, P., Bhogaraju, S., Pahari, S., Prakash, B. (2009) Circularly permuted GTPase YqeH binds 30S ribosomal subunit: Implications for its role in ribosome assembly. *Biochem Biophys Res Commun* 386: 602-6.

86. Anand, B., Surana, P., Prakash, B. (2010) Deciphering the catalytic machinery in 30S ribosome assembly GTPase YqeH. *PLoS One* 5: e9944.

87. Scheffzek, K., Ahmadian, M.R. (2005) GTPase activating proteins: structural and functional insights 18 years after discovery. *Cell Mol Life Sci* 62: 3014-38.

88. Mishra, R., Gara, S.K., Mishra, S., Prakash, B. (2005) Analysis of GTPases carrying hydrophobic amino acid substitutions in lieu of the catalytic glutamine: implications for GTP hydrolysis. *Proteins* 59: 332-8.

89. Anand, B., Verma, S.K., Prakash, B. (2006) Structural stabilization of GTP-binding domains in circularly permuted GTPases: implications for RNA binding. *Nucleic Acids Res* 34: 2196-205.

CHAPTER 2

Biochemical characterization of the ribosome assembly GTPase RbgA in *Bacillus subtilis*

The contents of this chapter were published in Achila D., Gulati M., Jain N. and Britton R.A. (2012) Biochemical characterization of ribosome assembly GTPase RbgA in Bacillus subtilis. J Biol Chem. 287:8417-8423. MG contributed to Table 2.3 and Figure 2.5. MG and NJ collaborated on Figure 2.3 and DA contributed to Figures 2.1, 2.2 and 2.4.

Abstract

The ribosome biogenesis GTPase A protein (RbgA) is involved in the assembly of the large ribosomal subunit in *Bacillus subtilis* and homologs of RbgA are implicated in the biogenesis of mitochondrial, chloroplast, and cytoplasmic ribosomes in archaea and eukaryotes. The precise function of how RbgA contributes to ribosome assembly is not understood. Defects in RbgA give rise to a large ribosomal subunit that is immature and migrates at 45S in sucrose density gradients. Here we report a detailed biochemical analysis of RbgA and its interaction with the ribosome. We found that RbgA, like most other GTPases, exhibits a very slow k_{cat} (14 h^{-1}) and has a high K_m (90 μM). Homology modeling of the RbgA switch I region using the K-loop GTPase MnmE as a template suggested that RbgA requires K^+ ions for GTPase activity, which was confirmed experimentally. Interaction with 50S subunits, but not 45S intermediates, increases GTPase activity ~55 fold. Stable association with 50S subunits and 45S intermediates was nucleotide dependent and GDP did not support strong interaction with either of the subunits. GTP and GMPPNP were sufficient to promote association with the 45S intermediate while only GMPPNP was able to support binding to the 50S subunit, presumably due to the stimulation of GTP hydrolysis. These results support a model in which RbgA promotes a late step in ribosome biogenesis and that one role of GTP hydrolysis is to stimulate dissociation of RbgA from the ribosome.

Introduction

Ribosome assembly is a complex, tightly regulated process that involves the coordinated assembly of 3 RNA molecules and over 50 proteins [1,2]. Although more than 150 accessory proteins required for the assembly of ribosomes in eukaryotes have been identified [3], relatively few proteins dedicated to the assembly of ribosomes have been discovered in bacteria [4-6]. Several ribosome associated GTPases (RA-GTPase) such as RbgA (YlqF), Era, YqeH, YphC (EngA), CgtEA, YloQ (YjeQ, RsgA) and YsxC have been implicated in the assembly of either the 50S or 30S ribosomal subunits in bacteria, however their precise functions in ribosome assembly has remained elusive [6-13]. The RA-GTPase RbgA is required for a late maturation step of the 50S subunit in *B. subtilis* [8,10] and its homologs have been shown to be required for the assembly of the large ribosomal subunit in eukaryotes [14-17].

Depletion of RbgA in *B. subtilis* stalls 50S subunit assembly resulting in the accumulation of a large ribosomal intermediate that migrates more slowly (45S) through a sucrose gradient and lacks three ribosomal proteins, L16, L27, and L36 [8,10,11]. RbgA can interact with the 45S intermediate and 50S subunits, but the latter interaction was only observed in the presence of a non-hydrolyzable analog of GTP [8,10,11]. It was also observed that intact 50S stimulates the GTPase activity of RbgA [8]. These observations led to proposal of a model in which RbgA promotes a late step in ribosome assembly and that GTPase activation of RbgA occurs upon correct assembly of the 50S subunit followed by dissociation of RbgA from the subunit [8,10]. In this way RbgA would serve as a checkpoint to ensure proper formation of the 50S subunit. However, it was later reported that the GTPase activity of RbgA is maximally stimulated by the 45S intermediate (referred to as pre50S in this model) and “free” 50S subunits but not by mature 50S subunits (those isolated by dissociation of subunits from 70S ribosomes) [18]. These

additional results led to a revised model in which RbgA promotes a GTPase dependent structural rearrangement of the 45S complex that then allows L16 and L27 to subsequently bind. GDP bound RbgA remains associated with the ribosome until some undetermined signal triggers the release of RbgA [18]. The later model posits that structural difference exists between "free" 50S and mature 50S subunits to explain the differential activation of RbgA by free 50S subunits.

In order to address these two conflicting models we undertook a more thorough biochemical analysis of RbgA and explored its interaction with the ribosome in details. Our results demonstrate that the GTPase activity of RbgA is maximally stimulated by both mature and free 50S subunits, more than ten times over the stimulation observed with the 45S intermediate. Interaction assays of RbgA with the different ribosomal subunits shows that GDP-bound RbgA does not stably associate with the ribosome and suggests that the GTPase activity of RbgA promotes dissociation from the ribosome. We discuss our findings in the context of the two conflicting models and further clarify the role of GTPase activity in RbgA function during ribosome assembly.

Materials and Methods

Growth conditions and strain construction

All experiments were performed at 37°C in Luria-Bertani (LB) medium. When necessary, antibiotics were added at the following concentrations: Chloramphenicol (5 μg/ml), Ampicillin (100 μg/ml). All *B. subtilis* strains used in this study were derived from the wild-type strain JH642 (RB247). *B. subtilis* RB301 (Pspank-*rbgA*) and RB418 (Pspank-*infB*) strains were constructed as previously described [10]. RB301 and RB418 accumulate 45S and 50S subunits, respectively, when grown in the absence of IPTG and were used to purify 45S and free 50S

ribosomal subunits. *E. coli* BL21(DE3) transformed with plasmids containing full-length *rbgA* placed under the control of the T7 promoter was used to overexpress RbgA proteins [10].

Purification of RbgA proteins

RbgA protein with histidine tag (His_6) at the C-terminus was isolated as previously described [10]. Briefly, *E. coli* BL21(DE3) cells transformed with plasmid containing full-length *rbgA* under IPTG inducible T7 promoter [10] were grown to OD_{600} of 0.5 at 37°C in LB medium containing 100 μg/mL ampicillin then induced by addition of 1 mM isopropyl β-thiogalactoside (IPTG). The cells were harvested by centrifugation after 3 hours and resuspended in binding buffer (20 mM sodium phosphate, pH 7.5, 0.5 M NaCl and 20 mM imidazole). The cells were lysed by three consecutive passes through a French press at between 1400 to 1600 psi then clarified by centrifugation at 16000xg for 20 min. RbgA-His_6 was isolated from the cell lysate by affinity chromatography using HisTrapHP (Ni-NTA resin column) from GE Healthcare BioScience on a BioRad BioLogic LP chromatography system. Cell lysate was injected into the column pre-equilibrated with binding buffer and allowed to equilibrate for 5 minutes then washed with 5 column volumes of wash buffer (20 mM sodium phosphate, pH 7.5, 0.5 M NaCl and 60 mM imidazole) followed by step elution with binding buffer containing 250 mM imidazole. Elution was monitored by UV absorption at 280 nm and RbgA containing fractions were verified by SDS-PAGE gel then concentrated and desalted by exchanging buffer to desalting buffer (50 mM Tris-HCl pH 7.5, 750 mM KCl, 5 mM $MgCl_2$, 20 mM imidazole, 2 mM DTT and 10% glycerol) and then to storage buffer (50 mM Tris-HCl, pH 7.5, 750 mM KCl, 5 mM $MgCl_2$, 2 mM DTT and 10% glycerol). Purity of isolated concentrated RbgA was verified

by SDS-polyacrylamide gel electrophoresis (SDS-PAGE) before storage at -20ºC. K59A, P129R, S134A and F180A mutations were introduced into *rbgA* by the QuikChange II XL kit (Stratagene).

Preparation of ribosomal particles

Mature 50S, free 50S and 45S large ribosomal subunits were prepared by sucrose density centrifugation [19,20]. 50S and 45S complexes were isolated from lysates of RB418 and RB301 cells respectively. Mature 50S subunits were isolated by subjecting the RB247 lysate to low Mg^{2+} buffer (buffer B containing 1 mM Mg^{2+}), thereby dissociating the 70S ribosome into 50S and 30S subunits. The cells were grown were grown to OD_{600} of 0.5 at 37°C in LB medium with or without IPTG. RB301 and RB418 cells were grown without IPTG for several generations to deplete the cells of RbgA and IF-2, respectively, until a doubling time of about 150 min was reached. Chloramphenicol (Sigma) was added to a final concentration of 100 μg/ml 5 minutes prior to harvesting. Cells were harvested by centrifugation at 5000xg for 10 min and resuspended in lysis buffer (10 mM Tris-HCl (pH 7.5), 60 mM KCl, 10 mM $MgCl_2$, 0.5% Tween 20, 1 mM DTT, 1× Complete EDTA-free protease inhibitors (Roche) and 10 U/ml RNase-free DNase (Roche). Cells were lysed by three consecutive passes through a French press set at 1400 to 1600 psi, then clarified by centrifugation at 16000xg for 20 minutes. Clarified cell lysates were loaded on top of 10-25% sucrose density gradients equilibrated in buffer B (10 mM Tris-HCl, pH 7.6, 10 mM $MgCl_2$, 50 mM NH_4Cl) and centrifuged using an SureSpin 630 rotor (Sorvall) for 4.5 hours at 30,000 rpm. Gradients were then fractionated on BioRad BioLogic LP chromatography system by monitoring UV absorbance at 254 nm. Fractions corresponding to ribosomal subunits

of interest were pooled, concentrated using 100 kDa cutoff filters (Millipore) and stored in buffer A (10 mM Tris-HCl, pH 7.6, 10 mM $MgCl_2$, 60 mM KCl and 1 mM DTT) at -80°C. To purify mature 50S subunits, RB247 cells were grown in LB medium at 37°C to an OD_{600} of 0.5, harvested, and resuspended in lysis buffer containing only 1 mM Mg^{2+} concentration. The lysate was incubated on ice for 30 minutes and then centrifuged for 14 hours at 20,600 rpm through a 25-40% sucrose gradient prepared in buffer B containing 1 mM Mg^{2+} (10 mM Tris-HCl, pH 7.6, 1 mM $MgCl_2$, 50 mM NH_4Cl). 50S subunit peak fractions were pooled, concentrated, and stored in buffer A.

Characterization of GTPase activity of RbgA

GTP hydrolysis activity of RbgA was determined incubating RbgA with GTP for 30 minutes then measuring the released free phosphate by the malachite green–ammonium molybdate colorimetric assay (BioAssays) [21]. Intrinsic GTPase activity was assayed in triplicate at a constant RbgA protein concentration of 2 μM and a range of GTP concentrations (8 to 650 μM) (USB corp.). GTPase reactions was started by addition of protein to GTP solutions at 37°C in reaction buffer (50 mM Tris-HCl, pH 7.5, 200 mM KCl, 5 mM $MgCl_2$, and 1 mM DTT) for 30 minutes then terminated by addition of Malachite reagent. We determined that under these conditions GTP hydrolysis was in the linear range of the assay and less than 10% of the substrate had been consumed. Released phosphate was detected by monitoring color formation at 620 nm using a 96-well plate reader (Tecan Sunrise). Experiments were repeated a minimum of three times and values for K_m and k_{cat} were calculated by fitting the data to the Michaelis-Menten

equation with nonlinear regression curve fitting using GraphPad Prism (Graph-Pad Software Inc.; version 5.0).

Stimulation of GTPase activity of RbgA by ribosomal subunits

To probe the effect of ribosomal subunits on the GTPase activity of RbgA, 100 nM of purified ribosomal subunits (mature 50S subunits from dissociated 70S, free 50S subunits from IF-2 depleted cells, and 45S subunits from RbgA depleted cells) were individually incubated with 100 nM RbgA for 15 min at 37°C in reaction buffer (50 mM Tris-HCl, pH 7.5, 200 mM KCl, 5 mM $MgCl_2$, and 1 mM DTT) then added to 8-650 μM GTP to start the reaction. We predetermined that under these conditions the values were in the linear range of the assay. The activity of RbgA-subunit complex was determined by standard malachite green assay as described above for RbgA proteins alone. Three biological replicates (independent RbgA and ribosome preparations) were performed, each with three technical replicates.

Importance of potassium ion for GTPase activity of RbgA

For testing with the GTPase activity in the presence of K^+, the protein was purified as described above and stored in storage buffer (50 mM Tris-HCl, pH 7.5, 750 mM KCl, 5 mM $MgCl_2$, 2 mM DTT,10% glycerol).To test the effects of Na^+, the protein was exchanged and stored in NaCl buffer (50 mM Tris-HCl, pH 7.5, 750 mM NaCl, 5 mM $MgCl_2$, 2 mM DTT and 10% glycerol). The intrinsic activity of RbgA was assayed by incubation of 2 μM of RbgA with 200 μM GTP for 15 min at 37°C. Stimulation of GTPase activity was tested by incubation of 100 nM of free

50S subunits with 100 nM RbgA and 200 μM GTP for 15 min at 37°C. The activity was determined by standard malachite green assay as described above.

Homology modeling of the K-loop of RbgA

Homology modeling of the K-loop of RbgA was carried out with Modeler [22] using MnmE as a template. A multiple sequence alignment in which K-loop of MnmE was used as a template to model the RbgA K-loop, which is disordered in available crystal structures, while for the remainder of RbgA the existing crystal structure was used (PDB: 1PUJ).A total of 20 initial models were made the best model was chosen based on the lowest energy (molpdf) and the lowest discrete objective protein energy (DOPE) function. A ligand based superimposition of RbgA (PDB: 1PUJ) and MnmE (PDB: 2GJ8) was carried out using ligalign script [23] in PyMOL [24]. The figure was generated by using Chimera [25].

Interaction between RbgA and ribosomal particles

RbgA protein and ribosomal particles were purified as described above. The RbgA subunit binding assay was performed as previously described [8]. The protocol was however modified to include 15 min incubation with a high salt buffer, buffer C (10 mM Tris-HCl pH 7.5, 60 mM KCl, 500 mM NH_4Cl, 10 mM $MgCl_2$ and 1 mM DTT) to further test the specificity of RbgA/subunits interaction. Briefly, 60 pmol of RbgA was pre-incubated with 1.5 mM of different guanine nucleotides for 15 min followed by addition of 10 pmol purified subunits. The binding was allowed to proceed for 15 min at 37°C, then centrifuged once through Microcon 100 filters (Millipore) with a cut-off of 100 kDa. The RbgA-subunit complexes were washed once with buffer A, twice with buffer C before elution. Ribosome bound RbgA was detected by

separating the complexes on NuPAGE 12% Bis-Tris SDS gels (Invitrogen) followed by Western blot analysis, using rabbit polyclonal anti-RbgA and HRP-conjugated goat anti-rabbit antibodies. RbgA specific bands were visualized with the Western Lightning (PerkinElmer) chemiluminescent detection system.

Results

RbgA has a low intrinsic GTPase activity

Most RA-GTPases have low intrinsic GTPase activity in the absence of an effector protein or molecule. To characterize the intrinsic GTPase activity of RbgA, we purified RbgA-His_6 and measured GTP hydrolysis using a malachite green assay. Previously we have shown that the C-terminal fusion of six histidine residues to RbgA yields a functional protein that can support wild-type growth of *B. subtilis* as well as interaction with the ribosome [10]. We performed a steady state kinetic analysis of RbgA GTPase activity using the RbgA-His_6 protein (Figure 2.1). Wild-type RbgA had a k_{cat} of 14 h^{-1}, a K_m of 90 μM, and a k_{cat}/K_m of 47 $M^{-1}s^{-1}$ (Table 2.1). To confirm that the low rate of hydrolysis observed was due to RbgA and not a contaminant, we created three mutants that altered important residues in the P-loop (P129R, S134A) or the G4 region that specifies binding for guanine nucleotides (K59A) and tested their ability to hydrolyze GTP (Figure 2.1 and Table 2.2). All three mutants displayed lower GTPase activity and a reduced k_{cat}/K_m, indicating that the GTPase activity observed for wild-type RbgA was not due to a contaminant.

The GTPase activity of RbgA is maximally stimulated by mature or free 50S ribosomal subunits

To better understand the role of GTPase activity in the function of RbgA, we characterized GTP hydrolysis of RbgA in the presence of 50S subunits and 45S intermediates. We tested three types of large ribosomal subunits: mature 50S subunits isolated by dissociating subunits from 70S ribosomes, free 50S subunits isolated by depleting initiation factor 2 (IF-2) and 45S intermediates purified from RbgA depleted cells. Previous work had indicated that 45S intermediates and free 50S subunits had higher stimulatory activity than mature 50S subunits [18]. Ribosomal subunits were mixed with RbgA in a ratio of 1:1 and the GTPase activity of RbgA was monitored using a malachite green assay. Both mature and free 50S subunits were capable of stimulating the GTPase activity of RbgA ~55-fold (Figure 2.2 and Table 2.1). In contrast the 45S intermediate isolated from RbgA-depleted cells showed a markedly reduced ability to stimulate the GTPase activity of RbgA (5-fold) over intrinsic GTPase activity. Michaelis-Menten analysis of the GTPase activity of RbgA indicated that the increase in GTPase activity with 50S subunits was primarily governed by an increase in k_{cat} (Table 2.3). Conversely, interaction with the 45S intermediate decreased the K_m of RbgA for GTP to 4 μM, indicating a tighter affinity for GTP in the presence of the 45S complex while k_{cat} was largely unaffected. Our results show that GTPase activity of RbgA is maximally stimulated by the 50S subunits (free and mature), in contrast to previously published results [18].

Potassium is required for optimal GTPase activity

Recent work has indicated that three translation associated GTPases (MnmE, FeoB and YqeH) utilize a unique mechanism for GTP hydrolysis in which a K^+ ion participates in the activation of GTP hydrolysis [26-28]. The structures of these GTPases demonstrate that a K^+ ion functions as a GTPase Activating Element (GAE), analogous to GTPase activating proteins (GAP) in eukaryotic GTPases.

This K^+ ion occupies a position, usually occupied by an arginine residue, referred as "arginine finger" in GAPs of Ras related GTPases [29]. The positive charge provided by arginine or K^+ at this position stabilizes the transition state by neutralizing negative charges that builds up during the transition state. In GTPases that require K^+, the K^+ ion is held in position by a region of the GTP binding domain that has been designated the "K-loop"[28]. The K-loop is located upstream of switch I and interacts with K^+ through the peptide backbone of amino acids and shields the K^+ ion from the bulk solvent. An additional side-chain interaction is provided by a conserved asparagine residue situated within the P-loop. Inspection of the primary sequence of RbgA indicated a possible K-loop type sequence; however this part of the protein is not resolved in any of the crystal structures of RbgA to date. Therefore, we modeled this K-loop in RbgA using transition state structure of MnmE [28] (Figure 2.3A). Out of 20 homology models generated, the most energetically favorable model shows a high degree of similarity to the K-loop of MnmE. Moreover, the asparagine residue from P loop (GIPNVGKS in RbgA), that makes a direct contact with the K^+ in other 16 activated GTPases, is also oriented similar to P loop

asparagine in the RbgA crystal structure (Figure 2.3B). This suggests that RbgA may also utilize K^+ in the activation of GTPase activity similar to MnmE, FeoB and YqeH.

Next, we investigated whether K^+ was required for maximal stimulation of RbgA GTPase activity. The intrinsic GTPase activity and stimulation of RbgA GTPase was monitored in the presence of 250 mM NaCl or KCl. The intrinsic GTPase activity of RbgA is reduced 133-fold when NaCl is substituted for KCl, demonstrating that K^+ is required for optimal RbgA GTPase activity (Table 2.3). The stimulation of RbgA GTPase activity by the ribosome is also affected by Na^+ but to a lesser degree, showing a 22-fold reduction in GTPase activity when co-incubated with 50S subunits compared to K^+ conditions. These results show that K^+ is required for maximal GTPase activity.

RbgA interacts with the 50S ribosomes and 45S intermediates in a nucleotide specific manner

Previous work showed that RbgA interacts with the large ribosomal subunit when incubated with a non-hydrolyzable analog of GTP [8]. In order to explore interaction of RbgA with the subunits in detail, the interaction of RbgA with both purified 50S subunits and 45S intermediate was characterized in the presence of GTP, GDP, and GMPPNP. Saturating levels of guanine nucleotides were used to ensure all RbgA molecules were bound to nucleotide. 45S intermediates or 50S subunits were incubated with RbgA for 15 minutes at 37°C and were spun through a 100 kDa cutoff microcon filter to remove unbound RbgA. RbgA bound to the subunits was retained on top of the filter and was detected using RbgA specific polyclonal antibodies. We found that RbgA associates most stably with the 45S subunit in the GTP and GMPPNP bound forms and

that binding is greatly reduced in the presence of GDP (Figure 2.4). In the presence of the 50S subunit, RbgA binding is maximally enhanced in the presence of GMPPNP but is greatly reduced in the presence of GTP and GDP. The difference between GTP and GMPPNP is likely due to GTP hydrolysis in the presence of the 50S ribosome, resulting in dissociation from the ribosome. We also tested if the alarmone, pppGpp, affected RbgA interaction with the ribosome. We found that addition of pppGpp enhanced the interaction of RbgA with both the 45S intermediate and 50S subunits.

Discussion

Previous genetic and biochemical studies aimed at elucidating the role of RbgA in large ribosomal subunit assembly have yielded two conflicting models. One model posits that RbgA couples a final maturation step of the 50S subunit with the activation of GTP hydrolysis, which signals RbgA to leave the ribosome [8,10]. This maturation step involves the incorporation of ribosomal proteins L16, L27, and L36. However, a revised model was proposed suggesting that RbgA uses GTP hydrolysis to induce a conformational change in the 45S subunit that is independent of the incorporation of L16, L27, and L36 [18]. The revised model is based upon the finding that the 45S subunit can maximally stimulate RbgA GTPase activity in vitro, although one major complication of the model is that free 50S subunits, but not mature 50S subunits, can also stimulate GTP hydrolysis to the same level as the 45S intermediate. Because both of these models rely on limited biochemical evidence, we undertook a detailed analysis of RbgA interaction with the ribosome to clarify the role of GTP hydrolysis in RbgA function.

Several lines of evidence presented here support the model in which RbgA utilizes GTPase activity to dissociate from the ribosome. First, GTPase stimulation by 50S subunits, free or

mature, was ten times more than that observed with 45S intermediates. Second, RbgA interaction with 50S subunits was nucleotide dependent, with reduced levels of binding observed in the presence of GTP and GDP compared to the non-hydrolyzable analog GMPPNP. In contrast, the 45S intermediate displayed similar binding in the presence of GTP and GMPPNP with greatly reduced binding in the presence of GDP. Decreased binding of RbgA to the 50S subunit in the presence of GTP, but not GMPPNP, is consistent with GTP hydrolysis governing dissociation of RbgA from the ribosome. Third, steady state kinetic analysis of RbgA in the presence of the different ribosomal subunits showed that the k_{cat} of RbgA was dramatically increased only in the presence of the 50S subunit. This indicates that the 50S, but not the 45S intermediate, serves a GAP-like function for RbgA. Additionally K_m was decreased only in presence of 45S but not 50S, which suggest a cooperative binding of 45S and GTP to RbgA. These data support a model in which the GTPase activity of RbgA is required to dissociate RbgA from the 50S subunit. It is possible that RbgA either serves to monitor correct ribosome formation with its GTPase activity or that it couples the hydrolysis of GTP to a conformational change in the subunit while subsequently dissociating from the subunit.

An important question to address is why we observe maximal stimulation of RbgA GTPase activity in the presence of 50S subunits (free or mature) while previous work shows maximal stimulation with the 45S intermediate and free 50S subunits but not mature subunits [18]. Our steady-state kinetic analysis of RbgA indicates a potential answer to this question. The K_m for RbgA in the absence of the ribosome is ~90 μM, and given the slow forward reaction in the absence or presence of the ribosome the K_m is a good estimate for the K_D of RbgA for GTP. In the presence of 50S subunits the K_m is only marginally reduced (62 μM for mature 50S and 32

μM for free 50S subunits). However in the presence of the 45S intermediate the K_m of RbgA is reduced to 4 μM, indicating that interaction with the 45S intermediate fosters tighter association with GTP. In previous work GTPase assays were performed using a concentration of 10 μM GTP, well below the K_m of RbgA for GTP in the presence of the 50S subunit [18]. These assay conditions would result in most of the RbgA protein being unbound to GTP and should underestimate the activity of RbgA in the presence of 50S subunits. Since GTP concentration in the cell is in the range of 0.5-5 mM [30,31], our assay likely reflects a more physiologically relevant condition. Finally, our results demonstrate that RbgA is a member of a growing family of GTPases that utilize K^+ as part of the mechanism of GTP hydrolysis. Previous work on the biochemistry of RbgA was performed with NH_4Cl [18]. While NH_4^+ supports hydrolysis of GTP in YqeH, it is reduced 2-fold in its activity indicating that NH_4^+ is not sufficient to replace K^+ for full activity [26]. Future experiments on the biochemistry of RA-GTPases thus warrant investigation of K^+ as a possible GTPase activating element.

The results presented here support a model in which the guanine nucleotide state of RbgA regulates the association of RbgA with the ribosome (Figure 2.5). GDP significantly inhibits RbgA interaction with either the 45S intermediate or the 50S subunit, and the interaction with the 50S subunit is only stabilized in the presence of non-hydrolyzable analogs of GTP. These results indicate that GTP hydrolysis promotes RbgA dissociation from the 50S subunit, similar to other translation factor GTPases such as EF-Tu. EF-Tu couples proper accommodation of the aa-tRNA to GTPase activity, resulting in release of EF-Tu from the ribosome [32]. We propose that RbgA promotes a late step in large subunit assembly that allows the stable incorporation of ribosomal

proteins L16, L27, and L36. While the nature of this rearrangement is still unknown, once properly achieved we propose that RbgA "senses" the correct assembly of the ribosome which in turn promotes GTP hydrolysis and RbgA dissociation. Alternatively, RbgA could act directly on the 45S intermediate independently of incorporation of L16, L27, or L36. Finally, we previously proposed that regulating a late assembly process would allow RbgA to act as a checkpoint governing the release of active 50S subunits into the translation active pool of ribosomes in the cell. Previous work with BipA has also shown that pppGpp can regulate GTPase association with ribosomal subunits [33]. It is intriguing that alarmone pppGpp enhances association of RbgA with both 45S and 50S subunits, given the fact that RbgA likely binds to the subunit interface and would block association with the 30S subunit. Under times of translational stress pppGpp could block the additional maturation of 45S intermediates and prevent newly formed 50S subunits from participating in translation.

Ribosome	k_{cat} (h^{-1})	K_m (μM)	k_{cat}/K_m(M^{-1} s^{-1})
none	14 ± 2	90 ± 13	43
50S free	755 ± 207	32 ± 6	6533
50S mature	807 ± 158	62 ± 16	3616
45S intermediate	69 ± 16	4 ± 3	4791

Table 2.1 Kinetic parameters of RbgA in the presence and absence of ribosomal subunits.

The intrinsic activity of RbgA was assayed by incubation of 2 μM of RbgA with various concentrations of GTP for 30 min at 37°C. Stimulation of RbgA GTPase activity by ribosomes was assessed by determining the GTP hydrolysis rates of RbgA in the presence of various purified ribosomal particles. 100 nM of purified ribosome was incubated with 100 nM RbgA for 15 min at 37°C in the presence of various concentrations of GTP and assayed as described in the Materials and Methods section. Standard deviations of the mean of three biological replicates are presented.

RbgA Proteins	k_{cat} (h^{-1})	K_m (μM)	k_{cat}/K_m (M^{-1} s^{-1})
Wild Type	15 ± 0.4	72 ± 5	58
F180A	18 ± 0.8	65 ± 9	77
P129R	8 ± 0.8	290 ± 58	8
K59A	10 ± 1	286 ± 60	10
S134A	7 ± 0.6	146 ± 32	13

Table 2.2 Intrinsic GTPase activity of RbgA mutants.

The intrinsic activity of RbgA was assayed by incubating 2 μM of RbgA with various concentrations of GTP for 30 min at 37°C. P-loop mutants (P129R and S134A), linker region mutant (F180A) and G4 region mutant K59A were purified and assayed in a similar manner to RbgA wild type. Released free phosphate was determined by Malachite green assay. The experiments were done at least three times and the values of k_{cat} and K_m were determined by fitting the Michaelis-Menten equation using nonlinear regression algorithms provided by the GraphPad Prism software (GraphPad Software, Inc.). Standard deviations of the mean of at least three biological replicates are shown. As expected, the P-loop and G4 mutations increase the K_m and lower the k_{cat}. The linker region mutation (F180A) has no remarkable effect on the GTPase activity of RbgA.

	Intrinsic GTPase activity	Stimulation of GTPase activity in the presence of the 50S subunit
	V = pmol phosphate/pmol RbgA/ min	
RbgA 250 mM KCl	0.26 ± 0.02	13.8 ± 0.85
RbgA 250 mM NaCl	< 0.003	0.78 ± 0.1

Table 2.3 GTPase activity of RbgA in the presence of Na^+ and K^+ ions.

The intrinsic activity of RbgA was assayed by incubation of 2 μM of RbgA with 200μM GTP for 15 min at 37°C in the presence of 250 mM NaCl or 250 mM KCl. Stimulation of GTPase activity by the ribosome was tested by incubation of 100 nM of free 50S subunits with 100 nM RbgA and 200 μM GTP for 15 min at 37°C in the presence of 250 mM NaCl or 250 mM KCl. The activity was determined by standard malachite green assay as described in the materials and methods. Data for three biological replicates with standard deviation of the mean presented.

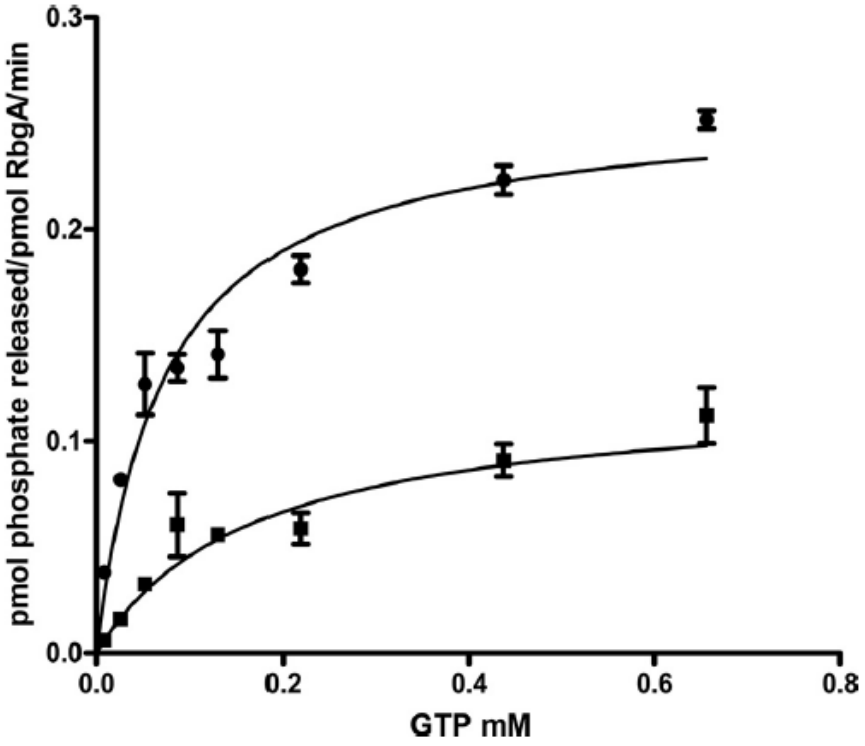

Figure 2.1 Kinetic analysis of GTP hydrolysis rates by RbgA proteins.

GTP hydrolysis rates of RbgA proteins were determined by monitoring release of free phosphate using malachite green/ammonium molybdate colorimetric assay as described in materials and methods. Reactions were carried out under initial rate conditions (less than 10% of substrate consumed). Values of k_{cat} and K_m were determined by fitting the Michaelis-Menten equation using nonlinear regression algorithms provided by the GraphPad Prism software (GraphPad Software, Inc.). Representative GTP hydrolysis curves of RbgA wild type (●) and the P-loop variant S134A (■) are shown. Error bars represent standard deviation of the mean of three technical replicates.

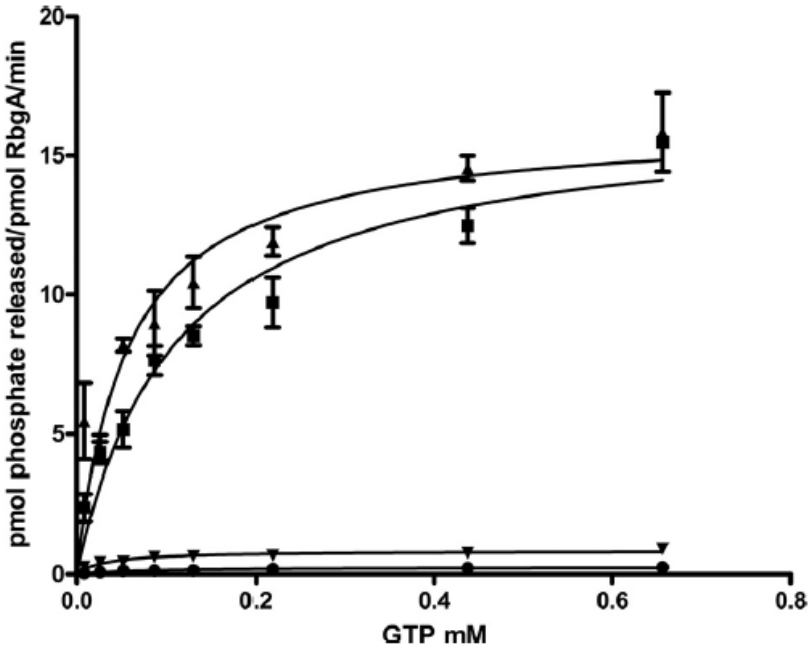

Figure 2.2 Stimulation of GTPase activity of RbgA by ribosomal particles.

Stimulation of RbgA GTPase activity by ribosomes was assessed by determining the GTP hydrolysis rates of RbgA in the presence of various purified ribosomal particles. 100 nM of purified ribosome was incubated with 100 nM RbgA for 15 min at 37°C in the presence of various concentrations of GTP and assayed as described in the Materials and Methods section. The representative curves are of GTP hydrolysis rates determined based on the free phosphate produced after the reactions had proceeded for 15 min at 37°C by reaction mixtures containing RbgA only (●), RbgA and mature 50S (■), RbgA and free 50S (▲), or RbgA and 45S (▼)**.** Error bars represent standard deviation of the mean of three technical replicates.

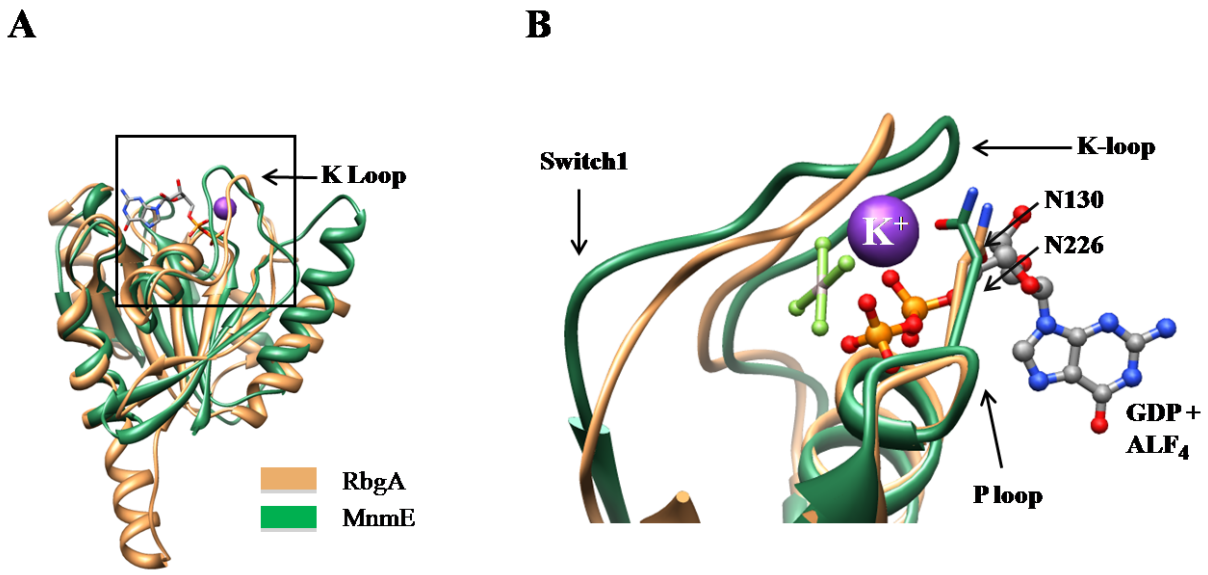

Figure 2.3 Superimposition of MnmE and homology model of RbgA.

A. MnmE and RbgA homology model was superimposed using ligalign script in PyMOL which align the two structures based on their ligand positions, which is GDP in this case. The K-loop of MnmE (green) and RbgA (brown) occupies similar position (as shown in rectangle) around the bound potassium in crystal structure. B. An enlarged view of catalytic pocket with GDP and bound potassium is shown in which N130 from P loop of RbgA (brown) coordinates bound K^+ ion (indicated by purple ball) in similar fashion as N226 from MnmE (green) P loop (indicated by arrows).

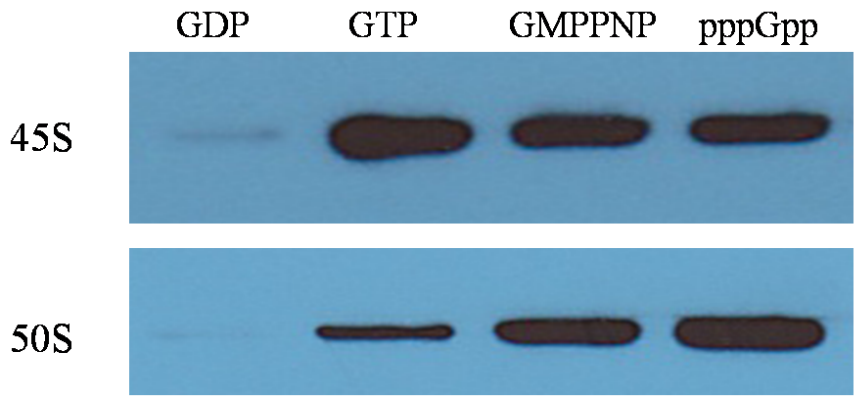

Figure 2.4 Interaction between RbgA and ribosome in the presence of different guanine nucleotides.

Binding of RbgA to purified ribosomal subunits was tested by an *in vitro* binding assay in which 60 pmoles of RbgA was pre-incubated with 1.5 mM GDP, GTP, GMPPNP or pppGpp before the addition of 10 pmoles of purified 45S or 50S ribosomal subunits. The mixtures were incubated further for 15 min at 37°C then free RbgA was filtered off by centrifugation through a 100 kDa cut-off Microcon columns. The columns were washed three times; first with buffer A and then twice with buffer C (high salt buffer). RbgA-ribosome complexes were eluted and bound RbgA was detected by immunoblotting using anti-RbgA antibody.

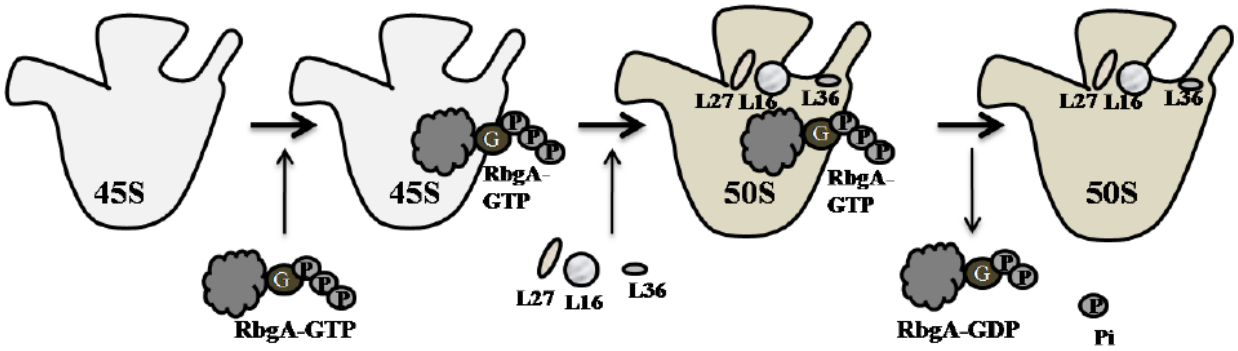

Figure 2.5 Proposed model for role of RbgA in 50S subunit maturation.

RbgA interacts with 45S in GTP bound form and introduces conformational changes that further facilitate the binding of late ribosomal proteins like L16, L27 and L36 (depicted by different ovals). Binding of these proteins promotes maturation of intermediate 45S subunit (white) to a mature 50S subunit (gray). Along with the complete maturation of 50S subunit, GTP at RbgA is hydrolyzed to GDP and this GDP bound RbgA and inorganic phosphate leave the mature 50S subunit, which is now ready to take part in translation. It is also possible that RbgA completes maturation of a late step that does not end in the final maturation of the 50S subunit.

ACKNOWLEDGEMENTS

We thank Marci Baranski and Loren Palmeri for technical assistance and Jade Wang (Baylor College of Medicine) for providing pppGpp.

REFERENCES

REFERENCES

1. Nierhaus, K.H. (1991) The assembly of prokaryotic ribosomes. *Biochimie* 73: 739-55.

2. Nomura, M., Erdmann, V.A. (1970) Reconstitution of 50S ribosomal subunits from dissociated molecular components. *Nature* 228: 744-8.

3. Dez, C., Tollervey, D. (2004) Ribosome synthesis meets the cell cycle. *Curr Opin Microbiol* 7: 631-7.

4. Culver, G.M. (2003) Assembly of the 30S ribosomal subunit. *Biopolymers* 68: 234-49.

5. Wilson, D.N., Nierhaus, K.H. (2007) The weird and wonderful world of bacterial ribosome regulation. *Crit Rev Biochem Mol Biol* 42: 187-219.

6. Britton, R.A. (2009) Role of GTPases in bacterial ribosome assembly. *Annu Rev Microbiol* 63: 155-76.

7. Gollop, N., March, P.E. (1991) A GTP-binding protein (Era) has an essential role in growth rate and cell cycle control in *Escherichia coli*. *J Bacteriol* 173: 2265-70.

8. Matsuo, Y.*, et al.* (2006) The GTP-binding protein YlqF participates in the late step of 50 S ribosomal subunit assembly in Bacillus subtilis. *J Biol Chem* 281: 8110-7.

9. Schaefer, L.*, et al.* (2006) Multiple GTPases participate in the assembly of the large ribosomal subunit in Bacillus subtilis. *J Bacteriol*.

10. Uicker, W.C., Schaefer, L., Britton, R.A. (2006) The essential GTPase RbgA (YlqF) is required for 50S ribosome assembly in Bacillus subtilis. *Mol Microbiol* 59: 528-40.

11. Uicker, W.C., Schaefer, L., Koenigsknecht, M., Britton, R.A. (2007) The essential GTPase YqeH is required for proper ribosome assembly in Bacillus subtilis. *J Bacteriol* 189: 2926-9.

12. Jiang, M.*, et al.* (2006) The Escherichia coli GTPase CgtAE is involved in late steps of large ribosome assembly. *J Bacteriol* 188: 6757-70.

13. Campbell, T.L., Daigle, D.M., Brown, E.D. (2005) Characterization of the Bacillus subtilis GTPase YloQ and its role in ribosome function. *Biochem J* 389: 843-52.

14. Bassler, J.*, et al.* (2001) Identification of a 60S preribosomal particle that is closely linked to nuclear export. *Mol Cell* 8: 517-29.

15. Jensen, B.C., Wang, Q., Kifer, C.T., Parsons, M. (2003) The NOG1 GTP-binding protein is required for biogenesis of the 60S ribosomal subunit. *J Biol Chem* 278: 32204-11.

16. Kallstrom, G., Hedges, J., Johnson, A. (2003) The Putative GTPases Nog1p and Lsg1p Are Required for 60S Ribosomal Subunit Biogenesis and Are Localized to the Nucleus and Cytoplasm, Respectively. *Mol Cell Biol* 23: 4344-55.

17. Saveanu, C.*, et al.* (2001) Nog2p, a putative GTPase associated with pre-60S subunits and required for late 60S maturation steps. *Embo J* 20: 6475-84.

18. Matsuo Y, O.T., Loh Pc, Morimoto T, Ogasawara N (2007) Isolation and characterization of a dominant negative mutant of Bacillus subtilis GTP-binding protein, YlqF, essential for biogenesis and maintenance of the 50 S ribosomal subunit. *J Biol Chem* 282: 25270-7.

19. Charollais, J., Pflieger, D., Vinh, J., Dreyfus, M., Iost, I. (2003) The DEAD-box RNA helicase SrmB is involved in the assembly of 50S ribosomal subunits in Escherichia coli. *Mol Microbiol* 48: 1253-65.

20. Lin, B., Thayer, D.A., Maddock, J.R. (2004) The Caulobacter crescentus CgtAC protein cosediments with the free 50S ribosomal subunit. *J Bacteriol* 186: 481-9.

21. Lanzetta, P.A., Alvarez, L.J., Reinach, P.S., Candia, O.A. (1979) An improved assay for nanomole amounts of inorganic phosphate. *Anal Biochem* 100: 95-7.

22. Sali, A., Potterton, L., Yuan, F., Van Vlijmen, H., Karplus, M. (1995) Evaluation of comparative protein modeling by MODELLER. *Proteins* 23: 318-26.

23. Heifets, A., Lilien, R.H. LigAlign: flexible ligand-based active site alignment and analysis. *J Mol Graph Model* 29: 93-101.

24. Schrödinger, L. (Version 1.2r3pre) The PyMOL 1.2r3pre ed. pp. Molecular Graphics System.

25. Pettersen, E.F.*, et al.* (2004) UCSF Chimera--a visualization system for exploratory research and analysis. *J Comput Chem* 25: 1605-12.

26. Anand, B., Surana, P., Prakash, B. Deciphering the catalytic machinery in 30S ribosome assembly GTPase YqeH. *PLoS One* 5: e9944.

27. Ash, M.R., Maher, M.J., Guss, J.M., Jormakka, M. The initiation of GTP hydrolysis by the G-domain of FeoB: insights from a transition-state complex structure. *PLoS One* 6: e23355.

28. Scrima, A., Wittinghofer, A. (2006) Dimerisation-dependent GTPase reaction of MnmE: how potassium acts as GTPase-activating element. *EMBO J* 25: 2940-51.

29. Scheffzek, K.*, et al.* (1997) The Ras-RasGAP complex: structural basis for GTPase activation and its loss in oncogenic Ras mutants. *Science* 277: 333-8.

30. Neidhardt, F.C., Ingraham, J.L., Schaechter, M. (1990) Physiology of the Bacterial Cell: A Molecular Approach: Sinauer Associates.

31. Lopez, J.M., Marks, C.L., Freese, E. (1979) The decrease of guanine nucleotides initiates sporulation of Bacillus subtilis. *Biochim Biophys Acta* 587: 238-52.

32. Schmeing, T.M.*, et al.* (2009) The crystal structure of the ribosome bound to EF-Tu and aminoacyl-tRNA. *Science* 326: 688-94.

33. Delivron, M.A., Robinson, V.L. (2008) Salmonella enterica serovar Typhimurium BipA exhibits two distinct ribosome binding modes. *J Bacteriol* 190: 5944-52.

CHAPTER 3

Mutational analysis of the ribosome assembly GTPase RbgA provides insight into ribosome interaction and ribosome-stimulated GTPase activation

The contents of this chapter were published in Gulati M., Jain N., Anand B., Prakash B and Britton R.A. (2013) Mutational analysis of the ribosome assembly GTPase RbgA provides insight into ribosome interaction and ribosome-stimulated GTPase activation. Nucleic Acids Res. 41(5):3217-27. MG and NJ collaborated on Figures 3.7 and 3.8 and Table 3.2

Abstract

Ribosome biogenesis GTPase A protein (RbgA) is an essential GTPase required for the biogenesis of the 50S subunit in *Bacillus subtilis.* Homologs of RbgA are widely distributed in bacteria and eukaryotes and are implicated in ribosome assembly in the mitochondria, chloroplast and cytoplasm. Previous work has shown that cells depleted of RbgA accumulate an immature large subunit that is missing key ribosomal proteins. RbgA, unlike many members of the Ras-superfamily of GTPases, lacks a defined catalytic residue for carrying out GTP hydrolysis. To probe RbgA function in ribosome assembly we used a combined bioinformatics, genetic and biochemical approach. We identified a RNA binding domain, ANTAR which are known to bind structured RNA within the C-terminus of RbgA. Mutation of key residues in the ANTAR domain altered RbgA association with the ribosome. We identified putative catalytic residue His9 part of three amino acid motif PGH, which is similar to a domain within EF-Tu that is directly involved in GTP hydrolysis upon interaction with the ribosome. Finally, our results support a model in which the GTPase activity of RbgA directly participates in the maturation of the large subunit rather than solely promoting dissociation of RbgA from the 50S subunit.

Introduction

Ribosomes are complex molecular machines that, in bacteria, contain three RNA molecules and over 50 proteins [1-4]. The accurate and timely assembly of ribosomes is critical for organisms to achieve the fast growth rates observed [4]. Though active ribosomes can be generated *in vitro* without the need for additional assembly factors, non-physiological temperatures and salt conditions are required [1,2,5]. In light of this observation Nomura and co-workers suggested that ribosome assembly factors would be required *in vivo* at key steps that required these non-physiological conditions *in vitro*. However, these assembly factors have remained elusive in bacteria [4,6]. Over the past decade studies have shown that several GTPases likely play a critical role in ribosome assembly (RA-GTPases) in both bacteria and eukaryotes [6-8]. However the precise molecular function carried out by RA-GTPases during *in vivo* ribosome assembly remains unknown.

RbgA (ribosome biogenesis GTPase A) is an essential, widely conserved GTPase that is required for the assembly of the 50S subunit in *Bacillus subtilis [9-12]*. RbgA homologs are widely distributed evolutionarily and eukaryotic homologs of RbgA such as Mtg1 (mitochondria), Lsg1, Nug1, and Nog2 have been implicated in ribosome assembly [13-16]. RbgA proteins have several unique features that distinguish them from conventional Ras like GTPases. First, RbgA belongs to a family of circularly permuted GTPases (cpGTPases) in which the order of the highly conserved G motifs (G1-G4) is altered such that the G4 motif precedes the G1 motif in the sequence of the protein [17]. Although the reason for this circular permutation of the G domain is unclear, in almost every case cpGTPases contain a second protein domain directly downstream of the Switch II (G3) region. This would allow guanine nucleotide dependent movement of this second protein domain, which is likely involved in binding to RNA or

interacting with ribonucleoprotein structures [17]. Secondly, RbgA and its homologs are also classified as hydrophobic amino acid substituted GTPases (HAS-GTPases) [18]. HAS-GTPases are involved in a wide variety of cellular functions such as ribosome biogenesis, tRNA modification and cell cycle regulation [18]. In this family of GTPases the catalytic glutamine that is usually present in Ras-like GTPases is replaced by a hydrophobic amino acid. Several prokaryotic GTPases such as FeoB, MnmE, YphC YqeH, Obg and Era fall into this family [19-25]. These GTPases utilize alternative mechanisms for GTP hydrolysis that have been deduced with the help of crystal structures in two cases, MnmE and FeoB, but not for RbgA [26,27].

Cells depleted of RbgA do not form mature 50S subunits but rather accumulate a novel 45S complex lacking three ribosomal proteins – L16, L27 and L36 [9,11]. In yeast, the RbgA homolog Lsg1 is proposed to participate in the association of Rpl10p (L16 homolog) with the 60S subunit at a late stage during large subunit biogenesis [14]. Incorporation of L16 is also predicted to occur at a late stage of 50S assembly and is accompanied by a large conformational change *in vitro* [28], suggesting that RbgA proteins regulate an evolutionarily conserved step in ribosome assembly. The GTPase activity of RbgA is stimulated ~60-fold by 50S subunits and physical association with 50S subunits is maximal in the presence of a non-hydrolyzable analog of GTP [12], indicating that GTP hydrolysis is responsible for dissociating RbgA from the ribosome. Interaction with the 45S yields only a mild increase in GTPase activity and the association of RbgA with 45S subunits is equal in the presence of GTP or a non-hydrolyzable analog of GTP [12]. These and other observations have led to a model in which RbgA functions by interacting with the large ribosomal subunit prior to the incorporation of L16 and either directly recruits L16 to the ribosome complex or indirectly facilitates L16 binding by remodeling

the ribosome [12]. The molecular basis of RbgA mediated ribosome assembly, in particular the role of specific amino acid residues, is poorly understood.

To elucidate how RbgA participates in ribosome assembly we utilized a site-directed mutagenesis approach combined with *in vivo* and biochemical characterization of RbgA mutants. We have discovered a RNA binding motif that mediates, in part, RbgA interaction with the 50S subunit. We also identified a potential catalytic residue that mediates GTP hydrolysis. We discuss our findings in relation to other ribosome associated GTPases and suggest that future studies of RbgA in bacteria will also provide additional insight into mitochondrial and eukaryotic ribosome assembly.

Materials and Methods

Growth conditions

All strains were grown at 37°C in LB (lysogeny broth) medium. Antibiotics were added at the following concentrations when required: chloramphenicol (5 μg/ml), kanamycin (25 μg/ml), spectinomycin (100 μg/ml) and ampicillin (100 μg/ml). In addition IPTG was added at a concentration of 1 mM unless mentioned otherwise and xylose was added at a concentration of 2% when needed.

Construction of strains

All strains used in this study were derived from wild type *Bacillus subtilis* strain JH642 (RB247). Strain RB301 was constructed as described [9]. Strain RB562 was constructed by switching the antibiotic resistance cassette linked to P_{spank} and *rbgA* in RB301 from chloramphenicol to spectinomycin. RB611 was constructed by transforming RB562 with plasmid pMAP65 [29] that

overexpresses *lacI* repressor to control the expression of wild type *rbgA* gene under the control of P_{spank} promoter. Strain RB613 was constructed by cloning wild type *rbgA* into the pSWEET plasmid [30] with a chloramphenicol resistance cassette and *rbgA* under the control of the P_{xylA} promoter. This construct was linearized and inserted at the *amyE* locus in RB611, creating strain RB613. Chloramphenicol-resistant colonies were confirmed to have lost the ability to degrade starch, indicating disruption of the *amyE* gene. The desired mutations were introduced into the pSWEET plasmid using the QuikChange II XL kit (Stratagene) by following the manufacturers instructions. The resultant plasmids with mutated *rbgA* gene were linearized and transformed in RB611 strain. Resultant strains are dependent on IPTG for growth and are listed in Table 3.1. *Escherichia coli* BL21(DE3) cells transformed with plasmid pET21b containing full-length *rbgA* placed under the control of the T7 promoter were used to overexpress RbgA proteins [9]. Desired mutations were constructed using the QuikChange II XL kit (Stratagene) by following the manufacturers instructions.

Characterization of association between RbgA or mutants and 45S or 50S complexes

Wild type and mutant proteins were purified as described [12]. 50S subunits and 45S intermediates were prepared by sucrose density gradient [12]. 50S and 45S complexes were isolated from lysates of RB418 and RB301 cells respectively. The cells were grown were grown to OD_{600} of 0.5 at 37°C in LB medium with or without IPTG. RB301 and RB418 cells were grown without IPTG for several generations to deplete the cells of RbgA and IF-2, respectively, until a doubling time of about 150 min was reached. Chloramphenicol (Sigma) was added to a final concentration of 100 μg/ml 5 minutes prior to harvesting. 50S subunits and 45S complex

were isolated as described [12]. The association assay was performed with varying levels of RbgA protein to 45S or 50S to determine the linear range of the assay. At each ratio the nucleotide concentration was 400 μM, which is well above the K_m of RbgA to ensure maximal RbgA protein was bound to the nucleotide. All assays reported here were performed at 37°C with 50 nM RbgA or mutant protein, 10 nM 45S or 50S and 400 μM nucleotide (GDP, GTP or GMPPNP). The binding protocol was used as described [12]. Briefly, 60 pmol of RbgA was pre-incubated with 1.5 mM of different guanine nucleotides for 15 min followed by addition of 10 pmol purified subunits. The binding was allowed to proceed for 15 min at 37°C, then centrifuged once through Microcon 100 filters (Millipore) with a cut-off of 100 kDa. The RbgA-subunit complexes were washed once with buffer A, twice with buffer C before elution. Four controls were performed for every assay - 45S/50S with no RbgA/mutant protein and RbgA/mutant protein with each of the three nucleotides but no subunit. This was to ensure that no RbgA was bound to the subunit while preparation of subunits and RbgA/mutant protein was not retained on the filter in the absence of subunit respectively. The subunit bound RbgA was detected by separating the complex on SDS-PAGE gels (12% Bis-Tris NuPAGE gel, Invitrogen) followed by western blot analysis using polyclonal rabbit anti-RbgA and HRP-conjugated goat anti-rabbit polyclonal antibodies (PerkinElmer Life Sciences). The bands were visualized using Western Lightening chemiluminescent detection system (PerkinElmer Life Sciences). A series of incremental exposures was obtained to determine that chemiluminescent signal was in the linear range of detection. A single time point from the linear range was chosen and mutant and wild type protein, present on the same blot membrane was quantified using FujiFilm Multi Gauge v3.0 software. The binding level of RbgA/mutant protein was determined and the data is reported

as a percentage of wild-type RbgA association with either the 45S or the 50S subunit in the presence of GMPPNP, which displays maximal binding.

Characterization of GTPase activity of RbgA/mutants

The assay was performed as described [12]. Briefly for measuring GTPase activity in the presence of 50S subunits 100 nM RbgA/mutant protein was incubated with 100 nM 50S subunit and 200 μM GTP at 37°C for 30 minutes and for measuring intrinsic GTPase activity 2 μM RbgA/mutant protein was incubated with 200 μM GTP at 37°C for 30 minutes. We predetermined that under these conditions the values were in the linear range of the assay. The phosphate released was measured by malachite green colorimetric system (BioAssay systems). The mutant proteins were assayed on the same 96 well plate (Corning) as the wild type protein.

Bioinformatics analysis and superimposition

Coordinates from the C-terminus of RbgA were used to search for similar structures using the DALI server (http://ekhidna.biocenter.helsinki.fi/dali_server/) [31] and resulting structures were superimposed using PyMol [32]. Superimposition of free EF-Tu (PDB: 1EFT) and ribosome bound EF-Tu (PDB: 3FIC) were superimposed on RbgA (PDB:1PUJ) using ligalign script [33] in PyMol. All the figures were made in Chimera [34].

Results

Multiple sequence alignment of RbgA homologs revealed 4 regions of high conservation

RbgA contains two structural domains, an N-terminal circularly permuted G-domain and a C-terminal domain that contains no sequence similarity to any known functional protein domain.

To identify key residues within conserved regions in RbgA we generated a multiple sequence alignment of bacterial RbgA homologs using CLUSTAL-W (Figure 3.1A). In addition to the universally conserved G-domain motifs G1-G4 we identified four regions of high conservation designated CR1-CR4 (Figure 3.1A). Although these conserved regions are dispersed throughout the protein sequence, they lie in close vicinity in the crystal structure of the protein (Figure 3.1C). The first two regions, CR1 and CR2 are contained in the N-terminal domain of RbgA and precede the circularly permuted G-domain. Of these two CR1 was of particular interest as this stretch of 15 amino acids found at the N-terminus of RbgA is largely conserved among all bacterial RbgA homologs as well as eukaryotic Mtg1 proteins (Figure 3.1B). Most of CR1 is unstructured in all available RbgA crystal structures deposited to date, indicating its dynamic nature and thus its role in RbgA function cannot be assessed by its structure. CR3 is a highly conserved loop that links the N-terminal domain to the C-terminal domain and contains the Switch II motif. Thus it is likely to participate in communication between the N and C terminal domains when bound to either GTP or GDP. The C-terminal domain following the CR3 showed low sequence similarity and only one moderately conserved region (CR4) was identified in this domain.

The C-terminal domain of RbgA contains an ANTAR RNA binding domain

Because the C-terminal domain of RbgA contained low sequence similarity to proteins of known function in the NCBI database (other than RbgA homologs) we asked if the C-terminal domain is structurally similar to any previously characterized domains. To identify proteins that contain a structurally similar domain, we used the structure of only the C-terminal domain (177-269 residues) of RbgA as a query to search the DALI database [31]. The first 4 hits (Table 3.2) were

from crystal structures of either RbgA or its homologs as expected (DALI Z-score= 7.3-14.8, rmsd=0-2.8 Å). The DALI score provides a measure of structural similarity between a given pair of protein domains and structures that have significant similarities have a Z-score greater than 2. The first non-RbgA hit was the C-terminal domain of a NasR, a protein that mediates transcription anti-termination (Z =4.1, rmsd=3.6 Å) [35]. The next few hits were with incomplete domains of exodeoxyribonuclease and Cdc4, followed by other potential transcription anti-terminators including AmiR [36]. These results showed that the C-terminal domain of RbgA had significant structural similarity to the C-terminal domains of two proteins that are involved with promoting transcription antitermination, AmiR and NasR (Table 3.2). This C-terminal domain present in both AmiR and NasR interacts with structured RNA and encompasses a RNA binding domain denoted the ANTAR (AmiR-NasR Transcription Anti-termination Regulators) domain [37]. The ANTAR domain, characterized by a three-helix structure, is structurally similar to the C-terminal domain of RbgA (Figure 3.2) [37]. Superimposition of the RbgA C-terminal structure on the C-terminal regions of NasR and AmiR shows a topologically similar three-helix arrangement, typical of ANTAR domains (rmsd=3.6 and 3.4 Å respectively) (Figure 3.2). It is noteworthy that the structural similarity notwithstanding, the sequence similarity of these proteins with the RbgA C-terminal domain is remarkably low (13% for NasR and15% for AmiR).

Site-directed mutagenesis and phenotypic analysis of RbgA mutants

Since *rbgA* is an essential gene, null mutations will not survive and cannot be studied. Therefore, we developed a strain that allowed mutations that negatively affect RbgA function to be generated and characterized. A conditional *rbgA* mutant strain was created by placing a wild-

type copy of the *rbgA* at its native locus under the control of the P_{spank} promoter, yielding a strain that is dependent on IPTG for growth. Mutant versions of a second copy of the *rbgA* gene were placed under the control of the P_{xyl} promoter and introduced at the *amyE* locus. The expression of the mutant *rbgA* gene is therefore dependent on the presence of xylose in the growth media. In order to study mutations in *rbgA* we constructed strains in the presence of IPTG and then interrogated their phenotype by growing cells in the presence of xylose and absence of IPTG. As a control we created a strain (RB613) that contains a wild-type copy of the *rbgA* gene under the control of the P_{xyl} promoter at the *amyE* locus. As expected, RB613 grows equally well in the presence of 1 mM IPTG or 2% xylose (data not shown).

Using this system we screened 44 mutations in *rbgA* to assess their growth phenotypes by streaking each mutant *rbgA* strain on plates containing either 1 mM IPTG or 2% xylose. A representative result is shown in Figure 3.3. Previous work on GTPases has shown that mutating the S/T residue in the P-loop (motif G1 -GXXXXGKS/T) abolishes GTP hydrolysis [38]. We constructed the corresponding RbgA mutant strain (S134A) and found that this mutation was lethal and no colonies were observed on plates containing 2% xylose, in contrast to the control strain RB613 (Figure 3.3C). Both strains displayed wild-type growth when streaked on plates containing 1 mM IPTG (Figure 3.3B) while no growth was observed in the absence of either inducer (Figure 3.3D). Using this system we identified 17 mutations that negatively affected cell growth (Figure 3.4). We further quantified the effect of each mutation by measuring growth rates in liquid media. Mutations that reduced the growth rate 3 fold or less compared with wild type growth were classified as causing a mild growth effect while mutations that reduced cell growth more than 3 fold were classified as severely affecting cell growth. We found that 12 mutations

cause a severe growth defect while 5 mutations have a milder effect on cell growth (Table 3.3 and Figure 3.5). To verify that defective RbgA proteins that did not support growth were able to accumulate inside the cell, we confirmed that the expression of all mutant RbgA proteins was similar to wild-type expression levels with the exception of one case (D228A/E229A) (data not shown). Mutations that alter the CR1, CR3 and ANTAR residues and that caused a severe growth defect were characterized further and are discussed below.

In constructing our strains we did not find any indication of a strong dominant negative effect of any mutation in RbgA. Previously it was reported that a deletion of the first 10 amino acids of RbgA (referred to as ΔN10) resulted in a dominant negative phenotype [39]. We tested all of our mutants and theΔN10 RbgA mutant for dominant negative effects using 1 mM IPTG and 2% xylose. Under these conditions none of the mutations tested displayed any phenotype, including ΔN10, as all cells grew at a wild-type growth rate. Reduction of IPTG levels to 100 μM, which reduces expression of the wild-type copy of *rbgA,* still allows cells to proliferate at wild-type growth levels. Growing cells with 100μM IPTG and 2% xylose uncovered the dominant negative phenotype of theΔN10 mutant. Under these conditions we identified three additional mutations in our collection that also had dominant negative effects, F6A and H9A in CR1 and Y225A in the ANTAR domain (Table 3.4). We note that when cells are grown under 100 μM IPTG and 2% xylose the protein expression level of mutant copy of RbgA is at least 10-fold higher than the wild-type copy, indicating that these RbgA mutations have a weak dominant negative phenotype.

Biochemical characterization of RbgA mutants

In order to fully characterize the effects of mutations that were found to be severely deleterious to growth we A) monitored the ability of RbgA mutants to associate with both 50S subunits and 45S complexes and B) assessed their ability to catalyze GTP hydrolysis in the presence and absence of 50S subunits. The results of these two experiments are discussed in the following two sections. Seven mutants were selected for these studies based on their location in the protein and their phenotype of severely reduced growth rates relative to wild-type RbgA. Three are from CR1 (F6A, H9A, K12E/R14E), one from CR3 (F180A), and three (A206D, Y225A, I241D) from the ANTAR domain. These RbgA mutants were purified as C-terminal His-tag fusions; previous work has shown that wild-type RbgA with a C-terminal His-tag is fully functional [9].

Mutations in the ANTAR domain alter RbgA:ribosome association

We have previously shown that RbgA stably binds to the 45S complex and 50S subunit in a nucleotide-dependent manner [12]. RbgA binds to the 50S subunit in the presence of a non-hydrolyzable GTP analog, GMPPNP, and binding in the presence of GTP is reduced, likely due to GTP hydrolysis upon interaction with the 50S subunit [12]. In contrast, both GTP and GMP-PNP enhance binding of RbgA to the 45S complex equally [12]. We hypothesized that the ANTAR domain of RbgA is essential for association with the ribosome and targeted five key structural residues in the ANTAR domain for mutation as described below.

The ANTAR domain comprises three alpha-helices and is stabilized by coiled-coil interactions (Figure 3.2). ANTAR domains display low sequence conservation amongst homologs and contain only five strictly conserved residues which have their side-chains exposed into the cavity formed between the three helices and hence stabilize the structural fold [37]. RbgA contains four

of these conserved residues at the corresponding position in the domain: A206, A235, F238 and I241. Our results show that substitutions in two of these residues (A206D and I241D) caused a severe growth defect, while substitutions in A235 or F238 had no effect on growth (Figure 3.4 and Table 3.3). We also generated a fifth mutant, Y225A, which likely disrupts non-covalent interactions between the helices and may alter the structure of the domain. Y225A caused a severe growth defect and displayed a weak dominant negative phenotype (Figure 3.4 and Table 3.4). We proceeded to test association of mutated RbgA proteins with the 45S intermediate and the 50S subunit under different nucleotide conditions using a quantitative *in vitro* binding assay. Purified RbgA proteins were incubated with either purified 50S subunits or 45S intermediates for 15 minutes at 37°C. These complexes were then centrifuged through a 100 kDa Millipore filter to remove unbound RbgA from the sample. The remaining RbgA that is associated with the ribosomal subunit was then analyzed and quantified by Western blot analysis. A representative example of the results is depicted in Figure 3.6. Wild-type RbgA binds most efficiently to the 50S subunit in the presence of GMPPNP, with a ~5-fold reduction in association in the presence of GTP and ~30-fold reduction in the presence of GDP. A206D, a strictly conserved residue in the ANTAR domain renders RbgA unable to associate with the 50S subunit (Figure 3.6) or 45S intermediate (Table 3.5) under any nucleotide condition. Since A206D retains some GTPase activity (see below), we do not expect that the lack of binding observed is solely due to complete loss of the tertiary structure of the entire protein.

The binding of each RbgA mutant protein was determined in a similar manner and the results are reported as a percentage of wild-type RbgA association with either the 45S or the 50S subunit in the presence of GMPPNP, which displays maximal binding. Notably, of the eight mutant proteins tested, the most striking results were seen with substitutions in the ANTAR domain that

changed the binding of RbgA to the 50S or 45S subunits. Mutations in CR1 were only altered in GTP bound form, a result of the altered GTPase activity of these mutants which will be discussed in the next section and mutation in CR3 displayed near wild-type levels of binding and retained the same nucleotide dependence as wild-type RbgA. In contrast, all three mutants targeting the ANTAR domain displayed altered binding and surprisingly had different phenotypes. A206D completely lost all ability to stably associate with the ribosomal subunits, while I241D displayed reduced association (~10 fold) with the 50S or 45S subunits in the presence of GTP. The most surprising result was observed with the Y225A mutant RbgA protein. This RbgA derivative was greatly reduced in its association with the subunits in the presence of GMPPNP, displaying binding levels comparable to those observed with GDP (Figure 3.6). However, Y225A associated with both the 50S and 45S subunits in the presence of GTP at higher levels than observed with the wild-type RbgA protein, indicating that this mutation may stabilize interaction in state of partial GTP hydrolysis (Figure 3.6). Thus all three ANTAR domain mutants display altered association with both the 45S and 50S subunits, highlighting the importance of this domain in association with the ribosomal subunit.

Mutations in CR1 severely reduce GTPase activity of RbgA

RbgA has a low intrinsic GTPase activity which is stimulated ~60 fold in the presence of mature 50S subunits [12]. We therefore assessed the ability of the 50S subunit to stimulate the GTPase activity of RbgA mutants. As a negative control we utilized a mutant protein containing the S134A substitution in the P-loop, which shows no detectable intrinsic GTPase activity and is inert to simulation in the presence of the 50S subunit. Our results show that mutations in CR1 and the ANTAR domain impact the GTPase activity of RbgA, while the mutation in CR3 had no

effect (Table 3.6). However, mutations in the ANTAR domain also disrupted interaction of RbgA with both the 45S as well as the 50S subunit and therefore the attenuated GTPase activity seen in A206D and I241D is likely due, in part, to an indirect effect of poor association with the 50S subunit (Table 3.5, and discussion above).

Mutations in CR1 had a strong impact on the GTPase activity of RbgA. Mutation F6A resulted in a ~11 fold reduction in intrinsic GTPase activity and was stimulated ~15 fold in the presence of the mature 50S subunit, demonstrating that this mutant is reduced but still capable of GTP hydrolysis. Mutation K12E/R14E had a moderate reduction in intrinsic GTPase activity but was stimulated only 2-fold in the presence of the 50S subunit. These results suggest that the flexible, highly conserved N-terminal region of RbgA encompassing CR1 is required for GTPase activation in the presence of the ribosomal subunit.

A recent crystal structure of EF-Tu in complex with the ribosome demonstrated that interaction between the ribosome and His84 of EF-Tu was required for efficient hydrolysis of GTP [40]. Voorhees *et al*. noted that His84 is preceded by a proline and glycine (denoted the PGH motif), which were proposed to be critical for the correct positioning of His84 upon interaction with nucleotide A2662 of the ribosome during activation. We observed that the CR1 region of RbgA also contains a PGH motif (amino acids 7-9) that is highly conserved in bacterial and eukaryotic RbgA homologs (Figures 3.1A and 3.1B). An alignment of crystal structures of RbgA and free EF-Tu indicate that His9 from PGH motif of RbgA is in a similar position as the catalytic His84 of EF-Tu (Figure 3.7 and Figure 3.8). To test the role of this histidine residue (His9) in the GTPase activity of RbgA, we generated a H9A mutant and characterized its GTPase activity in the absence and presence of the 50S subunit. Our results show that mutation H9A reduced intrinsic GTPase activity of RbgA by ~6 fold relative to the wild-type protein. Most significantly

this mutant displayed no detectable GTPase activity in the presence of the 50S subunit (Table 3.6). Together this result, in conjunction with the phenotype of F6A and K12E/R14E, shows that mutations in CR1 reduce GTPase activity of RbgA and that His9 is required for GTPase activity in the presence of the 50S subunit. The absence of GTPase activity in the mutant is unlikely to be due to reduced association with the 50S subunit as this mutant in particular and other CR1 mutants associated with the 50S subunit at similar levels compared to wild type RbgA (Table 3.5).

Linker region is required for RbgA function

All cpGTPases have a C-terminal domain linked to the G3 motif (Switch II) [17]. In RbgA a highly conserved loop (CR3) links the C-terminal ANTAR domain to the G3 motif (Switch II). We hypothesized that the CR3 could be crucial for communicating conformational changes during GTP hydrolysis between the G3 motif and the ANTAR domain. We identified one mutation in CR3, F180A that was lethal. We tested this mutation utilizing the *in vitro* binding assay described previously to determine if this residue was required for association of RbgA to the ribosomal subunits and found that this mutation did not alter association of RbgA to the 45S complex or the 50S subunit (Table 3.5). Next, we characterized the GTPase activity of this mutant and found that mutation F180A has a mild effect on GTPase activity of RbgA with and without the 50S subunit (Table 3.6). Thus, even though this mutation is defective neither in ribosome association nor in ribosome stimulated GTPase activity it is unable to support growth and yields ribosome assembly defects *in vivo*.

Strains expressing mutated RbgA proteins do not accumulate a novel intermediate

A previously proposed model suggested that GTP bound RbgA binds to the 45S intermediate and either directly or indirectly recruits the ribosomal protein L16 to the intermediate [12]. Stable integration of L16 and formation of a mature 50S subunit likely triggers GTP hydrolysis and dissociation of RbgA from the mature 50S subunit. We hypothesized that strains that show a growth defect phenotype due to the expression of a compromised RbgA protein may accumulate a trapped intermediate that differs from the 45S intermediate observed upon depletion of the wild type protein. We analyzed ribosome profiles of strains expressing RbgA mutants that negatively affected cell growth and isolated the 45S intermediate from each mutant (a representative set is shown in Figure 3.9). Our results show that strains expressing mutated RbgA proteins do not trap a new intermediate. These strains also accumulated the 45S intermediate similar to RbgA depleted cells and this intermediate also lacked the ribosomal protein L16 (Figure 3.10). Thus, no novel ribosomal intermediate could be detected for the RbgA mutants that were analyzed.

Discussion

Ribosome assembly GTPases (RA-GTPases) are critical for the efficient and accurate biogenesis of cellular, mitochondrial, and chloroplast ribosomes; however their roles in the assembly process are poorly understood [4,6,8]. RbgA, and its closest eukaryotic homolog Mtg1, are involved in the assembly of the large ribosomal subunit in bacteria and mitochondria, respectively [9,11,13]. RA-GTPases use a variety of RNA binding domains to interact with RNA including OB-folds (Obg) and KH-domains (Era) [24,41]. The crystal structure of RbgA showed that the C-terminal domain (201-269) is connected to the N-terminal G-domain (1-176) through a linker helix (177-200) (Figure 3.2). We have identified a novel RNA binding domain within

the C-terminus of RbgA, the ANTAR domain, which was discovered in proteins that bind structured mRNA leader regions and promote transcription antitermination [37]. ANTAR domain containing proteins such as NasR and EutV promote antitermination by interacting with mRNA and promoting the formation of stem-loop structures that preclude the formation of intrinsic transcription terminators [35,42,43]. It is attractive to speculate that RbgA may influence ribosome assembly by interacting with rRNA via its ANTAR domain and stabilizing the formation of a critical stem-loop in the 23S rRNA that does not form spontaneously and prevents the formation of other nonproductive loops that may hamper further assembly. It is possible that in *in vitro* experiments these nonproductive loops are circumvented by high temperature or high salt conditions thereby facilitating proper assembly. Efforts to identify the RbgA binding site on the ribosome are currently underway. Mutations in the ANTAR domain reduced association of RbgA to the 45S or 50S to varying degrees. Residue A206 is likely important for the structural stability of the ANTAR domain. This residue is one of four highly conserved alanine residues seen in most ANTAR structures [37]. In addition mutants such as Y225A could prove to be good candidates for structural and CryoEM studies as they show a unique binding profile compared to wild-type RbgA and could shed light on the interaction of RbgA with the 50S subunit.

Most ANTAR domain proteins are two domain proteins in which the ANTAR domain is precluded from interacting with RNA until a signal or ligand is sensed by the receiver domain, which opens up ANTAR for RNA binding [42,43]. One example of this arrangement is seen in the recently published NasR structure where the signal receiver domain (NIT) and the ANTAR domain are joined by a linker [35]. Thus, a similar arrangement in RbgA suggests that the guanine nucleotide dependent conformational change of the N-terminal G-domain could be

communicated to the ANTAR domain through the conserved linker region. In principle, the mechanistic reverse wherein binding of the ANTAR domain to rRNA could be coupled to a conformational change in the N-terminal G-domain that facilitates GTP hydrolysis could also occur. In both scenarios communication between the N- and C- terminal domains is important for RbgA function and would likely rely on the linker CR3. Our results indicate that mutation in this region is deleterious to growth though neither the association with subunit nor the GTPase activity of this mutant protein is affected suggesting that while the function of either domain is not lacking when tested independently the mutant protein cannot function *in vivo*.

The GTPase activity of RbgA is essential to its function and mutations in conserved G-domains that abolish GTP hydrolysis are lethal.. However due to the absence of a crystal structure of RbgA bound to 50S the exact mechanism of GTP hydrolysis remains elusive. Recent structural evidence demonstrating how EF-Tu carries out GTP hydrolysis upon interaction with the ribosome during accommodation has shown that positioning of His84 via interaction with 23S rRNA nucleotide A2662 is critical for GTP hydrolysis [40]. His84 is part of a PGH motif that is conserved in nearly all EF-Tu homologs identified to date and a similar PGH motif is found in bacterial and eukaryotic homologs of RbgA. A key difference between the conserved PGH motifs in EF-Tu and RbgA is the fact that whereas His84 is found in the Switch II (G3) region (His84 substitutes for the catalytic Gln normally found in Ras-superfamily GTPases), His9 in RbgA is found in the highly flexible CR1 region and is not ordered in the available crystal structures (1PUJ) [44]. In RbgA the Switch II region is instead linked to the C-terminal ANTAR domain. Mutation of His9 of RbgA resulted in a severely attenuated intrinsic rate of GTP hydrolysis and no stimulation of GTPase activity in the presence of the 50S subunit could be detected. Importantly this mutation had no significant effect on association with the 50S subunit.

Mutations in other parts of CR1 also greatly impacted GTP hydrolysis, however all other mutations showed at least some stimulation in the presence of the 50S subunit. Our data is consistent with a model in which the highly flexible CR1 region, upon interaction with the ribosome, adopts a conformation that suitably positions His9 for GTP hydrolysis.

This assertion is also supported by analysis of the EF-Tu crystal structure [40]. Vorhees et al. suggested that the EF-Tu GTP hydrolysis mechanism could be a general mechanism used by translation GTPases to carry out GTP hydrolysis. To this end we superimposed the G-domain of RbgA and EF-Tu (Figure 3.7 and Figure 3.8) by utilizing the GDPNP bound to each of these proteins in the crystal structure as a point of reference. In the superimposed structure, His9 from RbgA is in close proximity to His84 in the structure of free EF-Tu consistent with our assertion above (Figure 3.7 and Figure 3.8). It should be noted that the position of catalytic His84 in EF-Tu is different in the free EF-Tu structure compared to the ribosome bound structure (Figure 3.7 and Figure 3.8). Since only the structure of free RbgA is available it is difficult to predict if His9 would move to the exact position as EF-Tu His84 upon interaction with the ribosome and if it would interact with the same 23S rRNA nucleotide A2662. It is also noteworthy that due to relocation of the putative catalytic residue His9 in RbgA from Switch II to the N-terminal helix, a direct interaction between histidine and the activated water positioned to attack the γ-phosphate, requires a small translocation of Switch II and potentially the ANTAR domain as well.

Based on previously published mechanisms of GTP hydrolysis this can be accomplished by one of the following ways. First, binding of the ANTAR domain to the 50S subunit could result in a conformational change that is transmitted through the linker CR3 to Switch II. This would likely be coupled with the rearrangement of the N-terminal helix with concomitant positioning of His9

that would facilitate catalysis. The presence of a dynamic and unstructured N-terminal CR1 as evidenced by relatively high B-factors of this region in the RbgA crystal structure, as well as a flexible linker domain connecting Switch II to the ANTAR domain, further strengthen this possibility. A nucleotide dependent large domain rearrangement has also been shown to occur in other ribosomal GTPases such as YphC [21]. A second possibility is that the histidine residue might take part in catalysis through additional intermediate water molecule(s), as has previously been shown for other HAS-GTPases (MnmE and FeoB) [26,27]. In these GTPases the catalytic residue interacts with a secondary (in the case of MnmE or tertiary in the case of FeoB) water molecule that in turn activates the catalytic water molecule and results in GTP hydrolysis [26,27]. Further, it is also possible that the mechanism in RbgA might be a combination of both these mechanisms. Additional structural and biochemical studies are required to test either of these mechanisms and to further ascertain if the nucleotide equivalent to A2662 in *B. subtilis* is required for hydrolysis. This will require the development of tools to isolate mutant ribosomes from this organism similar to the tools that have been developed for *E. coli* [45,46]. The GTPase activity of RbgA was unaffected by *E. coli* 50S ribosomes, which was not unexpected given that *E. coli* lacks a RbgA homolog and thus we could not test the interaction of RbgA with A2662 from the *E.coli* 50S subunit.

Although we have uncovered important insights into the biochemistry of RbgA and how RbgA interacts with the ribosome, several important questions regarding RbgA (and RA-GTPases in general) remain. First, does the GTPase activity of RbgA play a direct role in the assembly process? If the GTPase activity was solely involved in displacing RbgA from the ribosome once assembly had been completed then we expected to identify RbgA mutations that completed assembly but not dissociate from the ribosome. This was not the case as all mutations that were

deleterious to growth yielded a 45S complex that lacked L16, which supports a direct role for GTP hydrolysis in the assembly process. Second, what part of the 23S rRNA does RbgA interact with during the assembly process? At this point there is limited chemical footprinting data that shows RbgA interacting with the central protuberance [11]. We are currently mapping the structure of the 23S rRNA in the 50S subunit and 45S complex to identify key sites that are altered in the 45S complex. In addition, since RbgA homologs are not found in *E. coli*, we are also targeting unique stem-loops within the *B. subtilis* 23S rRNA as possible sites where RbgA may act. Third, does RbgA serve as a checkpoint to monitor large subunit assembly and correct incorporation of L16? Recent work in yeast has uncovered a novel type of translational checkpoint utilized by ribosome assembly factors [47]. Finally, why do most organisms, ranging from bacteria to humans, require RbgA to form ribosomes while many proteobacteria have lost this requirement? Future work will uncover the precise role of RbgA in the assembly of ribosomes in all three kingdoms of life.

Strain	Relevant genotype	Source
B. subtilis		
RB301	JH 642 P*spank-rbgA cat* pMAP65	[9]
RB419	JH 642 P*spank-infB cat* pMAP65	[9]
RB611	JH 642 P*spank-rbgA Spc*^{r} pMAP65	This study
RB613	JH 642 P*spank-rbgA Spc*^{r} *amyE*::P*xyl-rbgA cat* pMAP65	This study
RB667	JH 642 P*spank-rbgA Spc*^{r} *amyE*::P*xyl-rbgA-Q4L cat* pMAP65	This study
RB720	JH 642 P*spank-rbgA Spc*^{r} *amyE*::P*xyl-rbgA-F6A cat* pMAP65	This study
RB653	JH 642 P*spank-rbgA Spc*^{r} *amyE*::P*xyl-rbgA-H9A cat* pMAP65	This study
RB633	JH 642 P*spank-rbgA Spc*^{r} *amyE*::P*xyl-rbgA-K12E/R14E cat* pMAP65	This study
RB750	JH 642 P*spank-rbgA Spc*^{r} *amyE*::P*xyl-rbgA-R14E cat* pMAP65	This study
RB752	JH 642 P*spank-rbgA Spc*^{r} *amyE*::P*xyl-rbgA-R15E cat* pMAP65	This study
RB754	JH 642 P*spank-rbgA Spc*^{r} *amyE*::P*xyl-rbgA-R34E cat* pMAP65	This study
RB744	JH 642 P*spank-rbgA Spc*^{r} *amyE*::P*xyl-rbgA-S38A/S39A cat* pMAP65	This study
RB655	JH 642 P*spank-rbgA Spc*^{r} *amyE*::P*xyl-rbgA-K59A cat* pMAP65	This study
RB654	JH 642 P*spank-rbgA Spc*^{r} *amyE*::P*xyl-rbgA-N58A cat* pMAP65	This study
RB635	JH 642 P*spank-rbgA Spc*^{r} *amyE*::P*xyl-rbgA-D61A cat* pMAP65	This study
RB708	JH 642 P*spank-rbgA Spc*^{r} *amyE*::P*xyl-rbgA-K107E cat* pMAP65	This study
RB656	JH 642 P*spank-rbgA Spc*^{r} *amyE*::P*xyl-rbgA-K107A cat* pMAP65	This study
RB711	JH 642 P*spank-rbgA Spc*^{r} *amyE*::P*xyl-rbgA-K114E cat* pMAP65	This study
RB657	JH 642 P*spank-rbgA Spc*^{r} *amyE*::P*xyl-rbgA-K114E cat* pMAP65	This study
RB622	JH 642 P*spank-rbgA Spc*^{r} *amyE*::P*xyl-rbgA-R122A cat* pMAP65	This study
RB756	JH 642 P*spank-rbgA Spc*^{r} *amyE*::P*xyl-rbgA-R122E cat* pMAP65	This study

Table 3.1 List of *B. subtilis* strains used in this study.

Table 3.1 (cont'd)

RB1155	JH 642 P*spank-rbgA Spc*^{r} *amyE*::P*xyl-rbgA-S134A cat* pMAP65	This study
RB758	JH 642 P*spank-rbgA Spc*^{r} *amyE*::P*xyl-rbgA-T135A cat* pMAP65	This study
RB631	JH 642 P*spank-rbgA Spc*^{r} *amyE*::P*xyl-rbgA-P129R cat* pMAP65	This study
RB623	JH 642 P*spank-rbgA Spc*^{r} *amyE*::P*xyl-rbgA-P129A cat* pMAP65	This study
RB718	JH 642 P*spank-rbgA Spc*^{r} *amyE*::P*xyl-rbgA-T155A cat* pMAP65	This study
RB742	JH 642 P*spank-rbgA Spc*^{r} *amyE*::P*xyl-rbgA-T155A/T155A cat* pMAP65	This study
RB704	JH 642 P*spank-rbgA Spc*^{r} *amyE*::P*xyl-rbgA-F180A cat* pMAP65	This study
RB722	JH 642 P*spank-rbgA Spc*^{r} *amyE*::P*xyl-rbgA-Q158A cat* pMAP65	This study
RB621	JH 642 P*spank-rbgA Spc*^{r} *amyE*::P*xyl-rbgA-E181A cat* pMAP65	This study
RB659	JH 642 P*spank-rbgA Spc*^{r} *amyE*::P*xyl-rbgA-W177F cat* pMAP65	This study
RB1153	JH 642 P*spank-rbgA Spc*^{r} *amyE*::P*xyl-rbgA-W177A cat* pMAP65	This study
RB658	JH 642 P*spank-rbgA Spc*^{r} *amyE*::P*xyl-rbgA-K196A cat* pMAP65	This study
RB851	JH 642 P*spank-rbgA Spc*^{r} *amyE*::P*xyl-rbgA-A206D cat* pMAP65	This study
RB863	JH 642 P*spank-rbgA Spc*^{r} *amyE*::P*xyl-rbgA-Y225A cat* pMAP65	This study
RB617	JH 642 P*spank-rbgA Spc*^{r} *amyE*::P*xyl-rbgA-D228A/E229A cat* pMAP65	This study
RB865	JH 642 P*spank-rbgA Spc*^{r} *amyE*::P*xyl-rbgA-I241D cat* pMAP65	This study
RB921	JH 642 P*spank-rbgA Spc*^{r} *amyE*::P*xyl-rbgA-C247A cat* pMAP65	This study
RB853	JH 642 P*spank-rbgA Spc*^{r} *amyE*::P*xyl-rbgA-A206L cat* pMAP65	This study
RB819	JH 642 P*spank-rbgA Spc*^{r} *amyE*::P*xyl-rbgA-K244A/R245A cat* pMAP65	This study
RB821	JH 642 P*spank-rbgA Spc*^{r} *amyE*::P*xyl-rbgA-K244A/R245A/R265A cat* pMAP65	This study

Table 3.1 (cont'd)

RB823	JH 642 P*spank-rbgA Spc*^{r} *amyE*::P*xyl-rbgA-K244A/R245A/K271A cat* pMAP65	This study
RB825	JH 642 P*spank-rbgA Spc*^{r} *amyE*::P*xyl-rbgA-R224A/K244A/R245A/R265A cat* pMAP65	This study
RB619	JH 642 P*spank-rbgA Spc*^{r} *amyE*::P*xyl-rbgA-E232A/D233A cat* pMAP65	This study
RB855	JH 642 P*spank-rbgA Spc*^{r} *amyE*::P*xyl-rbgA-A235D cat* pMAP65	This study
RB857	JH 642 P*spank-rbgA Spc*^{r} *amyE*::P*xyl-rbgA-A235L cat* pMAP65	This study
RB859	JH 642 P*spank-rbgA Spc*^{r} *amyE*::P*xyl-rbgA-F238A cat* pMAP65	This study
RB861	JH 642 P*spank-rbgA Spc*^{r} *amyE*::P*xyl-rbgA-Y256A cat* pMAP65	This study

S. No.	Chain	Z	rmsd	lalign	n_{res}	%id	Description
1	1puj-A	14.8	0	105	261	100	conserved hypothetical protein Ylqf
2	3cno-A	7.7	2.4	92	227	22	putative uncharacterized protein
3	3cnn-A	7.5	2.5	93	227	22	putative uncharacterized protein
4	3cnl-A	7.3	2.8	93	233	22	putative uncharacterized protein
5	4akk-A	4.1	3.6	53	368	11	nitrate regulatory protein
6	2qxf-A	3.7	2.7	70	433	13	exodeoxyribonuclease I
7	3hp9-A	3.7	2.7	69	452	13	exodeoxyribonuclease I
8	1fxx-A	3.5	2.6	69	459	13	exonuclease I
9	3c94-A	3.5	3	72	458	13	exodeoxyribonuclease I
10	1nex-B	3.5	4	72	444	8	centromere dna-binding protein complex cbf3
11	3c95-A	3.4	2.8	69	446	13	exodeoxyribonuclease I
12	1sd5-A	3.4	5.7	58	188	12	putative antiterminator
13	2jvw-A	3.3	5	67	82	13	uncharacterized protein
14	1s8n-A	3.3	5.6	58	190	12	putative antiterminator
15	1qo0-D	3.3	3.4	46	189	15	AmiC
16	1ucp-A	3.2	3.2	65	91	14	apoptosis-associated speck-like protein
17	4akk-B	3.2	3.9	52	367	12	nitrate regulatory protein
18	1qo0-E	3.2	3.8	50	194	14	AmiC

Table 3.2 Results from a search of structures similar to RbgA C-terminal domain in DALI server.

Mutation	Domain	Doubling time in 2% xylose (minutes)
RB613		26 ± 1
Q4L	CR1	66 ± 2
F6A	CR1	118 ± 4
H9A	CR1	138 ± 3
K12E+R14E	CR1	99 ± 2
K59A	G-domain	105 ± 3
K107E		46 ± 2
K114E		44 ± 1
P129R	G-domain	108 ± 3
S134A	G-domain	148 ± 1
T135A		68 ± 3
T155A	G-domain	104 ± 3
F180A	CR3	169 ± 3
A206D	ANTAR	109 ± 4
Y224A	ANTAR	174 ± 4
I241D	ANTAR	114 ± 3
C247A	ANTAR	70 ± 3

Table 3.3 Growth rate of RbgA mutants.

Strains were grown in LB + 2% Xylose at 37°C. Strain RB613 is a control strain with wild type *rbgA* gene under the control of P_{xyl} promoter. In the other strains mutated *rbgA* gene is under control of P_{xyl} promoter. The data represents three independent growth experiments. Mutations that reduced growth by 3-fold compared with wild type were classified as mild – these include Q4L, K107E, K114E, T135A and C247A. The mutations that reduced the growth rate by more than 3-fold were classified as severe – these include F6A, H9A, K12E/R14E, K59A, P129R, S134A, T155A, W177A,F180A, A206D, Y225A and I241D.

Mutation	Domain	Doubling time in 100 µM IPTG (minutes)	Doubling time in 100µM IPTG + 2% xylose (minutes)
Wild type		29 ± 2	26 ± 1
F6A	CR1	31 ± 1	59 ± 4
H9A	CR1	30 ± 2	62 ± 1
Y225A	ANTAR	30 ± 1	50 ± 2

Table 3.4 Dominant negative phenotype observed under specific growth conditions.

Strains were grown in LB + 1mM IPTG (full induction of wild type RbgA protein) and LB + 100 µM IPTG + 2% xylose to assess the dominant negative phenotype. The reduced 100 µM IPTG reduces the wild type RbgA protein level and 2% xylose induces the expression of mutated RbgA protein.

Domain/ Region	Mutation	50S			45S		
		GDP*	GTP	GMP-PNP	GDP	GTP	GMP-PNP
	RbgA wt	5%	22%	100%	4%	84%	100%
ANTAR	A206D	<0.6%	<0.6%	<0.6%	<0.6%	<0.6%	<0.6%
	Y225A	4%	380%	5%	7%	180%	7%
	I241D	1%	2%	58%	2%	5%	68%
CR1	F6A	1%	68%	71%	2%	70%	73%
	H9A	1%	65%	69%	3%	69%	72%
	K12E+R14E	4%	64%	67%	2%	71%	75%
CR3	F180A	6%	16%	79%	5%	86%	91%

Table 3.5 Results for *in vitro* binding of RbgA mutants to the 45S and 50S subunits under different nucleotide conditions.

The values represent the average of three independent experiments ± S.D.

Domain/ Region	Mutation	Intrinsic GTPase activity	Stimulation of GTPase activity with 50S	Fold stimulation in the presence of 50S
		V in pmol phosphate/ pmol RbgA/min		
	RbgA wt	0.207 ± 0.008	12.57 ± 0.18	61 ± 3
CR1	F6A	0.018 ± 0.002	0.283 ± 0.05	15± 4
	H9A	0.031 ± 0.006	<0.002	
	K12E+R14E	0.121 ± 0.004	0.226 ± 0.07	2 ± 0.5
G-domains	S134A	<0.002	<0.002	
ANTAR	A206D	0.040 ± 0.001	0.978 ± 0.06	24 ± 2
	Y225A	0.139 ± 0.005	3.97 ± 0.30	29 ± 3
	I241D	0.104 ± 0.007	0.597 ± 0.11	6 ± 0.5
CR3	F180A	0.097 ± 0.012	8.08 ± 0.19	84 ± 11

Table 3.6 Measurement of GTPase activity of RbgA mutants in the presence and absence of the 50S subunit.

A.

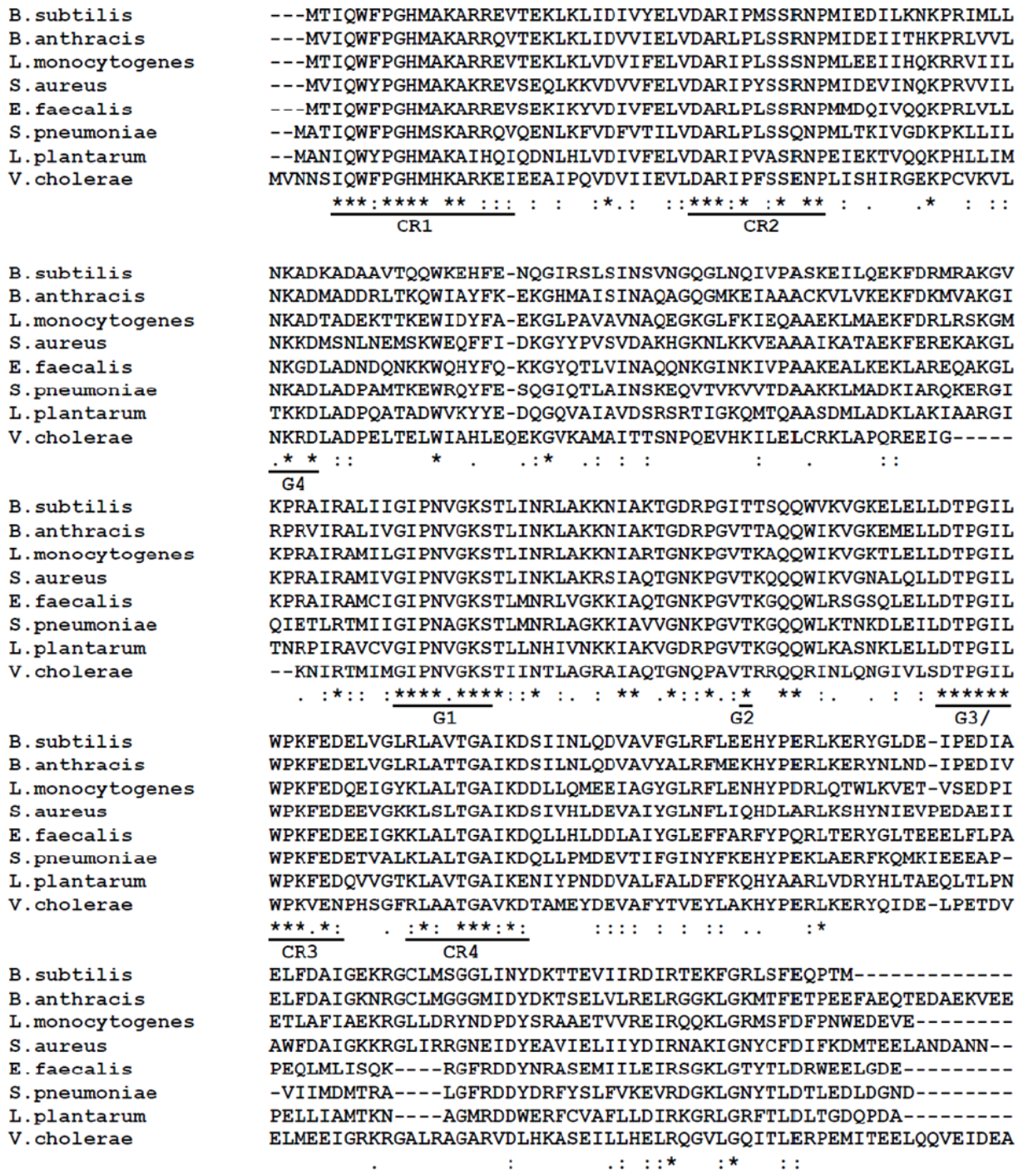

Figure 3.1 Sequence alignment of RbgA with its homologs.

A. Multiple sequence alignment of selected bacterial RbgA homologs. Highly conserved regions are underlined. G-domain motifs are indicated as G4 (NKXD), G1 (GXXXXGKS/T), G2 (T), and G3 (DXXG) in addition to four conserved regions (CR1-CR4).

Figure 3.1 (cont'd)

B.

B. Multiple sequence alignment of RbgA with eukaryotic homologs Mtg1 from humans and mouse highlighting conserved region CR1. G-domain motifs are indicated G1-G4. Alignments were constructed with ClustalW with default parameters and species indicated to the left. '*' indicates positions which have a single, fully conserved residue, ':' indicates conservation between groups of strongly similar physicochemical properties, '.' indicates conservation between groups of weakly similar physicochemical properties.

Figure 3.1 (cont'd)

C.

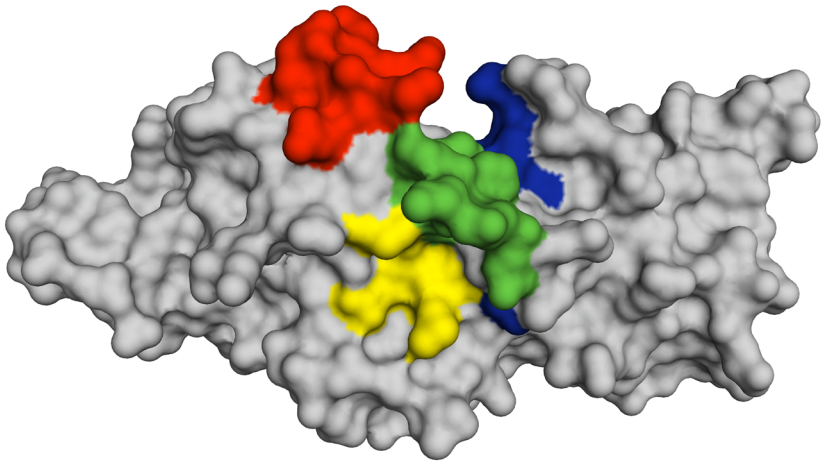

C. Structure of RbgA depicting CR1, CR2, CR3 and CR4. Crystal structure of RbgA (PDB: 1PUJ) depicting the three conserved regions. First 9 amino acid residues are not structured in the crystal. CR1 (9-17) is shown in red, CR2 (30-42) is shown in yellow, CR3 (175-182) is shown in green and CR4 (188-197) shown in blue. All four conserved regions are dispersed across the protein sequence and lie in close vicinity in the structure of the protein. For interpretation of the references to color in this and all other figures, the reader is referred to the electronic version of this thesis.

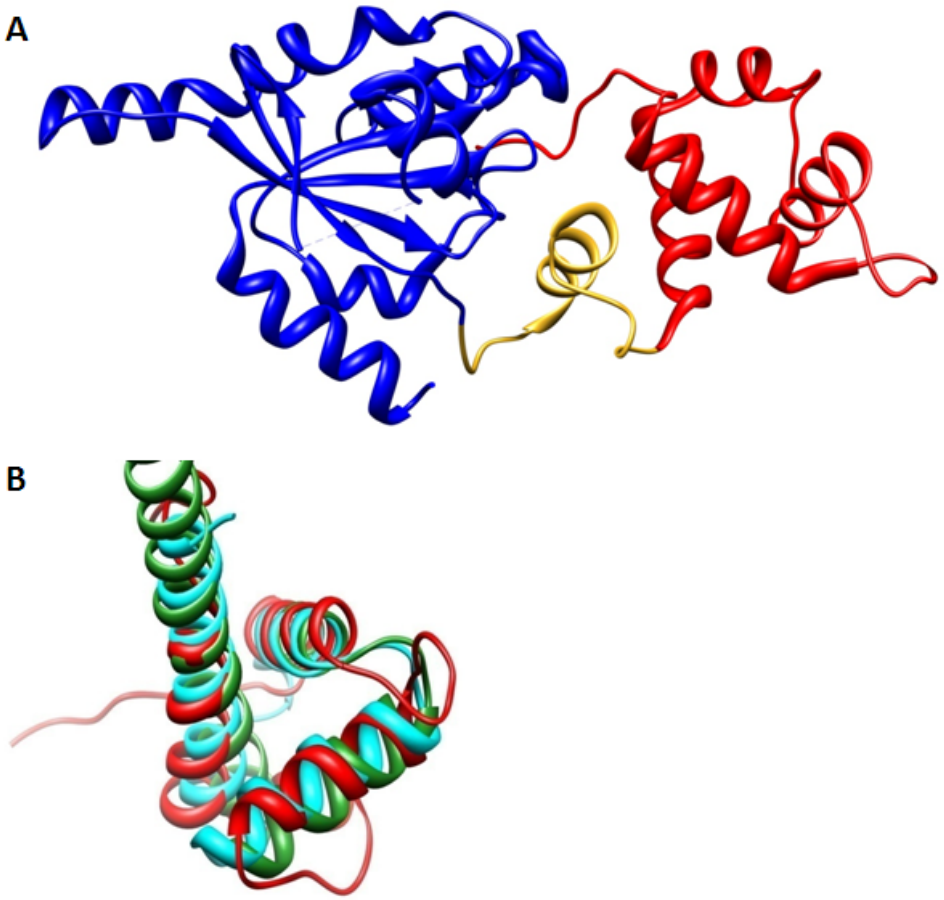

Figure 3.2 C-terminal domain of RbgA contains RNA binding domain ANTAR.

A. The crystal structure of RbgA (PDB: 1PUJ). The N-terminal G- domain is depicted in blue (9-176), the C-terminal domain is depicted in red (201-282) and a linker helix connecting the two domains is depicted in yellow (177-200). B. The superposition of the ANTAR domains of RbgA (red), AmiR (green) and NasR (Cyan).

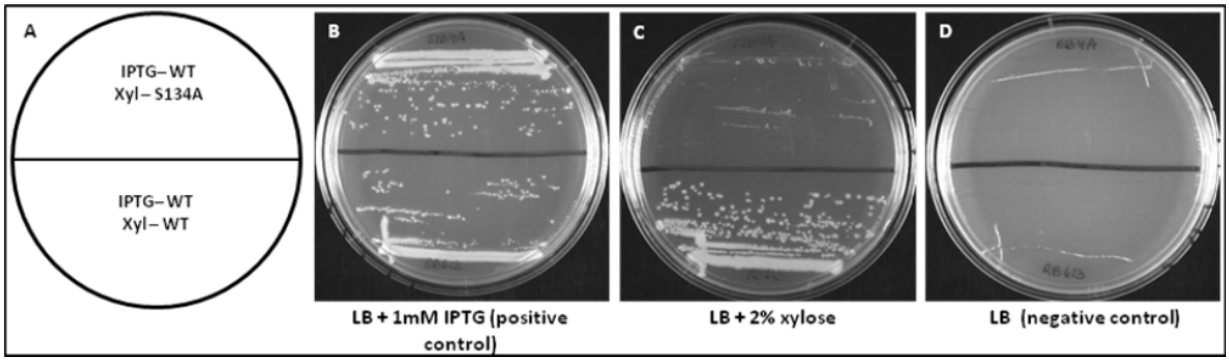

Figure 3.3 Testing the growth phenotype of RbgA mutants.

A. All strains were constructed with the wild-type *rbgA* gene under the control of an IPTG inducible promoter and a mutated *rbgA* gene (S134A is shown as an example here) under the control of a xylose inducible promoter. In contrast, the control strain had the wild-type *rbgA* gene under the control of both promoters B. The two strains were streaked on IPTG containing plates. Wild-type growth is seen in both strains due to the expression of *rbgA*. C. The two strains were streaked on plates containing xylose. No colonies were observed for S134A and hence the mutation was characterized as lethal. The RB613 control strain showed wild-type growth as *rbgA* is expressed from xylose inducible promoter D. The two strains were streaked on plates without IPTG or xylose. No growth is seen due to the absence of protein induction in either case.

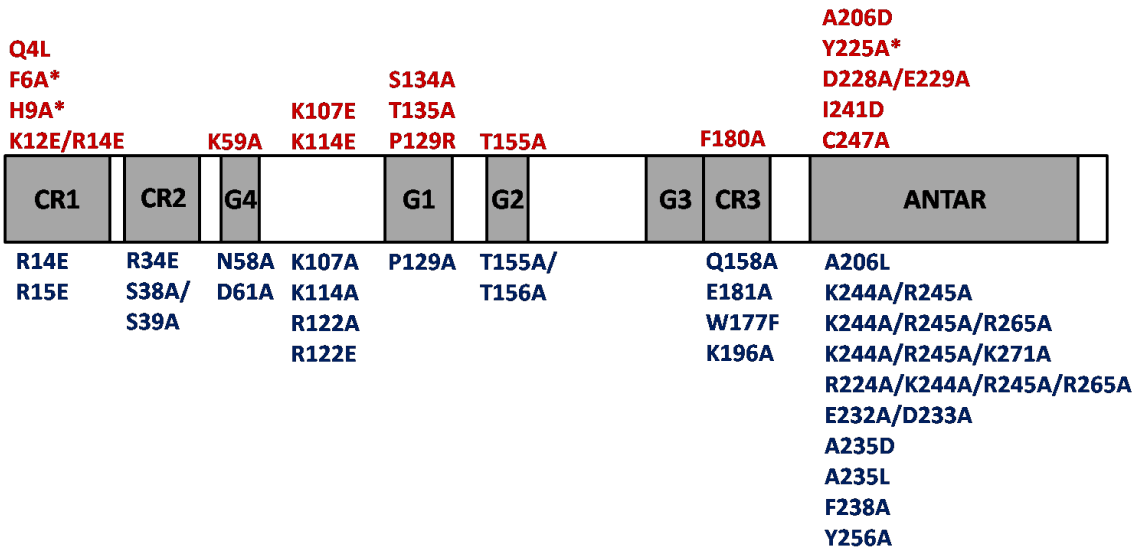

Figure 3.4 Consolidated results of mutational analysis of RbgA.

Domains are indicated in grey. CR1-3; conserved region, G1-G4; conserved GTP binding domains found in GTPase superfamily, ANTAR; AmiR-NasR transcription anti-termination domain. The mutations shown in red are sick or do not support growth and the mutations shown in blue do not effect growth. * indicates partial dominant negative effect.

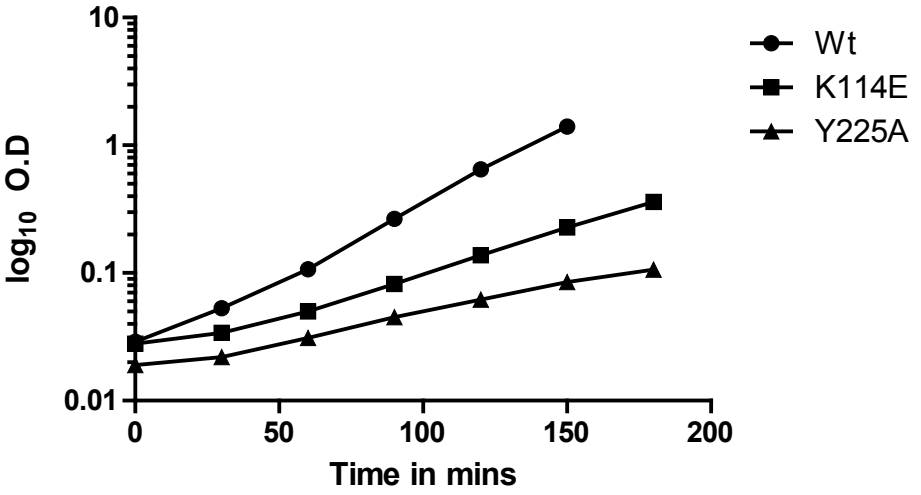

Figure 3.5 An example of growth curves comparing wild type growth with a mutation that causes a mild growth defect and a mutation that causes a severe growth defect.

Strains were grown in LB + 2% Xylose at 37°C. Strain RB613 is a control strain with wild type *rbgA* gene under the control of P_{xyl} promoter. In the other strains mutated *rbgA* gene is under control of P_{xyl} promoter. Represented here are examples of mutation that causes a mild growth defect (K114E) and a mutation that causes a severe growth defect (Y225A).

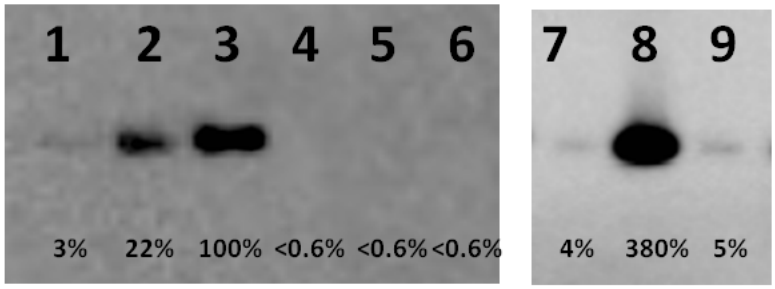

Figure 3.6 *In vitro* binding assay for RbgA mutants to 50S subunit under different nucleotide conditions.

Purified RbgA-his$_6$ or RbgA mutant-his$_6$ (50 nM) were incubated with purified 50S (10 nM) intermediates and GDP, GTP or GMP-PNP (400 μM) at 37°C. The presence of RbgA was tested by western blot with custom RbgA-antibody and quantified. Percentages were generated by assigning RbgA + 50S + GMP-PNP as 100%. Lane1: RbgA + 50S + GDP; lane2: RbgA + 50S + GTP; lane3: RbgA + 50S + GMPPNP; lane4: A206D + 50S + GDP; lane5: A206D + 50S + GTP; lane6: A206D + 50S + GMPPNP; lane7: Y225A + 50S + GDP; lane8: Y225A + 50S + GTP and lane 9: Y225A + 50S + GMPPNP.

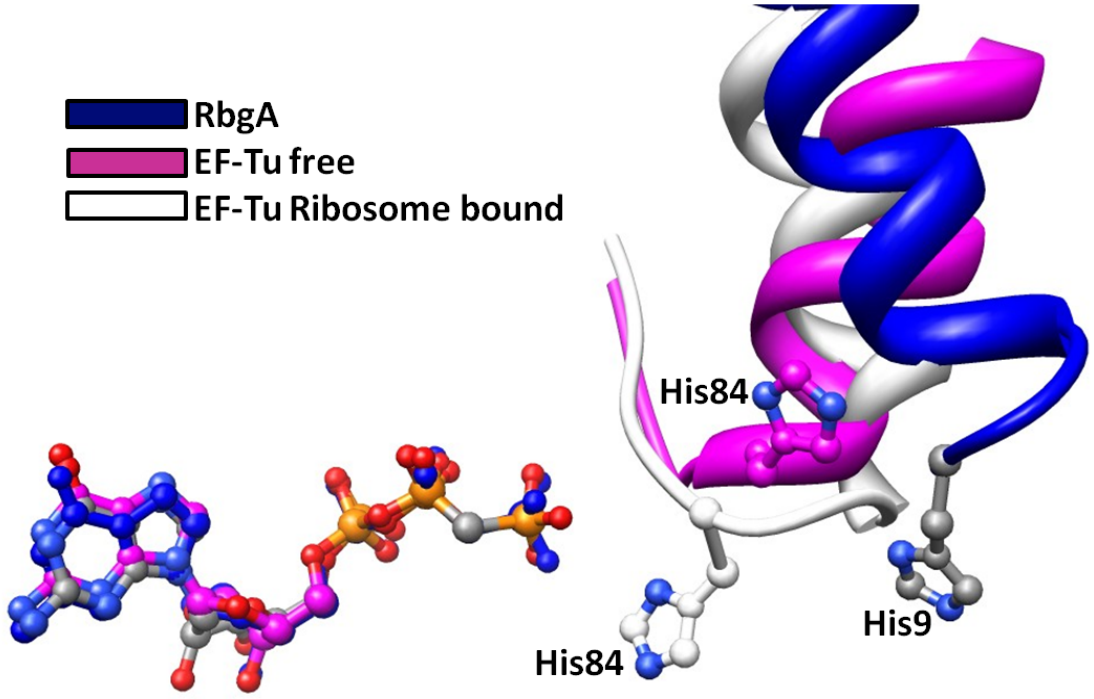

Figure 3.7 A ligand based structural superimposition of EF-Tu over the free RbgA.

Free EF-Tu is depicted in magenta, ribosome bound EF-Tu is depicted in light grey and free RbgA is depicted in blue color. For clarity only the helices containing the catalytic histidine residues are shown along with GTP analogue.

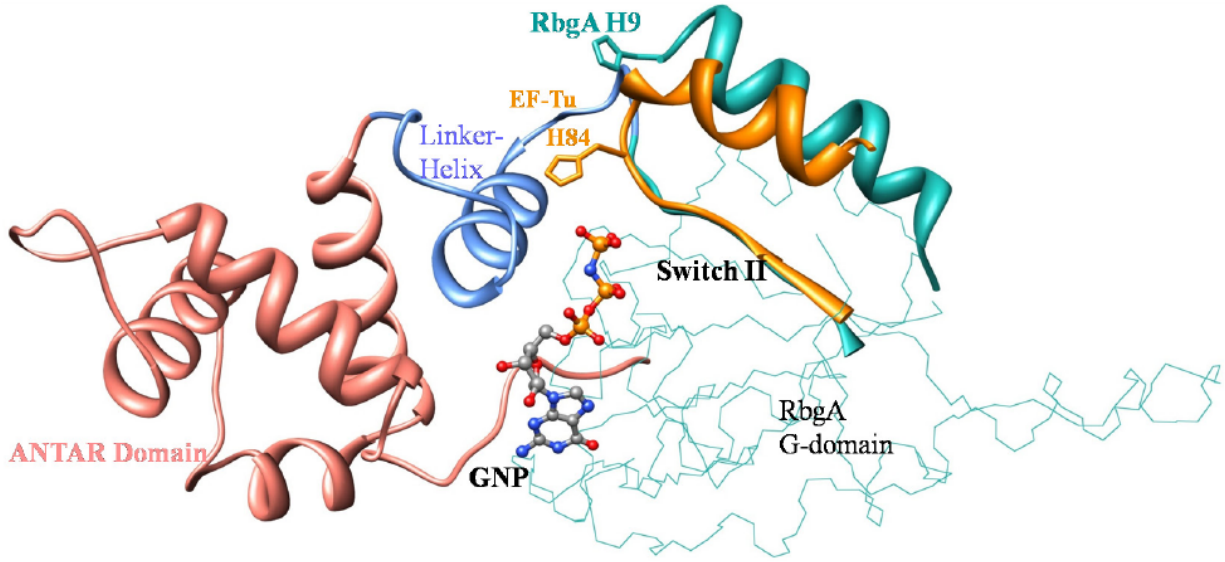

Figure 3.8 A ligand-based superimposition of RbgA and EF-Tu for comparison of catalytic machinery is shown.

RbgA G domain is shown in wire form and only switch II and following helix is shown from the EF-Tu structure (orange). Switch II in EF-Tu harbors catalytic residue His85 while in RbgA it connects the ANTAR domain (light brown) via the linker helix (light blue). Putative catalytic residue His9 in RbgA is relocated to a loop connected to a helix near the N terminus (cyan) which occupies a similar position to the EF-Tu helix connected to His85. Switch II in RbgA would prevent the direct involvement of His9 from the helix.

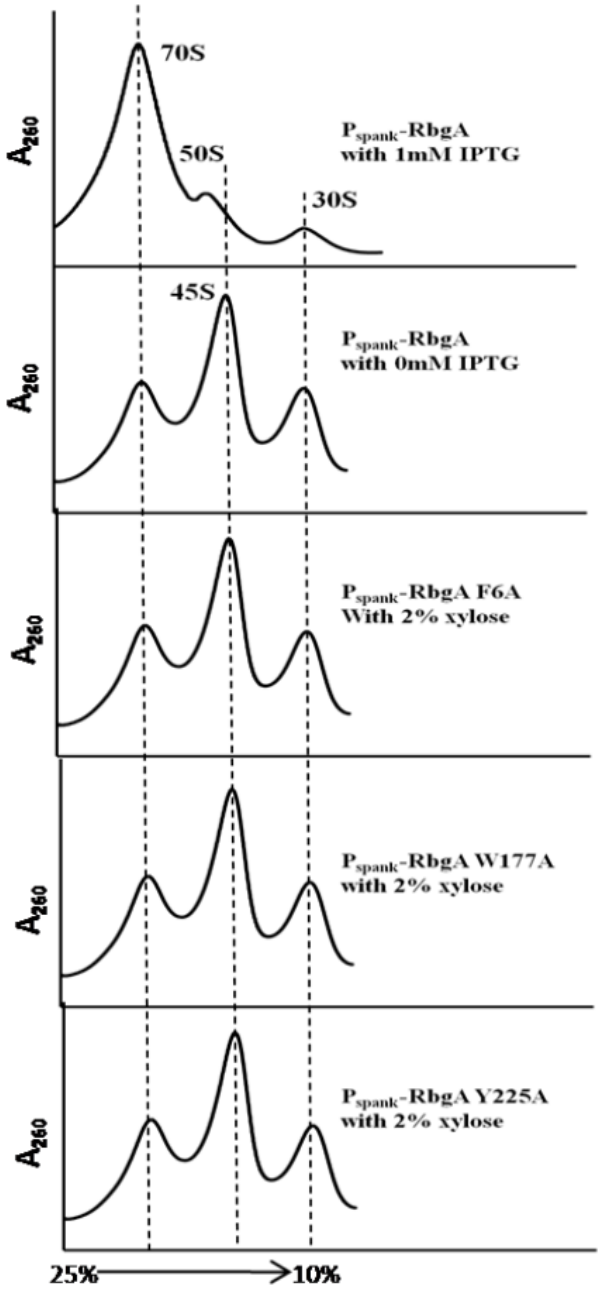

Figure 3.9 Ribosome profiles of RbgA mutants.

Strain RB301 was grown in the presence of IPTG (wild type) and in the absence of IPTG (depleting RbgA protein condition). The strains with mutated *rbgA* were grown in the presence of xylose to induce the RbgA mutant protein. Ribosome profiles were generated by centrifugation of lysates through sucrose density gradients (10-25%). Profiles are shown from the bottom of the gradient (left, 25%) to the top of the gradient (right, 10%). Dashed lines indicate where 70S, 45S and 30S complexes migrate in the gradients.

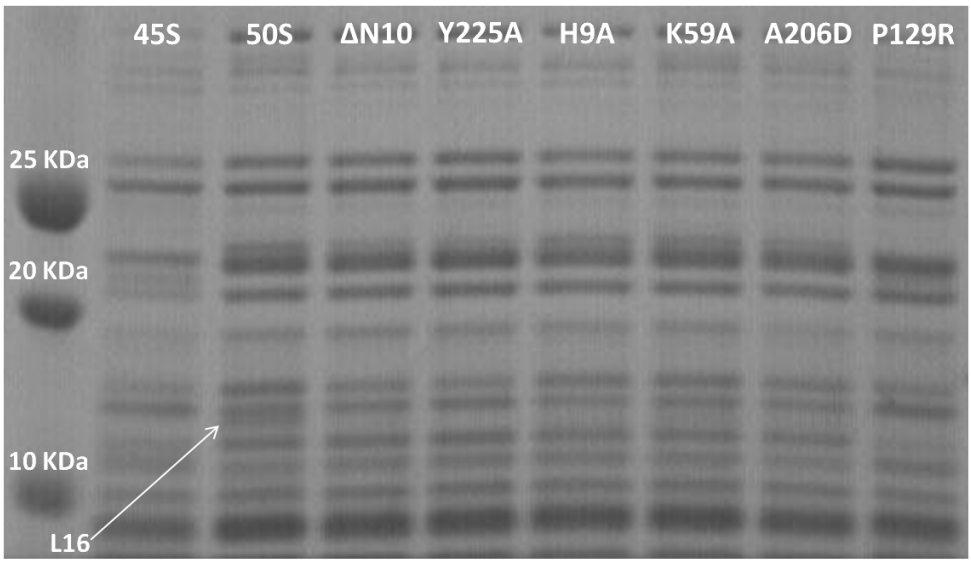

Figure 3.10 Proteomic analysis of ribosomal intermediate formed in strains expressing RbgA mutant protein.

45S complex was isolated from strains expressing mutated RbgA protein and from RbgA depleted strain. The 50S complex was isolated from RB301 grown in the presence of IPTG. The complexes were run on 12% SDS-PAGE gel and stained with Coomassie blue stain. The ribosomal intermediates formed in cells expressing mutant RbgA protein is similar in composition to the 45S intermediate formed in the absence of RbgA. All 45S complexes analyzed lacked ribosomal protein L16 seen in the 50S subunit – identified using mass spectrometry.

ACKNOWLEDGEMENTS

We thank David Achila and Brian Shy for technical assistance.

REFERENCES

REFERENCES

1. Nomura, M., Erdmann, V.A. (1970) Reconstitution of 50S ribosomal subunits from dissociated molecular components. *Nature* 228: 744-8.

2. Nierhaus, K.H. (1991) The assembly of prokaryotic ribosomes. *Biochimie* 73: 739-55.

3. Nierhaus, K.H., Dohme, F. (1974) Total reconstitution of functionally active 50S ribosomal subunits from Escherichia coli. *Proc Natl Acad Sci U S A* 71: 4713-7.

4. Wilson, D.N., Nierhaus, K.H. (2007) The weird and wonderful world of bacterial ribosome regulation. *Crit Rev Biochem Mol Biol* 42: 187-219.

5. Fahnestock, S., Erdmann, V., Nomura, M. (1973) Reconstitution of 50S ribosomal subunits from protein-free ribonucleic acid. *Biochemistry* 12: 220-4.

6. Britton, R.A. (2009) Role of GTPases in bacterial ribosome assembly. *Annu Rev Microbiol* 63: 155-76.

7. Granneman, S., Baserga, S.J. (2004) Ribosome biogenesis: of knobs and RNA processing. *Exp Cell Res* 296: 43-50.

8. Karbstein, K. (2007) Role of GTPases in ribosome assembly. *Biopolymers* 87: 1-11.

9. Uicker, W.C., Schaefer, L., Britton, R.A. (2006) The essential GTPase RbgA (YlqF) is required for 50S ribosome assembly in Bacillus subtilis. *Mol Microbiol* 59: 528-40.

10. Schaefer, L*., et al.* (2006) Multiple GTPases participate in the assembly of the large ribosomal subunit in Bacillus subtilis. *J Bacteriol* 188: 8252-8.

11. Matsuo, Y*., et al.* (2006) The GTP-binding protein YlqF participates in the late step of 50 S ribosomal subunit assembly in Bacillus subtilis. *J Biol Chem* 281: 8110-7.

12. Achila, D., Gulati, M., Jain, N., Britton, R.A. (2012) Biochemical characterization of ribosome assembly GTPase RbgA in Bacillus subtilis. *J Biol Chem* 287: 8417-23.

13. Barrientos, A*., et al.* (2003) MTG1 codes for a conserved protein required for mitochondrial translation. *Mol Biol Cell* 14: 2292-302.

14. Kallstrom, G., Hedges, J., Johnson, A. (2003) The Putative GTPases Nog1p and Lsg1p Are Required for 60S Ribosomal Subunit Biogenesis and Are Localized to the Nucleus and Cytoplasm, Respectively. *Mol Cell Biol* 23: 4344-55.

15. Bassler, J., Kallas, M., Hurt, E. (2006) The NUG1 GTPase reveals and N-terminal RNA-binding domain that is essential for association with 60 S pre-ribosomal particles. *J Biol Chem* 281: 24737-44.

16. Im, C.H.*, et al.* (2011) Nuclear/nucleolar GTPase 2 proteins as a subfamily of YlqF/YawG GTPases function in pre-60S ribosomal subunit maturation of mono- and dicotyledonous plants. *J Biol Chem* 286: 8620-32.

17. Anand, B., Verma, S.K., Prakash, B. (2006) Structural stabilization of GTP-binding domains in circularly permuted GTPases: implications for RNA binding. *Nucleic Acids Res* 34: 2196-205.

18. Mishra, R., Gara, S.K., Mishra, S., Prakash, B. (2005) Analysis of GTPases carrying hydrophobic amino acid substitutions in lieu of the catalytic glutamine: implications for GTP hydrolysis. *Proteins* 59: 332-8.

19. Marlovits, T.C., Haase, W., Herrmann, C., Aller, S.G., Unger, V.M. (2002) The membrane protein FeoB contains an intramolecular G protein essential for Fe(II) uptake in bacteria. *Proc Natl Acad Sci U S A* 99: 16243-8.

20. Monleon, D.*, et al.* (2007) Structural insights into the GTPase domain of Escherichia coli MnmE protein. *Proteins* 66: 726-39.

21. Muench, S.P., Xu, L., Sedelnikova, S.E., Rice, D.W. (2006) The essential GTPase YphC displays a major domain rearrangement associated with nucleotide binding. *Proc Natl Acad Sci U S A* 103: 12359-64.

22. Uicker, W.C., Schaefer, L., Koenigsknecht, M., Britton, R.A. (2007) The essential GTPase YqeH is required for proper ribosome assembly in Bacillus subtilis. *J Bacteriol* 189: 2926-9.

23. Sullivan, S.M., Mishra, R., Neubig, R.R., Maddock, J.R. (2000) Analysis of guanine nucleotide binding and exchange kinetics of the Escherichia coli GTPase Era. *J Bacteriol* 182: 3460-6.

24. Jiang, M.*, et al.* (2006) The Escherichia coli GTPase CgtAE is involved in late steps of large ribosome assembly. *J Bacteriol* 188: 6757-70.

25. Wout, P.*, et al.* (2004) The Escherichia coli GTPase CgtAE cofractionates with the 50S ribosomal subunit and interacts with SpoT, a ppGpp synthetase/hydrolase. *J Bacteriol* 186: 5249-57.

26. Scrima, A., Wittinghofer, A. (2006) Dimerisation-dependent GTPase reaction of MnmE: how potassium acts as GTPase-activating element. *EMBO J* 25: 2940-51.

27. Ash, M.R., Maher, M.J., Guss, J.M., Jormakka, M. (2011) The initiation of GTP hydrolysis by the G-domain of FeoB: insights from a transition-state complex structure. *PLoS One* 6: e23355.

28. Teraoka, H., Nierhaus, K.H. (1978) Protein L16 induces a conformational change when incorporated into a L16-deficient core derived from Escherichia coli ribosomes. *FEBS Lett* 88: 223-6.

29. Petit, M.-A.*, et al.* (1998) PcrA is an essential DNA helicase of Bacillus subtilis fulfilling functions both in repair and rolling-circle replication. *Mol Microbiol* 29: 261-73.

30. Bhavsar, A.P., Zhao, X., Brown, E.D. (2001) Development and characterization of a xylose-dependent system for expression of cloned genes in Bacillus subtilis: conditional complementation of a teichoic acid mutant. *Appl Environ Microbiol* 67: 403-10.

31. Holm, L., Rosenstrom, P. (2010) Dali server: conservation mapping in 3D. *Nucleic Acids Res* 38: W545-9.

32. The Pymol Molecular Graphics System, V.R.P., Schrödinger, Llc The PyMOL Molecular Graphics System, Version 1.2r3pre, Schrödinger, LLC.

33. Heifets, A., Lilien, R.H. (2010) LigAlign: flexible ligand-based active site alignment and analysis. *J Mol Graph Model* 29: 93-101.

34. Pettersen, E.F.*, et al.* (2004) UCSF Chimera--a visualization system for exploratory research and analysis. *J Comput Chem* 25: 1605-12.

35. Boudes, M.*, et al.* (2012) The structure of the NasR transcription antiterminator reveals a one-component system with a NIT nitrate receptor coupled to an ANTAR RNA-binding effector. *Mol Microbiol* 85: 431-44.

36. O'hara, B.P.*, et al.* (1999) Crystal structure and induction mechanism of AmiC-AmiR: a ligand-regulated transcription antitermination complex. *EMBO J* 18: 5175-86.

37. Shu, C.J., Zhulin, I.B. (2002) ANTAR: an RNA-binding domain in transcription antitermination regulatory proteins. *Trends Biochem Sci* 27: 3-5.

38. Sprang, S.R. (1997) G protein mechanisms: insights from structural analysis. *Annu Rev Biochem* 66: 639-78.

39. Matsuo, Y., Oshima, T., Loh, P.C., Morimoto, T., Ogasawara, N. (2007) Isolation and characterization of a dominant negative mutant of Bacillus subtilis GTP-binding protein, YlqF, essential for biogenesis and maintenance of the 50 S ribosomal subunit. *J Biol Chem* 282: 25270-7.

40. Voorhees, R.M., Schmeing, T.M., Kelley, A.C., Ramakrishnan, V. (2010) The mechanism for activation of GTP hydrolysis on the ribosome. *Science* 330: 835-8.

41. Sharma, M.R.*, et al.* (2005) Interaction of Era with the 30S ribosomal subunit implications for 30S subunit assembly. *Mol Cell* 18: 319-29.

42. Ramesh, A.*, et al.* (2012) The Mechanism for RNA Recognition by ANTAR Regulators of Gene Expression. *PLoS Genet* 8: e1002666.

43. Stewart, V., Van Tilbeurgh, H. (2012) Found: The Elusive ANTAR Transcription Antiterminator. *PLoS Genet* 8: e1002773.

44. Kim Do, J., Jang, J.Y., Yoon, H.J., Suh, S.W. (2008) Crystal structure of YlqF, a circularly permuted GTPase: implications for its GTPase activation in 50 S ribosomal subunit assembly. *Proteins* 72: 1363-70.

45. Asai, T.*, et al.* (1999) Construction and initial characterization of Escherichia coli strains with few or no intact chromosomal rRNA operons. *J Bacteriol* 181: 3803-9.

46. Asai, T., Zaporojets, D., Squires, C., Squires, C.L. (1999) An Escherichia coli strain with all chromosomal rRNA operons inactivated: complete exchange of rRNA genes between bacteria. *Proc Natl Acad Sci U S A* 96: 1971-6.

47. Strunk, B.S., Novak, M.N., Young, C.L., Karbstein, K. (2012) A Translation-Like Cycle Is a Quality Control Checkpoint for Maturing 40S Ribosome Subunits. *Cell* 150: 111-21.

CHAPTER 4

Functional interaction between ribosomal protein L6 and RbgA during ribosome assembly

Part of the research presented in this chapter was

performed by Nikhil Jain, who contributed

Figures 4.11, 4.12 and 4.13

Abstract

RbgA is an essential GTPase that participates in the assembly of the large ribosomal subunit in *Bacillus subtilis* and its homologs are implicated in mitochondrial and eukaryotic large subunit assembly. How RbgA functions in this process is still poorly understood. To gain insight into the function of RbgA we isolated suppressor mutations that partially restored the growth of an RbgA mutation (RbgA-F6A) that caused a severe growth defect. Analysis of these suppressors identified mutations in *rplF*, encoding ribosomal protein L6. The suppressor strains all accumulated a novel ribosome intermediate that migrates at 44S in sucrose gradients. All of the mutations cluster in a region of L6 that is in close contact with helix 97 of the 23S rRNA. *In vitro* maturation assays indicate that the L6 substitutions allow the defective RbgA-F6A protein to function more effectively in ribosome maturation. Our results suggest that RbgA functions to properly position L6 on the ribosome, prior to the incorporation of L16 and other late assembly proteins.

Introduction

The assembly of the 30S and 50S ribosomal subunits is a complex and tightly coordinated series of events that consists of the synthesis, processing and modification of 5S, 16S and 23S rRNA and the addition of more than 50 ribosomal proteins (r-proteins) [1-3]. The *in vitro* reconstitution of a mature 50S subunit has been extensively studied in *Escherichia coli* and the formation of a mature 50S subunit from its constituent r-proteins and rRNA is a multi-step process that requires non-physiological conditions such as high ionic concentration, high temperatures and long incubation times [4-7]. Relatively fewer studies focused on ribosome assembly in other bacterial species, such as *Bacillus stearothermophilus*, and these demonstrated that the intermediates formed in this system are different than those in *E. coli*, however similar non-physiological steps are required for formation of a functional ribosomal subunit [5,8]. Moreover, recent studies have utilized biophysical techniques to study ribosome assembly *in vivo* and demonstrated that assembly of the ribosome subunits is a multistage process that appears to follow multiple parallel pathways in which the accumulation of assembly intermediates identified *in vitro* do not accumulate *in vivo* [9-11]. The slow kinetics and attenuated efficiency of *in vitro* assembly strongly suggest that assembly factors are involved *in vivo* and indeed, several classes of assembly factors such as GTPases, RNA helicases, RNA modification enzymes and chaperone proteins have been implicated in *in vivo* ribosome assembly in bacterial and eukaryotic cells [2,12-15]. However, while studies show that these factors are functionally significant and play a critical role in ribosome assembly, the molecular functions of these factors remain elusive. RbgA (ribosome biogenesis GTPaseA) is an essential GTPase that is required for late step assembly of the 50S subunit in *Bacillus subtilis* [16,17]. RbgA is a widely conserved protein and its eukaryotic homologs such as Mtg1, Lsg1, Nug1 and Nog2 have also been implicated in assembly

of the large ribosomal subunit [18-21]. RbgA depleted cells do not form mature 50S subunits but instead accumulate a 45S complex. Quantitative mass spectrometry analysis of this particle shows that the 45S completely lack ribosomal proteins L16, L28, L36 and contain severely reduced amount of L27, L33a and L35 [16,22]. Proteins L16 and L27 are crucial components of the peptidyltransferase center in 50S subunit and directly contact the A-site and the P-site respectively [23,24]. Functional studies have shown that both proteins play a role in stabilization of the peptide bond formation, the positioning of tRNA on their respective sites and are required for optimal functioning of the ribosome [25-27]. While there have been no reports of deletion of L16, the deletion of L27 in *E. coli* causes a severe growth defect [28]. However, studies in *B. subtilis* indicate that both proteins are essential and deletion mutants could not be obtained for either protein [29]. *In vitro* assembly experiments have demonstrated that incorporation of L16 into the growing complex occurs at a late stage in the assembly process and is accompanied by a large conformational change [30]. In yeast, the RbgA homolog Lsg1 has been proposed to play a role in the incorporation of the L16 homolog Rpl10 into the large ribosomal subunit, suggesting that RbgA and its homologs regulate an evolutionarily conserved step during biogenesis [31,32]. RbgA has been shown to interact directly with both the 45S complex and the 50S subunits and the GTPase activity of RbgA is enhanced ~60 fold in the presence of the mature 50S subunit [33]. Mutational analysis of RbgA has shown that a stretch of 15 amino acids in the N-terminal domain, which is largely conserved among all bacterial RbgA homologs as well as eukaryotic homologs, plays a crucial role in GTPase activity [34]. Mutations that affect GTP hydrolysis result in the accumulation of the 45S complex similar to RbgA depleted cells indicating that GTP hydrolysis plays a key role in maturation of the 50S subunit [34].

To further investigate the role of RbgA in the assembly of the 50S subunit we constructed a *B. subtilis* strain that expressed a mutated RbgA protein that results in a severe growth defect and screened for suppressors that alleviated this growth defect. We isolated and characterized eight independent suppressor strains and found they contained six distinct mutations in the *rplF* gene, which encodes for ribosomal protein L6. Analysis of ribosome assembly in these strains led to discovery of a novel ribosomal intermediate that differs from the 45S complex observed in the parental strain and also in RbgA-depleted cells. We discuss the implications of these results and present a possible model for the role of RbgA in assembly of the 50S subunit.

Materials and Methods

Growth conditions

All strains were grown at 37°C in LB medium and cultures were shaken at 250 rpm. Antibiotics were added at the following concentrations when required: chloramphenicol (5µg/ml), erythromycin (5µg/ml), lincomycin (12.5µg/ml), spectinomycin (100µg/ml) and ampicillin (100µgml). IPTG was added to a final concentration of 1mM when required for strain growth.

Plasmids

Plasmid pMA1 was derived from pSWEET, an *amyE* insertion vector with a chloramphenicol resistance cassette, by placing the *rbgA* gene under the control of a xylose inducible promoter. Plasmid pAS24, an *amyE* insertion vector with a spectinomycin resistance, was used to construct pMG28 by inserting a wild-type copy of *rbgA* under the control of its native promoter. Plasmid pMG29 bearing a F6A mutation in the *rbgA* gene (accomplished by a TTC to GCC codon change) was constructed from pMG28 using the QuikChange II XL kit (Stratagene) by following

the manufacturer's instructions. Plamid pJCL87 was derived from pDR111 and contains a chloramphenicol resistance cassette and the IPTG inducible $P_{hyperspank}$promoter. Plasmid pMG30 was constructed from pJCL87 by cloning the first 330 bp of the *map* gene under the control of the $P_{hyperspank}$promoter.

Construction of strains

All strains used in this study are derived from the wild type strain JH642 (RB247) and listed in Table 4.1. The construction of strain RB301 and RB418 has been described previously [16]. RB395 was constructed by transforming RB247 with pMA1 and knocking out the native *rbgA* gene by using a MLS cassette. Strain RB1006 was constructed by transforming RB247 with plasmid pMG28 at the *amyE* locus and knocking out the native *rbgA* gene by using a MLS cassette. The strains were checked for interruption of *amyE* by growth on starch plates. Strain RB1043 was constructed by transforming RB247 with plasmid pMG29 and knocking out the native *rbgA* gene by using chromosomal DNA from RB395. Independently, strain RB1044 was constructed in a manner identical to RB1043 to serve as a biological duplicate. All strains discussed in this study were confirmed for desired change using PCR to amplify the region of interest followed by sequencing.

Suppressor screen

Strains RB1043 and RB1044 were used for suppressor analysis. A single colony from each of these strains was inoculated per flask (25 colonies per strain, total of 50 colonies) and grown at 37°C for 16 hours. The undiluted culture from each flask as well as two serial dilutions (10-, and 100-fold) were plated on LB plates and incubated overnight at 37°C. The parental strains

RB1043 and RB1044 were also plated along with RB1006 carrying wild-type RbgA to serve as controls. Isolated colonies from eight strains-RB1051, RB1055, RB1057, RB1059 (from RB1043) and RB1061, RB1063, RB1065, and RB1068 (from RB1044) that grew faster than parental strains were identified and characterized further.

Whole genome sequencing and bioinformatics analysis

Genomic DNA from RB247, RB1043, RB1051, RB1055, RB1057, RB1059, RB1061, RB1063, RB1065 and RB1068 was isolated using the Wizard genomic DNA isolation kit (Promega). The genomic DNA was analyzed on a 0.8% agarose gel to ensure that the quality was suitable for sequencing. Whole genome sequencing was performed on a Genome Analyzer II instrument equipped with a paired end module (Illumina) at the MSU RTSF. The sequencing reads obtained were quality tested using FASTQC and trimmed if needed. Next we aligned sequence reads from RB247 and RB1043 against the reference *B. subtilis* strain 168 genome using R2R software. We identified the insertion of pMG29 in RB1043 when compared with RB247 reads and the insertion of the MLS cassette in RB1043 at the native *rbgA* locus. The sequence of suppressor strains RB1051, RB1055, RB1057, RB1059, RB1063, RB1065 and RB1068 was then compared to RB1043 (the parental strain). In addition to the expected insertions found in RB1043 and each suppressor strain (corresponding to pMG28 at the *amyE* locus and the MLS cassette at the native *rbgA* locus) we identified only a single change in each suppressor strain in the *rplF* gene. The suppressor mutations that were identified utilizing the R2R platform were confirmed by PCR amplification of the *rplF* gene and sequencing the amplified product.

Structure analysis

Homology model of L6 from *B. subtilis* was obtained by using Modeller 9.12 [35], utilizing the crystal structure of L6 (PDB code: 1RL6) from *B. stearothermophilus* as a template. Out of 20 models constructed, the model with lowest energy (molpdf) was chosen for further analysis. All structural analysis for figure 7 were carried out in Chimera using the 50S structure (PDB: 2AW4) [35,36].

Constructions of strains for determining the phenotype of the L6 protein in a wild-type background

Strain RB1095 was constructed by transforming RB247 with pMG30 such that that the expression of the *map* gene (at the end of the operon that contains the *rplF* gene) was controlled by the IPTG inducible $P_{hyperspank}$ promoter. RB1102 was constructed by transforming suppressor strain RB1051 with chromosomal DNA from RB1095 and selecting cells on IPTG, chloramphenicol and MLS (lincomycin and erythromycin) such that the *rbgA*-F6A gene at *amyE* locus was selected and the mutated *rplF* gene operon was tagged with chloramphenicol marker. RB1103, RB1106 and RB1107 were constructed similarly by using RB1055, RB1065 and RB1068 as the parental strains, respectively. RB1117 was constructed by transforming RB247 with chromosomal DNA from RB1102 and selecting cells on IPTG and chloramphenicol, thus ensuring that this strain had wild type *rbgA* gene at the native locus and the mutated *rplF* gene (operon was tagged with the chloramphenicol marker). RB1118, RB1121 and RB1122 were constructed similarly by utilizing chromosomal DNA from RB1103, RB1106 and RB1107 respectively. RB1123 was constructed by growing RB1117 on LB plates without chloramphenicol and IPTG such that the plasmid pMG30 was excised out leaving the mutated

rplF gene in a wild type background. RB1125, RB1131and RB1133 were constructed similarly from RB1118, RB1121 and RB1122 respectively.

Analysis of ribosome profiles and ribosome complexes

Ribosomal subunits were prepared by sucrose density centrifugation. 50S and 45S complexes were isolated from lysates of RB418 and RB301 cells, respectively as previously described [34]. RB1051, RB1055, RB1057, RB1063, RB1065 and RB1068 were grown to OD_{600} of 0.5 at 37°C in LB medium. Chloramphenicol (Sigma) was added to a final concentration of 100µg/ml 5 minutes prior to harvesting. Cells were harvested by centrifugation at 5000g for 10 min and resuspended in lysis buffer [10 mMTris-HCl (pH 7.5), 60 mMKCl, 10 mM $MgCl_2$, 0.5% Tween 20, 1 mM DTT, 1x Complete EDTA-free protease inhibitors (Roche) and 10 U/ml RNase-free DNase (Roche)]. Cells were lysed by three consecutive passes through a French press set at 1400 to 1600 psi and clarified by centrifugation at 16000xg for 20 minutes. Clarified cell lysates were loaded on top of 10-25% sucrose density gradients equilibrated in buffer B (10 mMTris-HCl, pH 7.6, 10 mM $MgCl_2$, 50 mM NH_4Cl) and centrifuged using a SureSpin 630 rotor (Sorvall) for 4.5 hours at 30,000 rpm. Gradients were then fractionated on a BioLogic LP chromatography system (BioRad) by monitoring UV absorbance at 254 nm. Fractions corresponding to ribosomal subunits of interest were pooled, concentrated using 100kDa cutoff filters (Millipore) and stored in buffer A (10 mM Tris-HCl, pH 7.6, 10 mM $MgCl_2$, 60 mM KCl and 1 mM DTT) at -80°C. Ribosomal subunit peak fractions were pooled, concentrated, and stored in buffer A (10 mMTris-HCl, pH 7.6, 10 mM $MgCl_2$, 60 mMKCl and 1 mM DTT) at -80°C. To visualize L16 in the subunits/intermediates 5 pmoles of each subunit to be analyzed was run on 12% NuPAGE SDS-

PAGE gel (Invitrogen) at 120V in MOPS buffer (Invitrogen) and stained using SimplyBlue SafeStain (Invitrogen) following the manufacturer's instructions. To visualize L6 protein in the subunits/intermediates 10 pmol was loaded on a 28cm long 15% Bis-Tris gel and stained using Coomassie blue stain. L6 protein was identified by LC/MS/MS. To visualize L6 on a mini gel 5 pmol of subunits were loaded on a 16% Tricine gel (Invitrogen) and stained using SimplyBlue SafeStain.

***In vitro* maturation**

Cell lysates from RB1043 and RB1055 were obtained as described above. Lysates were concentrated using 4mL Amicon ultra-4 centrifugal filters with 4 kda cutoff (Millipore). An equal volume of lysate was incubated at 37^{o}C or 0^{o}C for 1 hour then loaded onto 18-43% sucrose gradient made in buffer C (10 mMTris-HCl, pH 7.6, 20 mM $MgCl_2$, 50 mM NH_4Cl) followed by centrifugation at ~82000 g for 14 hours at 4^{o}C in Surespin 630 rotor (Sorvall). Gradients were fractionated on BioLogic LP system (BioRad) monitoring absorbance at 254 nm.

GTPase activity

The assay was performed as described [34]. Briefly, for measuring GTPase activity in the presence of ribosomal subunits/intermediates 100nM RbgA protein was incubated with 100nM 50S subunit or 45S subunit or 44S subunit and 200μM GTP at 37°C for 30 minutes and for measuring intrinsic GTPase activity 2μM RbgA protein was incubated with 200μM GTP at 37°C for 30 minutes. We predetermined that under these conditions the values were in the linear range of the assay. The phosphate released was measured using the Malachite Green Phosphate Assay Kit (BioAssaySystems).

Results

Construction of a strain containing a *rbgA* mutation with a growth phenotype suitable for a genetic suppressor screen

To generate a strain that displayed a strong growth defect that would be amenable to suppressor analysis, we analyzed the phenotypes of over 40 site-directed mutations in the *rbgA* gene [34]. We were interested in identifying substitutions in RbgA that displayed reduced GTPase activity upon association with the ribosome and were still able to bind to the ribosome. One such mutation, *rbgA*-F6A, was identified as meeting both of these criteria. Our results showed that GTPase activity of RbgA-F6A was reduced ~12 fold, however the mutation did not prevent stable association with the 45S complex and the 50S subunit [34]. Therefore we constructed a strain in which *rbgA*-F6A was the only functional copy of *rbgA* in the cell expecting that cells harboring *rbgA*-F6A would be viable but display reduced growth. To achieve this we constructed strain RB1043 by cloning the *rbgA* gene (containing a mutation that results in a F6A substitution) fused to its native promoter into the plasmid pAS24 and inserted this construct at the *amyE* locus (Table 4.1). A control strain (RB1006) that contains a wild-type copy of the *rbgA* gene at the *amyE* locus was also constructed in similar manner as a control. The native *rbgA* gene was inactivated in both strains by the insertion of a MLS cassette by marker replacement, which led to the complete removal of the *rbgA* gene. Comparison of the two strains showed that the strain expressing RbgA-F6A (RB1043) was severely growth compromised and exhibited a growth rate~7 fold slower than the RB1006 strain (Figure 4.1A). This severe growth defect was utilized to isolate suppressors that restored the ability of this strain to grow more rapidly.

To isolate independent, spontaneous suppressor mutations we inoculated a single colony of the RB1043 (*rbgA*-F6A) strain per flask into a total of 50 flasks and isolated suppressors that exhibited faster growth at 37°C (only one per flask). We identified eight independent suppressor strains that partially alleviated the growth defect of RB1043 (Figure 4.1 and Table 4.2). Individual suppressors were grown in liquid medium and their growth rates were compared to the parental RB1043 strain and the control strain RB1006. The wild-type control strain RB1006 and the parental RB1043 strains exhibited a doubling time of 23 minutes and 173 minutes, respectively, whereas the growth rate of the suppressor strains ranged from 46 to 77 minutes (Table 4.2). Next, we sequenced the *rbgA*-F6A gene to check for reversion mutations and found that all eight strains did not contain any intragenic suppressor mutations. We then proceeded to backcross each suppressor strain with the wild-type RB247 strain and inactivated the native *rbgA* gene. The reappearance of RB1043 phenotype (~ 7-fold increase in doubling time) in each backcrossed strain indicated that the suppressor mutation was unlinked to the *rbgA*-F6A mutation.

Suppressor mutations localize to the *rplF* gene, which encodes the ribosomal protein L6

To identify the genetic changes responsible for the partial suppression of the growth defect we obtained the whole genome sequence of all eight suppressor strains, RB247 (wild-type background) and the parental RB1043. The resultant sequence reads were mapped back to the *B. subtilis* reference genome. The sequence reads from parental RB1043 strain were compared with each suppressor strain sequentially. After accounting for mutations that have arisen in our genetic background or were sequencing errors in the original *B. subtilis* sequencing project [37], the analysis revealed that each suppressor strain had a single point mutation compared to the

RB1043. In each case a single point mutation in the *rplF* gene, encoding ribosomal protein L6, was found. Three suppressor strains had the same mutation (Table 4.2) and thus we obtained six unique suppressor mutations that caused single amino acid substitutions in L6; R3C, G5C, G5S, H66L (3 isolates), T68R and R70P. Alignment of L6 proteins from phylogenitcally diverse bacteria indicates that these residues are conserved in bacterial L6 proteins, with T68 demonstrating the most conservation when compared to L6 homologs from archaea and eukaryotes (Figure 4.2). We constructed a homology model of the *B. subtilis* L6 protein based on the structure of the L6 protein from *B. stearothermophilus* and mapped the suppressor mutations onto the modeled structure of the protein. Our analysis shows that all of the six suppressor substitutions reside in close vicinity in the protein structure (Figure 4.3) and are contained within the N-terminal structural domain.

Suppressor strains accumulate a novel ribosomal intermediate that is distinct from the 45S particle

To assess the status of ribosome assembly in the suppressor strains, we analyzed the ribosome profiles using 10-25% sucrose density gradients. Our results showed that all of the suppressor strains accumulated a novel ribosomal intermediate that migrated at ~44S and was distinct from the 45S complex that accumulates in RbgA-depleted cells and RB1043 strain expressing RbgA-F6A (Figure 4.4).

We isolated the 44S intermediates from each suppressor strain and analyzed the protein composition utilizing SDS-PAGE (Figure 4.5 and 4.6). The 44S intermediates from RB1055 (L6-R3C) and RB1065 (L6-G5S) exhibited significantly reduced levels of L6 whereas RB1057 (L6-H66L) and RB1063 (L6-G5C) showed a moderate reduction (Figure 4.5 and 4.6). Strains

RB1051 (L6-R70P) and RB1068 (L6-T68R) accumulated 44S intermediates with L6 protein levels similar to that observed for the 45S complex and the 50S mature subunit (Figure 4.6 and 4.6). Most of the 44S subunits lacked detectable L16, however we noticed that one 44S intermediate [RB1068 (T68R)] stably incorporated L16 to near wild-type levels (Figure 4.5 and 4.6). It is important to note that while the protein composition of the 44S intermediate with regard to the levels of L6 and L16 differs among the suppressor strains, the migration of this complex in each suppressor strain does not change, indicating that the difference in migration is likely due to additional conformational changes and/or other missing ribosomal proteins.

Next we analyzed the GTPase activity of RbgA in the presence of the 44S intermediate that accumulate in the suppressor strains. We isolated 44S particles from each suppressor strain to test if the levels of L6 or L16 in the complex influence the GTPase activity of RbgA. Our results show that GTPase activity of RbgA is stimulated ~4-6 fold in the presence of the 44S intermediates (Figure 4.7). This is similar to the fold change in GTPase activity in the presence of the 45S complex and highly reduced compared with the ~60 fold stimulation seen in the presence of the mature 50S subunit [33].

rplF mutations do not impair growth but are partially defective in ribosome subunit joining

We were interested in studying the effects of the alterations in ribosomal protein L6 on cell growth and ribosome assembly in an otherwise wild-type background. To do this we created strains in which the *rplF* mutations were linked to an antibiotic resistance marker and moved into a wild-type background RB247. . Once each mutation was transferred to a wild-type background, the antibiotic resistance marker was easily removed by passage on media without selection,

resulting in strains that only contained mutations in *rplF* (see materials and methods for details). We successfully constructed strains in which mutations in *rplF* resulting in the R3C (RB1125), G5S (RB1131), T68R (RB1133), and R70P (RB1123) substitutions were the only alterations in the chromosome (Table 4.1). Each L6 mutant strain grew at a doubling time that was indistinguishable from the congenic wild-type RB247 strain, demonstrating that the partial suppression of the RbgA-F6A growth phenotype was not due to an impairment of growth due to defects in L6.

Although the *rplF* mutations did not have an effect on cell growth, we were interested to identify if they had any impact on ribosome maturation. Ribosome profiling of strains RB1123, RB1125, RB1131 and RB1133 through 10-25% sucrose gradients was performed and in each case L6 substitutions resulted in abnormal ribosome profiles. Figure 4.8 depicts the ribosome profile of RB1123 (L6-R70P) and demonstrates that despite displaying a wild-type growth rate, the mutant has an increased level of individual ribosomal subunits when compared to wild-type cells. Each of the other three mutants tested also had altered ribosome profiles that were similar to RB1123, indicating that the L6 substitutions impact subunit joining or maintaining 70S ribosome stability (Figure 4.9). We further analyzed the 50S subunits that accumulated in these strains and found that both ribosomal proteins L6 and L16 were present in levels similar to wild-type 50S subunits (Figure 4.10) indicating that these substitutions in RplF (R3C, G5S, T68R and R70P) do not impact the association of L6 or L16 with the 50S subunit.

The 44S particle can be matured into a 50S subunit *in vitro*

One possible mechanism for how L6 substitutions may suppress the RbgA-F6A defect is that 44S particles may be more easily matured into 50S subunits than 45S particles. To address this

possibility we concentrated purified lysates from RB1043 (RbgA-F6A) and RB1055 (RbgA-F6A, L6-R3C) and incubated them at either 37°C and 0°C for 1 hour. After incubation, these lysates were centrifuged over 18-43% sucrose gradients in the presence of 20mM Mg^{2+} (to facilitate mature subunit joining since L6 mutants show subunit association defects in 10mM Mg^{2+}, see Figure 4.8). Concentration of lysates (see materials and methods) led to an increase in 70S formation in both of the RB1043 and RB1055 lysates (data not shown). Incubation of the RB1055 lysate at 37°C demonstrated that many of the 44S particles in the RB1055 lysate were converted into 50S subunits that subsequently partnered with the 30S subunits to form 70S ribosomes (Figure 4.11). 70S ribosomes showed a more than 100% increase during 37°C incubation with a concomitant decrease in 44S and 30S subunits (Figure 4.11). These data support the idea that 44S particles are able to be matured more quickly into 50S subunits than 45S particles.

Discussion

We provide evidence that mutations causing substitutions in the N-terminal domain of ribosomal protein L6 can suppress ribosome assembly defects associated with a mutation that impairs the function of the ribosome assembly factor RbgA. The suppressor substitutions in L6, when coupled with the RbgA-F6A defect, gave rise to novel 44S particles. We propose that the partial suppression of growth and ribosome assembly defects observed are not due to the fact that the L6 substitutions bypass the requirement for RbgA in the cell. This is supported by two observations. First, we have repeatedly attempted to generate an *rbgA* null mutation in the background of several of the *rplF* suppressor mutations but were unsuccessful. Second, the fact that L6 substitutions do not cause a growth defect or accumulate a 44S particle in a wild-type

background supports that the function of the RbgA-F6A protein is still required for maturation. We suggest that the L6 alterations allow the defective RbgA-F6A protein to function more effectively in ribosome assembly. The *in vitro* maturation assay further supports this idea, as evidenced by increased maturation of the 44S particle observed in RB1055 (RbgA-F6A, RplF-R3C) versus the RB1043 (RbgA-F6A) strain. In addition, all of the L6 supressors lead to increased 70S ribosome formation *in vivo*. Since the only copy of RbgA in both strains carries the F6A substitution, this indicates that the L6 substitutions, along with the partial function of RbgA, are required to facilitate large subunit maturation.

L6 is a two-domain protein that is located on the L7/L12 side of the 50S subunit and forms an L-like structure that appears to form a clamp from the front to the back of the subunit (Figure 4.12) [38,39]. The N-terminus of the protein interacts with helix 97 (h97) of 23S rRNA, while the C-terminus of L6 interacts with the sarcin/ricin loop (SRL) [38,40,41]. All of the L6 substitutions that suppress the RbgA-F6A defect map to a small region in the N-terminus of the protein and in some cases disrupt direct interactions between L6 and h97 (Figure 4.12). Although some of the suppressor mutations cause L6 to unstably associate with the 44S intermediate, the ability to suppress the RbgA-F6A defect does not seem to correlate with L6 binding as two of the 44S particles isolated from the suppressors (R70P, H66L) have near wild-type levels of L6. However, the conformation of mutated L6 might be different in 44S as the structures of the ribosome intermediates that form in the suppressor strains are clearly altered based on their slower migration within sucrose gradients. The consequence of the L6 substitutions in a wild-type background appears to be at the level of 70S stability. Individual 50S subunits that contain mutant L6 proteins appear to have normal amounts of both L6 and L16, indicating that once matured these proteins are stably incorporated. However, clearly there is some disruption of 50S

subunit structure that causes decreased stability of 70S ribosomes. This is possibly due to improper positioning of the intersubunit bridge helix 89, which is located between and makes direct contacts with L16 and L6.

What effect might mutations in L6 have in suppressing ribosome assembly defects associated with reduced function of RbgA? L6 binds prior to L16 and has been implicated in setting up the binding site for L16 [4,42]. In *E. coli*, the expression of ribosomes that are deleted for the SRL, which interacts with the C-terminus of L6, are dominant-lethal and result in the accumulation of 50S subunits that lack L16 [43]. Lancaster *et al*. propose that L6 binds to the assembling subunit via initial interactions between the N-terminus of L6 and h97, which then results in the subsequent assembly of the functional core of the 50S subunit [43]. This includes the formation of several key interactions between h97, h42, h89, h91, and h95, which are predicted to be initiated by the initial binding of L6 with h97. When the SRL is deleted these interactions are disrupted and the L16 binding site, along with other functional regions of the large subunit, are improperly assembled and non-functional. The L6-T68R mutant may therefore be an interesting mutant to study as it contains not only near normal levels of L6 and substantial levels of L16, despite still existing as a 44S particle.

Although we still do not know the precise role that RbgA plays during ribosome assembly, the identification of the second-site suppressors in L6 supports a model in which RbgA participates in facilitating the correct association of L6 with the ribosome to allow subsequent maturation events to take place (Figure 4.13). Recent studies have postulated that ribosomal subunits can be formed via multiple parallel pathways. We suspect that the large subunit pathways converge on a late assembly intermediate ($LAI_{50\text{-}1}$) and GTPases, such as RbgA, act on $LAI_{50\text{-}1}$ to complete maturation. We envision two scenarios in which RbgA could act on $LAI_{50\text{-}1}$ to facilitate

maturation. In scenario 1, RbgA binds to an undefined late assembly intermediate ($LAI_{50\text{-}2}$), and promotes the rearrangement or movement of helix 97 to facilitate the correct incorporation of L6. In scenario 2, L6 binds to the ribosome prior to RbgA (resulting $LAI_{50\text{-}3}$, equivalent to the 45S complex) in an unproductive interaction 275 and the role of RbgA binding is to promote the correct interaction of L6 with the helix 97 [43]. Recently, we have shown that the 45S particle is not a dead end particle and can be fully matured into a 50S particle *in vivo* [22]. The fact that L6 is not fully visible in the cryo-EM structures of the 45S complex provides support that L6 is not in its proper conformation [22]. In both scenarios, correct positioning of L6 and h97 allows for proteins L16, L27, L28, L33, L35, and L36 to be stably incorporated into the large subunit. Once RbgA senses that incorporation of these proteins has taken place GTP hydrolysis occurs, a final maturation event takes place, and RbgA leaves the subunit. Because we have not been able to isolate RbgA mutants that are deficient in GTPase activity that form 50S subunits, we predict that the GTP hydrolysis plays a dual role in both promoting conformational changes in the ribosome while also resulting in RbgA leaving the subunit. Support for this latter step stems from the fact that 50S subunits lacking only ribosomal proteins L16 and L28 do not stimulate the GTPase activity to levels observed with wild-type 50S subunits [22].

Although we do not know the order of binding of L6 and RbgA, in both scenarios the proposed role of RbgA is to properly position L6 and helix 97 to facilitate assembly. This interaction between L6 and h97 is evolutionarily conserved (see Figure 4.14) and, given that RbgA homologs are present in archaea and eukaryotes, the role of RbgA proteins in ribosome assembly is likely to be conserved as well. Thus it appears that in small subunit and large subunit ribosome biogenesis, one function of assembly factors is to prevent binding of late binding ribosomal proteins until the subunit is ready to receive them [22,44,45]. Whether or not these potential

checkpoints are related to quality control mechanisms that insure only functional ribosomes enter into translation remains to be seen [45]. Interestingly, *E. coli* and many other proteobacteria lack RbgA, a function that was present in the last common ancestor and subsequently lost in this lineage of bacteria. We are currently using a comparative genomics approach to identify differences between *E. coli* and *B. subtilis* ribosomes in an attempt to further localize the precise site and mechanism of RbgA function.

Strain	Relevant genotype	Source
RB301	JH 642 P*spank-rbgAcat* pMAP65	[16]
RB419	JH 642 P*spank-infBcat* pMAP65	[16]
RB1006	JH 642 Δ*rbgA*::MLS *amyE*::*rbgA*Spc^r	This study
RB1032	JH 642 Δ*rbgA*::MLS *amyE*::*rbgA-F6A*Spc^r	This study
RB1043	JH 642 Δ*rbgA*::MLS *amyE*::*rbgA-F6A*Spc^r	This study
RB1044	JH 642 Δ*rbgA*::MLS *amyE*::*rbgA-F6A*Spc^r	This study
RB1051	JH 642 Δ*rbgA*::MLS *amyE*::*rbgA-F6A*Spc^r*rplF*-R70P	This study
RB1055	JH 642 Δ*rbgA*::MLS *amyE*::*rbgA-F6A*Spc^r*rplF*-R3C	This study
RB1057	JH 642 Δ*rbgA*::MLS *amyE*::*rbgA-F6A*Spc^r*rplF*-H66L	This study
RB1059	JH 642 Δ*rbgA*::MLS *amyE*::*rbgA-F6A*Spc^r*rplF*-H66L	This study
RB1061	JH 642 Δ*rbgA*::MLS *amyE*::*rbgA-F6A*Spc^r*rplF*-H66L	This study
RB1063	JH 642 Δ*rbgA*::MLS *amyE*::*rbgA-F6A*Spc^r*rplF*-G5C	This study
Rb1065	JH 642 Δ*rbgA*::MLS *amyE*::*rbgA-F6A*Spc^r*rplF*-G5S	This study
RB1068	JH 642 Δ*rbgA*::MLS *amyE*::*rbgA-F6A*Spc^r*rplF*-T68R	This study
RB1095	JH 642 *adk*::Cm P_{spank} *map*	This study
RB1102	JH 642 Δ*rbgA*::MLS *amyE*::*rbgA-F6A*Spc^r*rplF*-R70P *adk*::Cm P_{spank} *map*	This study
RB1103	JH 642 Δ*rbgA*::MLS *amyE*::*rbgA-F6A*Spc^r*rplF*-R3C *adk*::Cm P_{spank} *map*	This study
RB1106	JH 642 Δ*rbgA*::MLS *amyE*::*rbgA-F6A*Spc^r*rplF*-G5S *adk*::Cm P_{spank} *map*	This study
RB1107	JH 642 Δ*rbgA*::MLS *amyE*::*rbgA-F6A*Spc^r*rplF*-T68R *adk*::Cm P_{spank} *map*	This study
RB1117	*rplF*-R70P *adk*::Cm P_{spank} *map*	This study
RB1118	*rplF*-R3C *adk*::Cm P_{spank} *map*	This study
RB1121	*rplF*-G5S *adk*::Cm P_{spank} *map*	This study
RB1122	*rplF*-T68R *adk*::Cm P_{spank} *map*	This study
RB1123	JH 642 *rplF*-R70P	This study

Table 4.1 List of strains used in this study

Table 4.1 (cont'd)

RB1125	JH 642 *rplF*-R3C	This study
RB1131	JH 642 *rplF*-G5S	This study
RB1133	JH 642 *rplF*-T68R	This study

Suppressor/Strain	Strain number	*rplF* gene	L6 protein	Doubling time (mins)
		codon change	Amino acid change	
Control strain	RB1006	Wild type	none	23 ± 1
Suppressor 1	RB1055	cgt to tgt	R3C	69 ± 1
Suppressor 2	RB1063	ggt to tgt	G5C	77 ± 1
Suppressor 3	RB1065	ggt to agt	G5S	52 ± 10
Suppressor 4, 5 and 6	RB1057, RB1059, RB1061	cat to ctt	H66L	66 ± 10
Suppressor 7	RB1068	acg to agg	T68R	49 ± 5
Suppressor 8	RB1051	cgc to ccc	R70P	46 ± 4
Parental strain (RbgA-F6A)	RB1043	Wild type	none	173 ± 5

Table 4.2 Suppressor mutations in ribosomal protein L6

Values represent three independent experiments ± S.D.

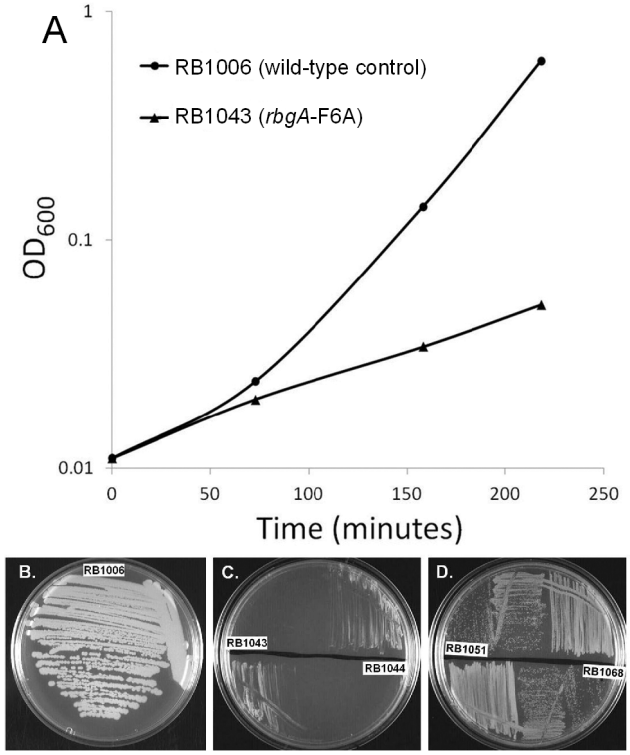

Figure 4.1 Phenotype of RB1043 (*rbgA*-F6A) and suppressor strains.

A. RbgA-F6A mutation causes a severe growth defect. Strains were grown in LB at 37°C. Strain RB1006, depicted by closed circles, is a control strain with wild type *rbgA* gene under the control of native promoter at *amyE* locus. RB1043, depicted by closed triangles, expresses *rbgA*-F6A gene under the control of native promoter at *amyE* locus. B. RB1006 (Wild-type control strain), C.RB1043 and RB1044. RB1044 is an independent isolate that contains the *rplF*-F6A mutation and has an identical phenotype. D. Two suppressor strains isolated from RB1043, (RB1051 and RB1068), that partially alleviate the growth defect. All strains were cultured on LB plates at 37°C overnight.

A.

```
Bacillus subtilis           MSRVGKKLLEIPSDVTVTLNDNNTVAVKGPKGELTRTFHPDMEIKVEDNVLTVARPSDQK 60
Bacillus stearothermophilus MXRVGKKPIEIPAGVTVTVNG-NTVTVKGPKGELTRTFHPDMTITVEGNVITVTRPSDEK 59
Clostridium difficile       MSRIGVKPIIIPAGVEVTIAEGNLVTVKGPKGTLTKQLSAELNIKKEENTIMVERPTDNK 60
Staphylococcus aureus       MSRVGKKIIDIPSDVTVTFDG-NHVTVKGPKGELSRTLNERMTFKQEENTIEVVRPSDSK 59
Neisseria gonorrhoeae       MSRVAKNPVTVPAGVEVKFGT-EALVIKGKNGELSFPLHSDVAIEFNDGKLTFVANNSSK 59
Vibrio cholerae             MSRVAKAPVAIPAGVEVKLNG-QEITIKGAKGELTRVFHNGVVIAQEDNQLTFGPREGVA 59
Escherichia coli            MSRVAKAPVVVPAGVDVKING-QVITIKGKNGELTRTLNDAVEVKHADNTLTFGPRDGYA 59
Salmonella typhi            MSRVAKAPVVVPAGVDVKING-QVITIKGKNGELTRTLNDAVEVKHADNALTFGPRDGYA 59
                            * *:.   : :*: * *..   : :.:** :* *:  :   : .      : .

Bacillus subtilis           EHRALHGTTRSLLGNMVEGVSKGFERGLELVGVGYRASKSGNKLVLNVGYSHPVEIVPEE 120
Bacillus stearothermophilus HHRALHGTTRSLLANMVEGVSKGYEKALELVGVGYRASKQGKKLVLSVGYSHPVEIEPEE 119
Clostridium difficile       KHRSLHGLTRTLLDNMVVGVNTGFEKKLELKGVGYRAQKQGKKLVMNLGFSHPVEMEDPE 120
Staphylococcus aureus       EDRTNHGTTRALLNNMVQGVSQGYVKVLELVGVGYRAQMQGKDLILNVGYSHPVEIKAEE 119
Neisseria gonorrhoeae       QANAMSGTARALVSNMVKGVSEGFEKKLQLMGVGYRAQAQGKILNLSLGFSHPIVYEMPE 119
Vibrio cholerae             NAWAQAGTARALVKNMVVGVTEGFTKKLVLKGVGYRAAMKGNAVGLTLGFSHPVEHELPA 119
Escherichia coli            DGWAQAGTARALLNSMVIGVTEGFTKKLQLVGVGYRAAVKGNVINLSLGFSHPVDHQLPA 119
Salmonella typhi            DGWAQAGTARALLNSMVIGVTEGFTKKLQLVGVGYRAAVKGNVVNLSLGFSHPVDHQLPA 119
                            .  :  * :*:*: .** **. *: : * * ******  .*: : :.:*:***:

Bacillus subtilis           GIEIEVPSQTKVVVKGTDKERVGAIAANIRAVRSPEPYKGKGIRYEGEVVRRKEGKSAK- 179
Bacillus stearothermophilus GLEIEVPSQTKIIVKGADKQRVGELAANIRAVRPPEPYKGKGIRYEGELVRLKEGKTGK- 178
Clostridium difficile       GITVEAPNQTELIVKGIDKQLVGNYAAKIRAWREPEPYKGKGIKYVDEVIRRKEGKTGKK 180
Staphylococcus aureus       NITFSVEKNTVVKVEGISKEQVGALASNIRSVRPPEPYKGKGIRYQGEYVRRKEGKTGK- 178
Neisseria gonorrhoeae       GVSVQTPSQTEIVLTGSDKQVVGQVASEIRAFRAPEPYKGKGVRYVGEVVVMKEAKKK-- 177
Vibrio cholerae             GVKAECPSQTEIVLTGCDKQVVGQVAADIRSYRAPEPYKGKGIRYADENVRSKEAKKK-- 177
Escherichia coli            GITAECPTQTEIVLKGADKQVIGQVAADLRAYRRPEPYKGKGVRYADEVVRTKEAKKK-- 177
Salmonella typhi            GITAECPTQTEIVLKGADKQVIGQVAADLRAYRRPEPYKGKGVRYADEVVRTKEAKKK-- 177
                             :  .  .:* : : * .*: :*  *:.:*: * ********::*  * :  **.*.
```

Figure 4.2 Multiple sequence alignment of L6 protein from selected bacterial species.

Substitutions in *rplF* partially suppress the growth defect of rbgA-F6A. The positions of the mutated residues are highlighted. Alignments were constructed with ClustalW with default parameters and species indicated to the left. '*' indicates positions which have a single, fully conserved residue, ':' indicates conservation between groups of strongly similar physicochemical properties, '.' indicates conservation between groups of weakly similar physicochemical properties.

Figure 4.2 (cont'd)

B.

```
Bacillus subtilis                        --MSRVGKKLLEIPSDVTVTLNDNNTVAVKGPKGELTRTFH-PD-MEIKVEDNVLTVARP   56
Haloarcula marismortui                   -----MPRVELEIPEDVDAEQDH-LDITVEGDNGSVTRRLWYPD-IDVSVDGDTVVIESD   53
Sulfolobus solfataricus                  -MQIVILREEIEIPKNVVVDLKG-SIIKIKGPKGEVVKDFSFAKGIQISLDGNKIVLETT   58
Methanothermococcus thermolithotrophicus MPVAAIMREEIDIPENVSVDING-SEVVVKSGGTELRRELSYPN-IVIKKEENKVVIEST   58
Aciduliprofundum boonei                  MPVADIVKHEITIPEGVEASLDG-FDLHIKGPKGELVREFKHTR-VKMKIEEGKIIVYCP   58
                                              : :  : **. * .  .    : ::.   .: : :     : :. :   : :

Bacillus subtilis                        SDQKEHRALHGTTRSLLGNMVEGVSKGFERGLELVGVGYRA--SKSGNKLVLN--VGYSH   112
Haloarcula marismortui                   EDNAKTMSTIGTFQSHIENMFHGVTEGWEYGMEVFYSHFPMQVNVEGDEVVIENFLGEKA   113
Sulfolobus solfataricus                  FANRRKKAVFYSIVSHIKNMITGVTKGYRYYLKIIYTHFPTSVKVVGNEVQITNLIGEKN   118
Methanothermococcus thermolithotrophicus FPRKKQAAMIGTYRAHIQNMIKGVTEGFEYKLKIRYAHFPMKVSVKGNEVIIDNFLGEKF   118
Aciduliprofundum boonei                  LPKKKEYALAGTWKAHVLNMIKGVTEGFEYHLKILYAHFPMKVTVKGNKVVIENFMGERS   118
                                           . .  :   :  : : **. **::*:.  :::    :    .  *::: :   :*

Bacillus subtilis                        PVEIVPEEGIEIEVPSQTKVVVKGTDKERVGAIAANIRAVRSPEPYKGKGIRYEGEVVRR   172
Haloarcula marismortui                   PRRTTIHGDTDVEID-GEELTVSGPDIEAVGQTAADIEQLTRINDKDV-RVFQDGVYITR   171
Sulfolobus solfataricus                  TRRAQILEGVKVTVK-GEDIVVEGPNLEAVAQTAANIESASKISGFDR-RIFSDGIFIYK   176
Methanothermococcus thermolithotrophicus PRKAKVMEGTKVKVS-GEDVIVTGADKEKVGQTAANIEQATKVKGRDI-RVFQDGIYIVE   176
Aciduliprofundum boonei                  PRYADIFGDAKVEIK-GDMVIVKSINKEHAGQTAANIERATRIKNRDP-RVFQDGIYIVK   176
                                                    .: :     : * . : * ..  **:*.     .  .   :  :*  : .

Bacillus subtilis                        KEGKSAK   179
Haloarcula marismortui                   KPNRGDA   178
Sulfolobus solfataricus                  KEVIE--   181
Methanothermococcus thermolithotrophicus KAGKVL-   182
Aciduliprofundum boonei                  KG-----   178
                                         *
```

Figure 4.2 (cont'd)

C

```
Bacillus subtilis            -MSRVGKKLLEIPSDVTVTLNDNNTVAVKGPKGELTRTFHP-DMEIKV---EDNVLTVAR   55
Homo sapiens                 MKTILSNQTVDIPENVDITLKG-RTVIVKGPRGTLRRDFNHINVELSLLGKKKKRLRVDK   59
Mus musculus                 MKTILSNQTVDIPENVEITLKG-RTVIVKGPRGTLRRDFNHINVELSLLGKKKKRLRVDK   59
Saccharomyces cerevisiae     MKYIQTEQQIEVPEGVTVSIKS-RIVKVVGPRGTLTKNLKHIDVTFTKVNNQ--LIKVAV   57
                                   :: :::*. * ::::  . * * **:* * : :.  :: :.    :   : *

Bacillus subtilis            PSDQKEHRALHGTTRSLLGNMVEGVSKGFERGLELVGVGYRASK-----SGNKLV-----   105
Homo sapiens                 WWGNRKELATVRTICSHVQNMIKGVTLGFRYKMRSVYAHFPINVVIQE--NGSLVEIRNF   117
Mus musculus                 WWGNRKELATVRTICSHVQNMIKGVTLGFRYKMRSVYAHFPINVVIQE--NGSLVEIRNF   117
Saccharomyces cerevisiae     HNGGRKHVAALRTVKSLVDNMITGVTKGYKYKMRYVYAHFPINVNIVEKDGAKFIEVRNF   117
                                 ::. *   *  * : **: **: *:.  :. * . :  .         .::

Bacillus subtilis            LNVGYSHPVEIVPEEGIEIEVPSQTKVVVKGTDKERVGAIAANIRAVRSPEPYKGKGIR-   164
Homo sapiens                 LGEKYIRRVRMRPGVACSVSQAQKDELILEGNDIELVSNSAALIQQATTV---KNKDIRK   174
Mus musculus                 LGEKYIRRVRMRTGVACSVSQAQKDELILEGNDIELVSNSAALIQQATTV---KNKDIRK   174
Saccharomyces cerevisiae     LGDKKIRNVPVRDGVTIEFSTNVKDEIVLSGNSVEDVSQNAADLQQICRV---RNKDIRK   174
                             *     : * :      ...   : ::::.*.. * *.  ** ::        : * **

Bacillus subtilis            --------YEGEVVRRKEGKSAK   179
Homo sapiens                 FLDGIYVSEKGTVQQADE-----   192
Mus musculus                 FLDGIYVSEKGTVQQADE-----   192
Saccharomyces cerevisiae     FLDGIYVSHKGFITED-------   190
                                    :* : .
```

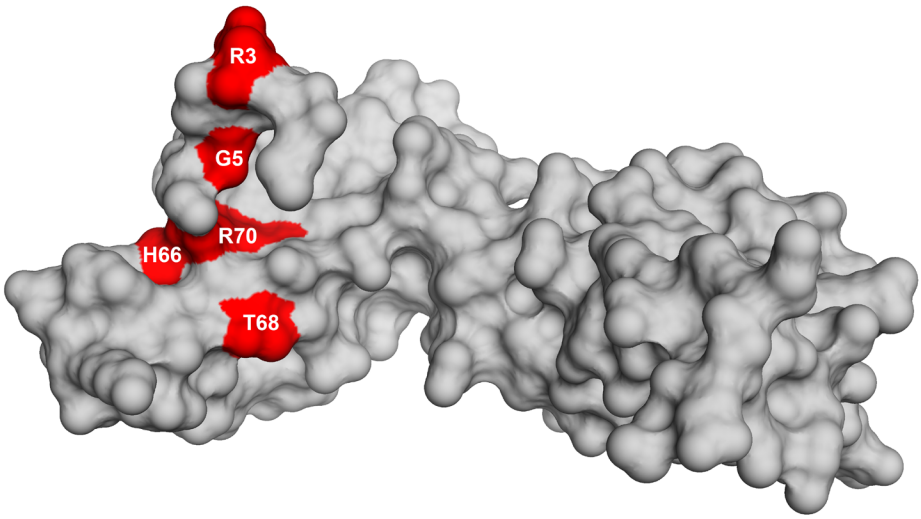

Figure 4.3 Homology model of L6 protein depicting the suppressor mutations**.**

Homology model of L6 protein of *B. subtilis* is shown as a surface representation in grey. The residues that are mutated in the suppressor strains, highlighted in red with the corresponding amino acid labeled.

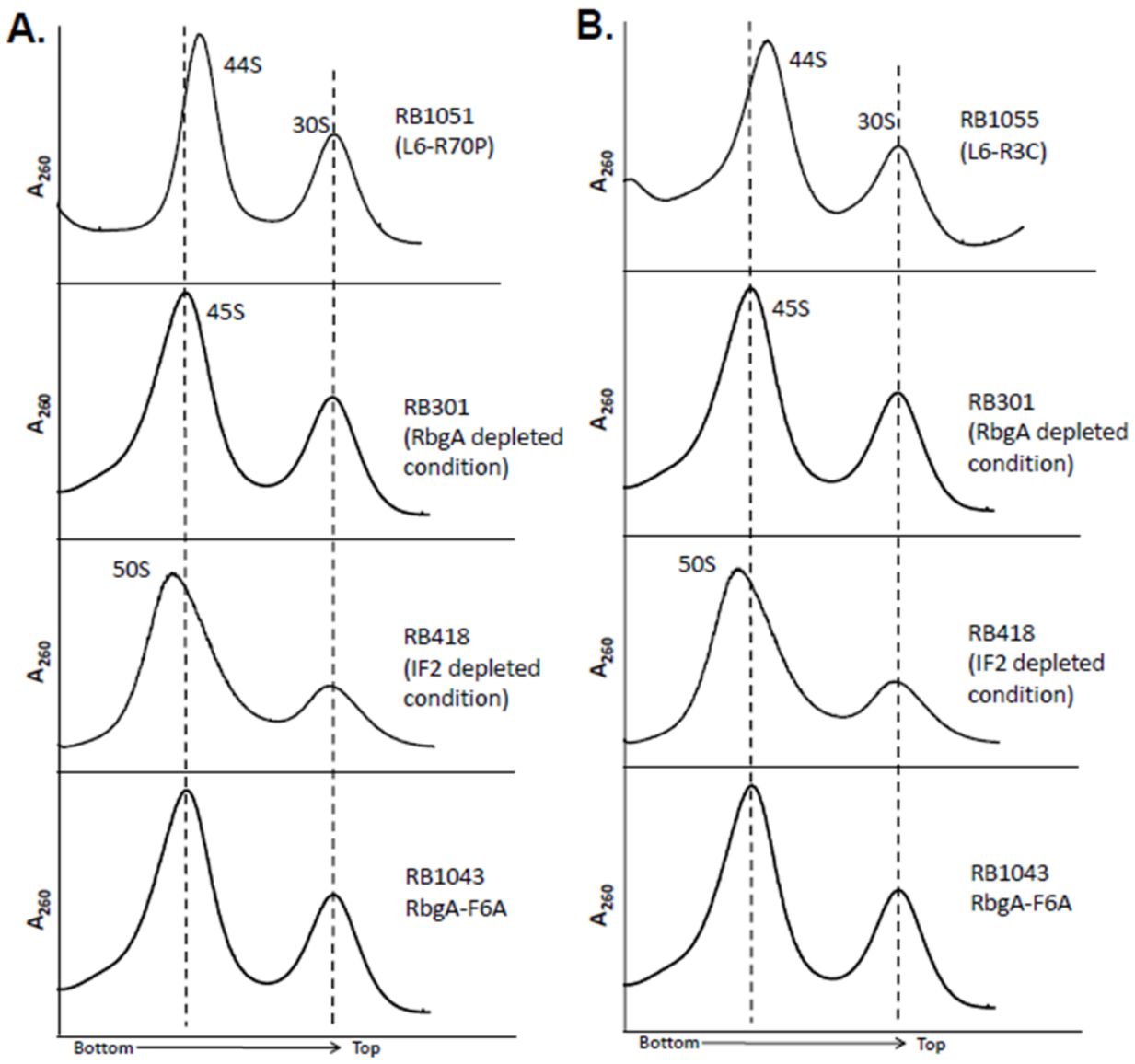

Figure 4.4 The ribosome profile of RbgA-F6A suppressor strain show an accumulation of a novel 44S complex.

Ribosome profiles were analyzed from RB1051 (A), RB1055 (B), RB1057 (C), RB1065 (D), RB1068 (E) and RB1063 (F). The ribosome profile from the suppressor strains were aligned with ribosome profiles from RbgA depleted cells (panel 2), IF-2 depleted cells (panel 3) and RB1043 (panel 4). Profiles are generated from the bottom of the gradient (25%) to the top of the gradient (10%) by ultracentrifugation for 16 hours. (G-H) Ribosome profiles were analyzed through a 10-25% sucrose density gradient after ultracentrifugation for 3.5 hours. All suppressor strains accumulated a 44S complex that differs in migration through the gradient from the 45S complex seen in the profile of RbgA depleted cells and parental strain RB1043 that expresses RbgA-F6A and the 50S ribosomal subunit seen in IF-2 depleted cells. Profiles are generated from the bottom of the gradient (25%) to the top of the gradient (10%). Dashed lines indicate the migration of the 45S and the 30S complex in the gradient.

Figure 4.4 (cont'd)

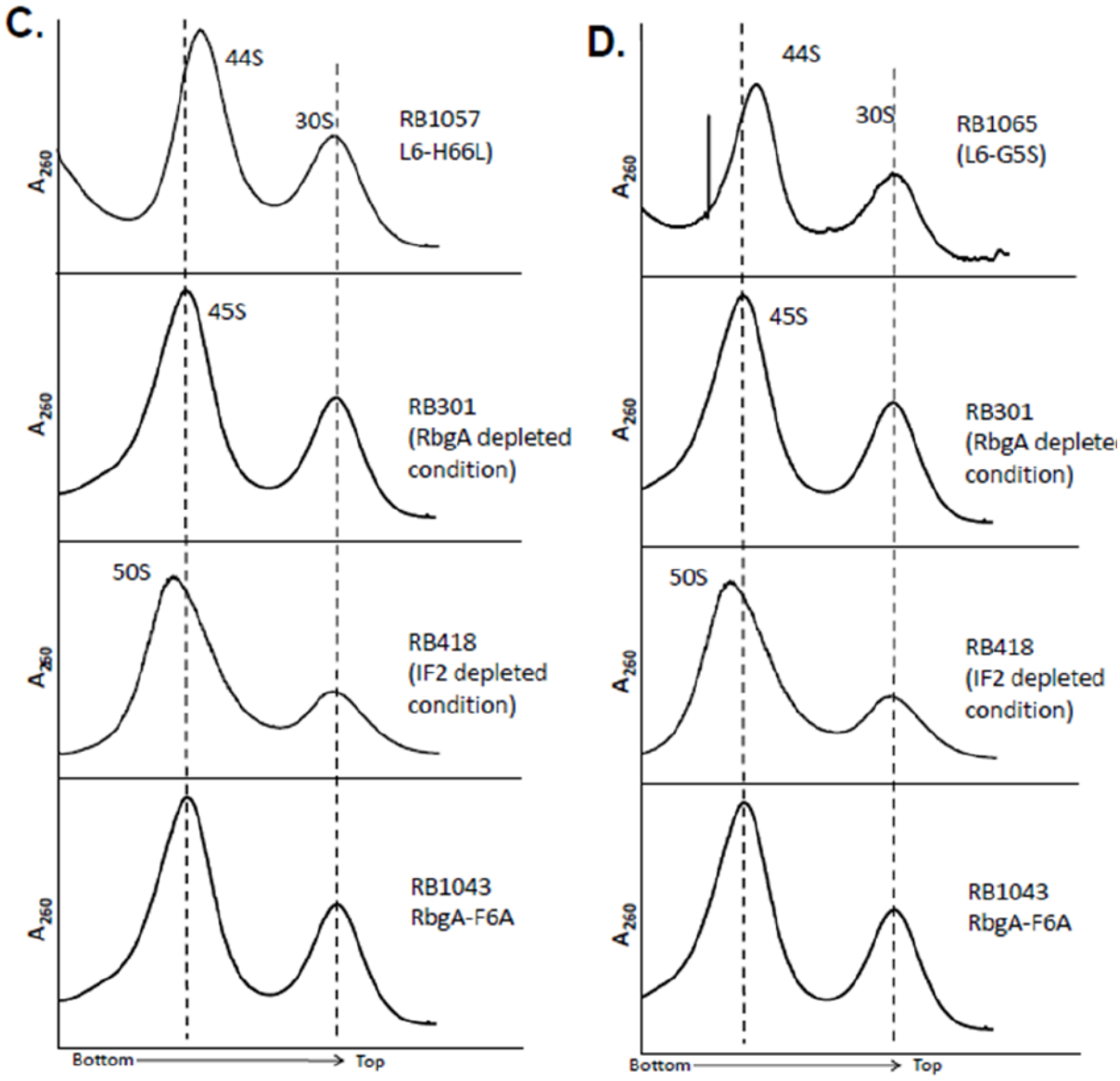

Figure 4.4 (cont'd)

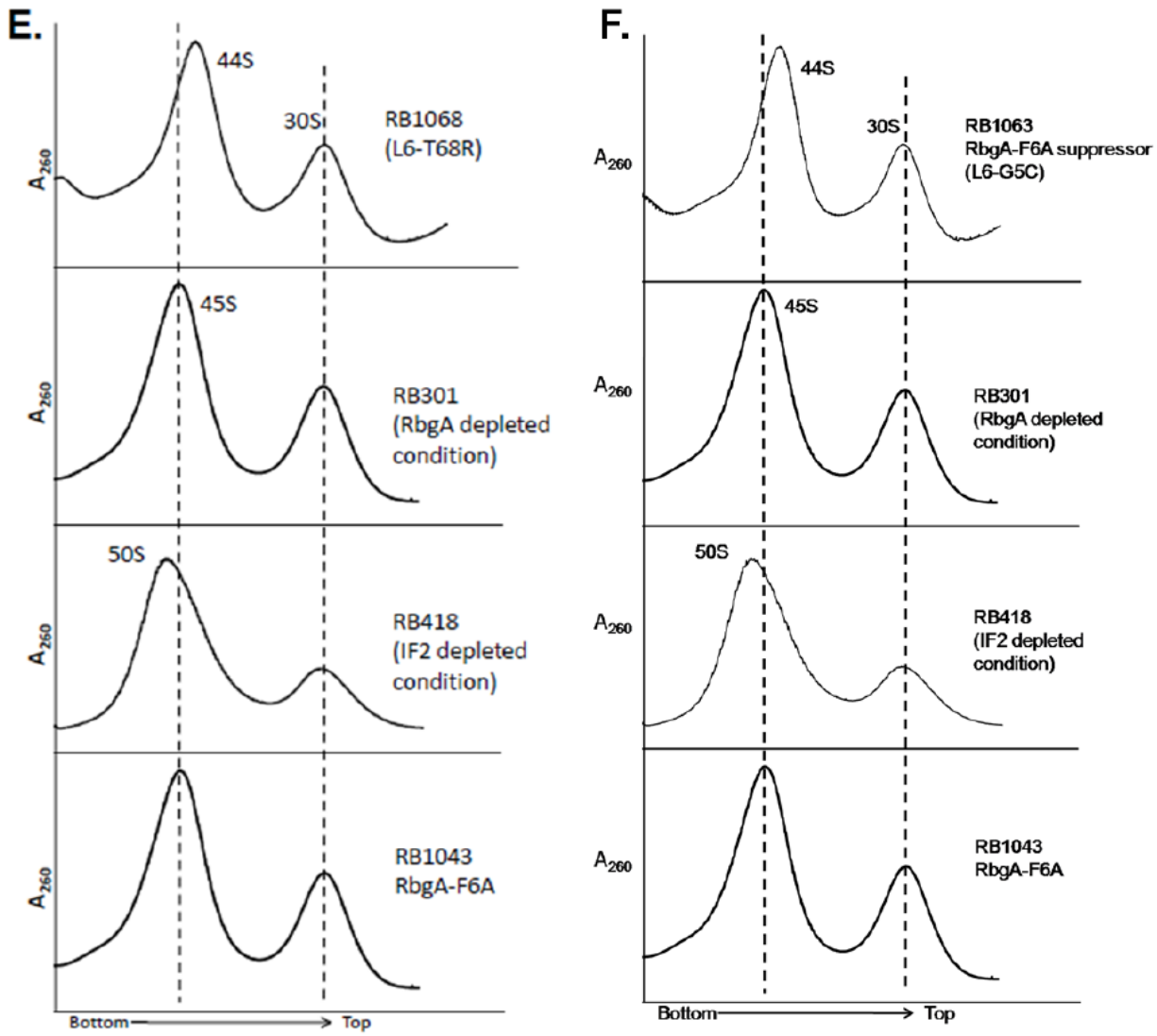

Figure 4.4 (cont'd)

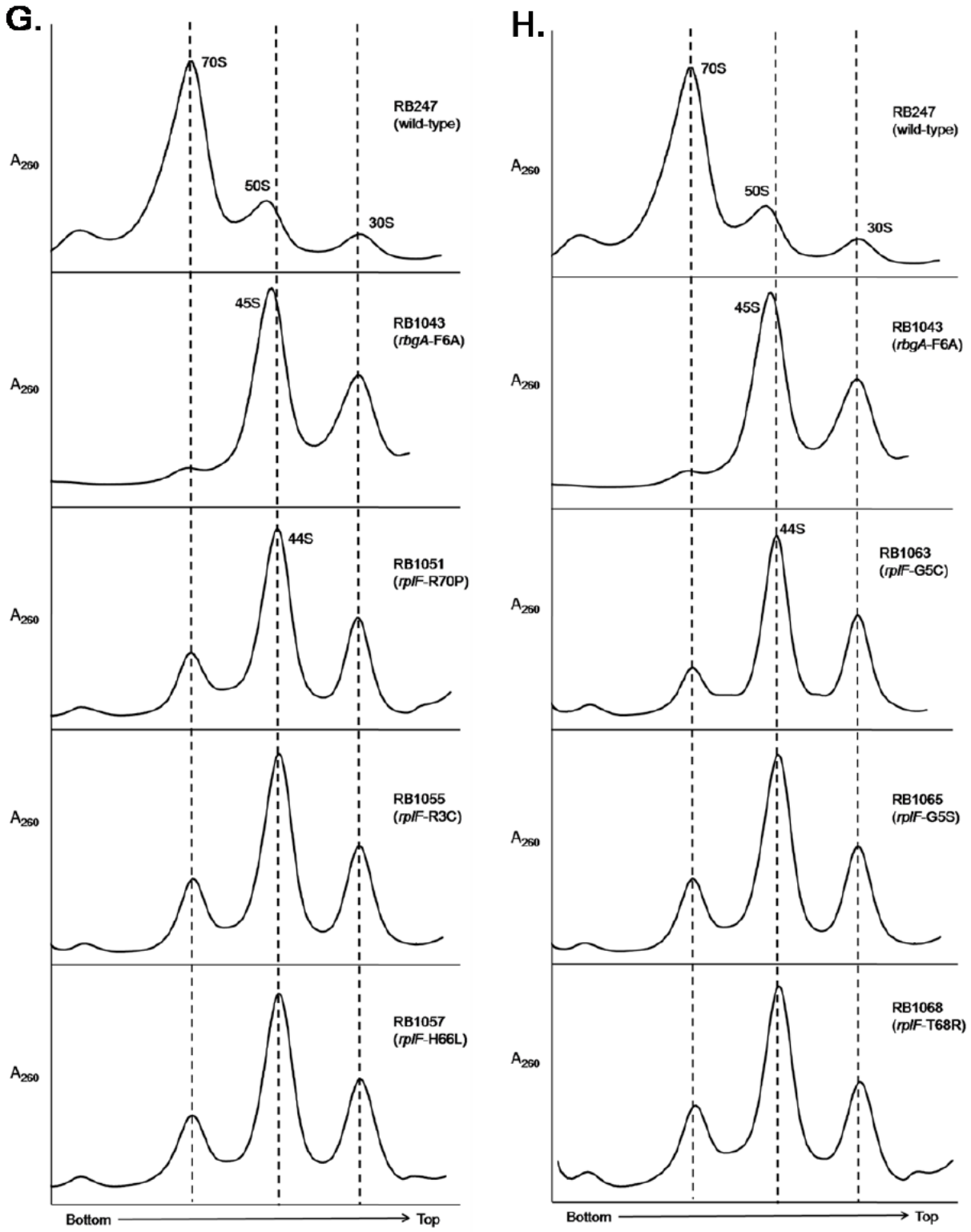

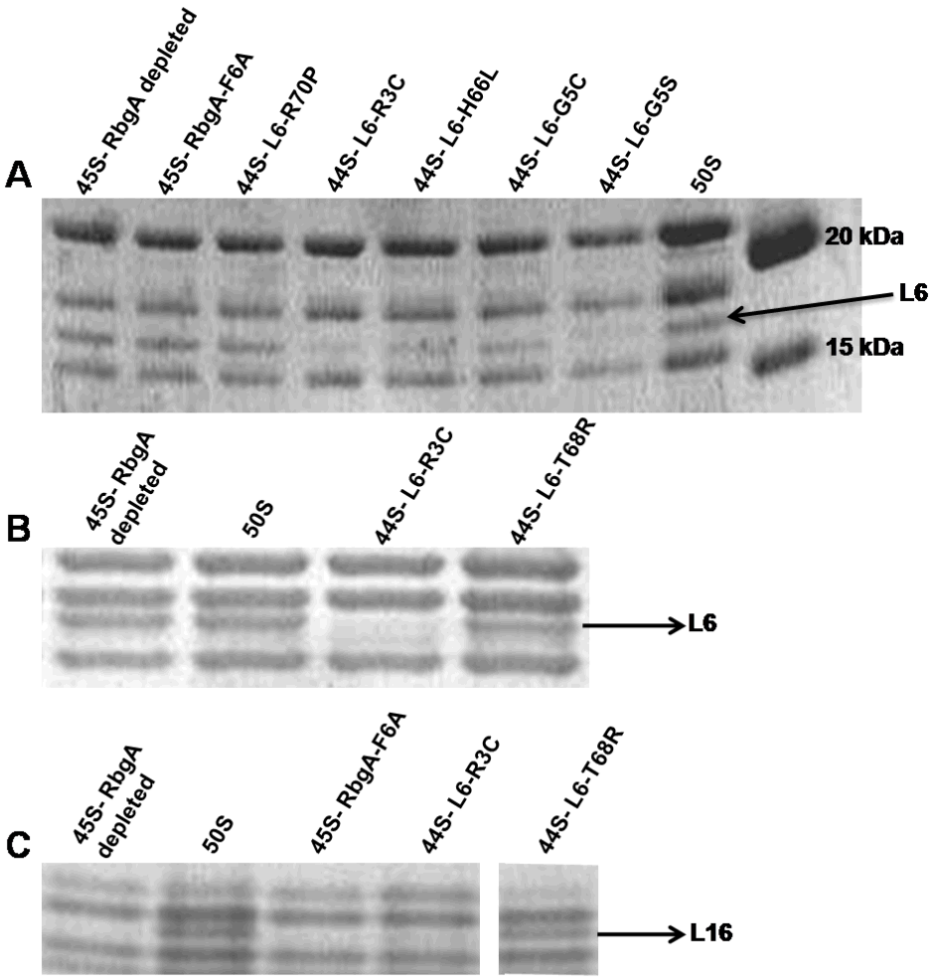

Figure 4.5 Analysis of ribosomal proteins in 44S intermediates**.**

A. Ribosomal protein L6 is not stably incorporated in all 44S intermediates isolated from the suppressor strains. Lane 1: 45S isolated from RB301 by depletion of RbgA; lane 2: 45S complex isolated from RB1043 (*rbgA*-F6A); lane 3: 44S complex isolated from RB1051 (*rplF*-R70P); lane 4: 44S complex isolated from RB1055 (*rplF*-R3C); lane 5: 44S complex isolated from RB1057 (*rplF*-H66L); lane 6: 44S complex isolated from RB1063 (*rplF*-G5C); lane 7: 44S complex isolated from RB1065 (*rplF*-G5S); lane 8: mature 50S subunit isolated from RB418 by depletion of IF2 and lane 9: BioRad PrecisionPlus AllBlue protein marker. L6 protein was confirmed by LC/MS/MS. All complexes were analyzed on a 28cm 15% Bis-Tris gel. B. Ribosomal protein L6 is stably integrated in 44S intermediate isolated from RB1068. Lane 1: 45S isolated from RB301 by depletion of RbgA; lane 2: mature 50S subunit isolated from RB418 by depletion of IF2; lane 3: 44S complex isolated from RB1055 (*rplF*-R3C) and lane 4: 44S complex isolated from RB1068 (*rplF*-T68R). All complexes were analyzed on 16% Tricine gel. (C) 44S complex isolated from RB1068 contains ribosomal protein L16. Lane 1: 45S isolated from RB301 by depletion of RbgA; lane 2: mature 50S subunit isolated from RB418 by depletion of IF2; lane 3: 45S complex isolated from RB1043 (*rbgA*-F6A); lane 4: 44S complex isolated from RB1055 (*rplF*-R3C) and lane 5: 44S complex isolated from RB1068 (*rplF*-T68R). All complexes were analyzed on 12% Bis-Tris gel.

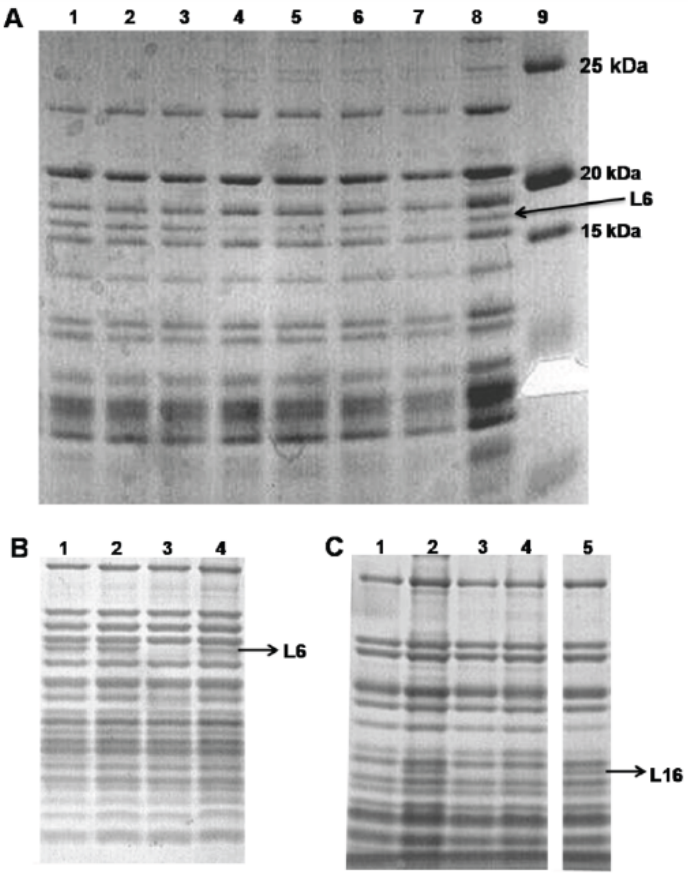

Figure 4.6 Analysis of ribosomal protein composition of 44S intermediates.

A. Ribosomal protein L6 is not stably incorporated in all 44S intermediates isolated from the suppressor strains. Lane 1: 45S isolated from RB301 by depletion of RbgA; lane 2: 45S complex isolated from RB1043 (*rbgA-F6A*); lane 3: 44S complex isolated from RB1051 (*rplF-R70P*); lane 4: 44S complex isolated from RB1055 (*rplF-R3C*); lane 5: 44S complex isolated from RB1057 (*rplF-H66L*); lane 6: 44S complex isolated from RB1063 (*rplF-G5C*); lane 7: 44S complex isolated from RB1065 (*rplF-G5S*); lane 8: mature 50S subunit isolated from RB418 by depletion of IF2 and lane 9: BioRad Precision Plus All Blue protein marker. L6 protein was confirmed by LC/MS/MS. All complexes were analyzed on a 28cm 15% Bis-Tris gel.
B. Ribosomal protein L6 is stably integrated in 44S intermediate isolated from RB1063. Lane 1: 45S isolated from RB301 by depletion of RbgA; lane 2: mature 50S subunit isolated from RB418 by depletion of IF2; lane 3: 44S complex isolated from RB1055 (*rplF-R3C*) and lane 4: 44S complex isolated from RB1068 (*rplF-T68R*). L6 protein was confirmed by LC/MS/MS. All complexes were analyzed on 16% Tricine gel. C. 44S complex isolated from RB1068 contains ribosomal protein L16. Lane 1: 45S isolated from RB301 by depletion of RbgA; lane 2: mature 50S subunit; lane 3: 45S complex isolated from RB1043 (*rbgA-F6A*); lane 4: 44S complex isolated from RB1055 (*rplF-R3C*) and lane 5: 44S complex isolated from RB1068 (*rplF-T68R*). L16 protein was confirmed by LC/MS/MS. All complexes were analyzed on 12% Bis-Tris gel.

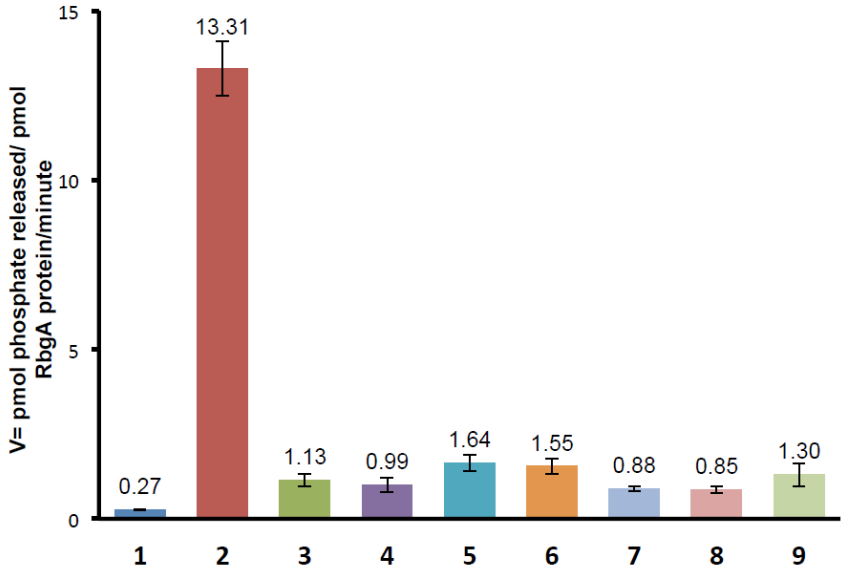

Figure 4.7 Measurement of GTPase activity of RbgA in the presence of 44S intermediate from suppressor strains.

The intrinsic GTPase activity of RbgA (lane 1) was determined by incubation of 2μM RbgA protein with 200μM GTP for 15 minutes at 37°C. Stimulation of GTPase activity was measured by incubation of 100nM RbgA protein with 100nM of mature 50S subunit (lane 2); 45S complex isolated from RbgA depleted cells (lane 3); 44S intermediate isolated from suppressor strain RB1051 (lane4); 44S intermediate isolated from suppressor strain RB1055 (lane5); 44S intermediate isolated from suppressor strain RB1057 (lane6); 44S intermediate isolated from suppressor strain RB1063 (lane7); 44S intermediate isolated from suppressor strain RB1065 (lane8) and 44S intermediate isolated from suppressor strain RB1068 (lane9). The values represent the average of three independent experiments and the error bars represent the S.D.

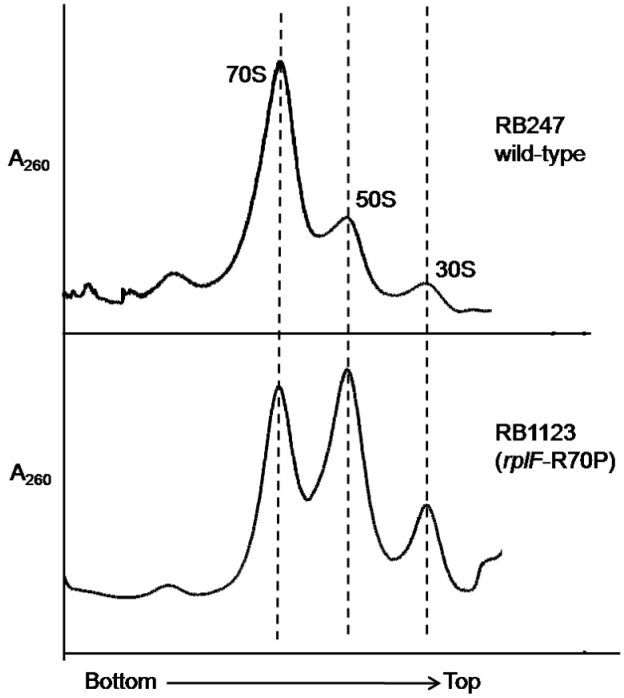

Figure 4.8 Mutations in L6 protein affect subunit joining/interaction.

Ribosome profiles of strains expressing mutated L6 protein [RB1123 (*rplF*-R70P) is depicted here as an example] show a higher concentration of individual ribosomal subunits and lower concentration of 70S ribosomes compared with ribosome profile of wild type cells. The X-axis indicates the direction of the profiles from the bottom of the gradient (25%) to the top of the gradient (10%). The Y-axis depicts absorbance at 260nm, which is equivalent for both plots depicted. Dashed lines indicate the migration of the 70S, 50S and the 30S complexes in the gradient.

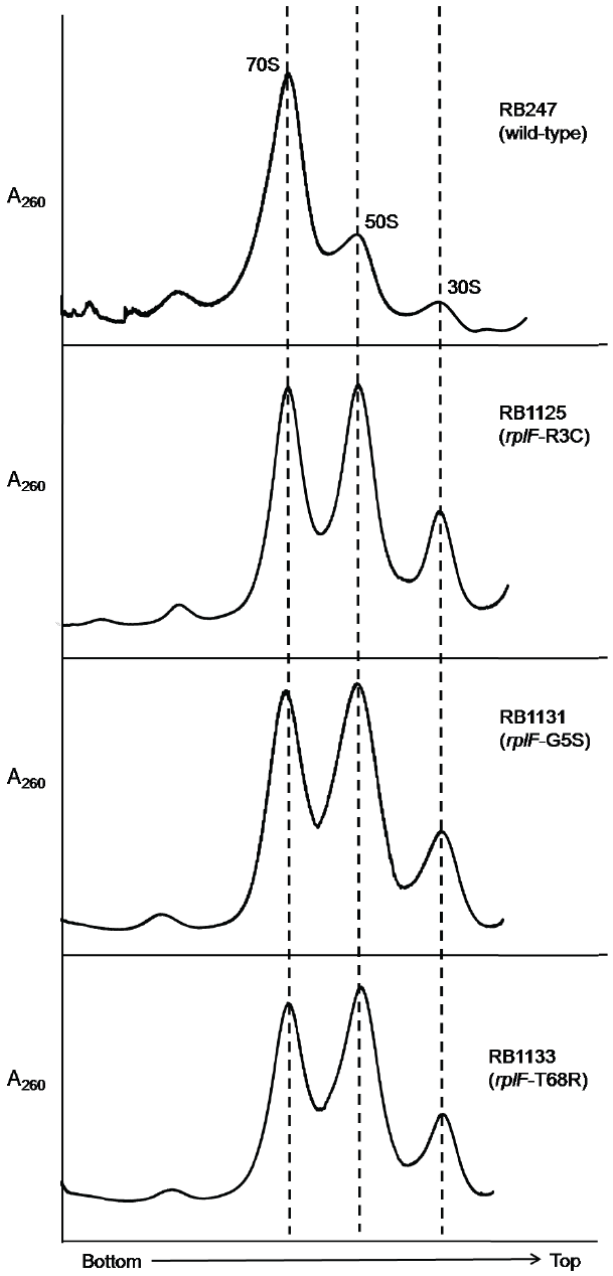

Figure 4.9 Mutations in L6 protein affect subunit joining/interaction.

Ribosome profiles of strains expressing mutated L6 protein RB1125 (panel 2), RB1131 (panel 3) and RB1133 (panel 4) show a higher concentration of individual ribosomal subunits and lower concentration of 70S ribosomes compared with ribosome profile of wild type cells (panel 1). The X-axis indicates the direction of the profiles from the bottom of the gradient (25%) to the top of the gradient (10%). The Y-axis depicts absorbance at 260nm, which is equivalent for all plots depicted. Dashed lines indicate the migration of the 70S, 50S and the 30S complexes in the gradient.

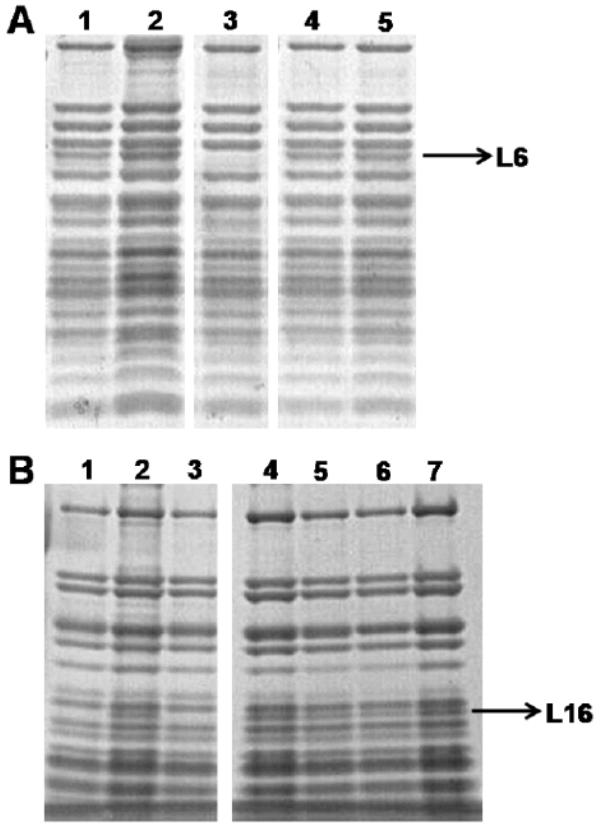

Figure 4.10 Analysis of ribosomal proteins L6 and L16 in 50S subunits that accumulate in strains expressing *rplF* substitutions in wild-type background.

A. Ribosomal protein L6 is stably integrated in 50S subunits isolated from strains expressing mutation L6 protein. Lane 1: 50S isolated from RB1123 (*rplF*-R70P); lane 2: 50S subunit isolated from RB1125 (*rplF*-R3C); lane 3: 44S complex isolated from RB1055 (*rplF*-R3C); lane 4: 50S subunit isolated from RB1131 (*rplF*-G5S) and lane 5: 50S subunit isolated from RB1133 (*rplF*-T68R). L6 protein was confirmed by LC/MS/MS. All complexes were analyzed on 16% Tricine gel. B. 50S subunits also stably integrate ribosomal protein L16. Lane 1: 45S isolated from RB301 by depletion of RbgA; lane 2: mature 50S subunit; lane 3: 45S complex isolated from RB1043 (*rbgA*-F6A); lane 4: 50S subunit isolated from RB1123 (*rplF*-R70P); lane 5: 50S subunit isolated from RB1125 (*rplF*-R3C); lane 6: 50S subunit isolated from RB1131 (*rplF*-G5S) and lane 7: 50S subunit isolated from RB1133 (*rplF*-T68R). L16 protein was confirmed by LC/MS/MS. All complexes were analyzed on 12% Bis-Tris gel.

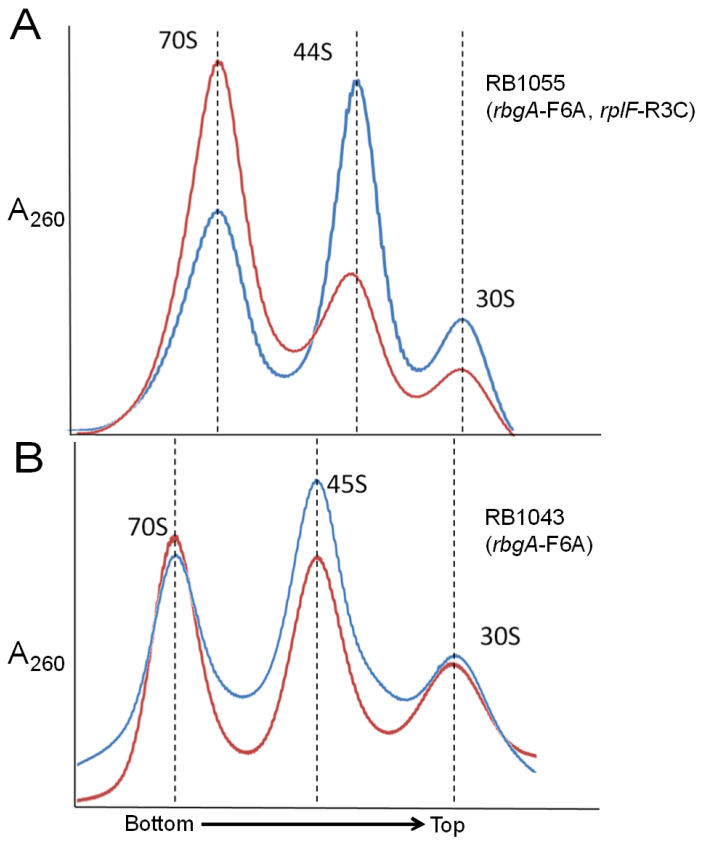

Figure 4.11 *In vitro* maturation of large subunit intermediates.

(A) *in vitro* maturation of 44S intermediate from RB1055. Ribosome profile from cell lysate of strain RB1055 expressing mutated L6 protein (R3C) and RbgA-F6A protein after incubation at 0°C (blue) and 37°C (red) for 60 minutes. The profiles show a maturation of the 44S subunit to the 50S subunit and a ~100% increase in the levels of 70S ribosomes after incubation at 37°C. (B) *in vitro* maturation of 45S intermediate from RB1043. Ribosome profiles from cell lysate of strain RB1043 expressing RbgA-F6A protein and wild-type L6 protein after incubation at 0°C (blue) or 37°C (red) for 60 minutes. The profiles show a moderate ~10% increase in the level of 70S ribosome after incubation at 37°C. The X-axis indicates the direction of the profiles from the bottom of the gradient (43%) to the top of the gradient (18%). The Y-axis depicts absorbance at 260nm, which is equivalent for both plots depicted. Dashed lines indicate the migration of the 70S, 50S, 44S and the 30S complexes in the gradient.

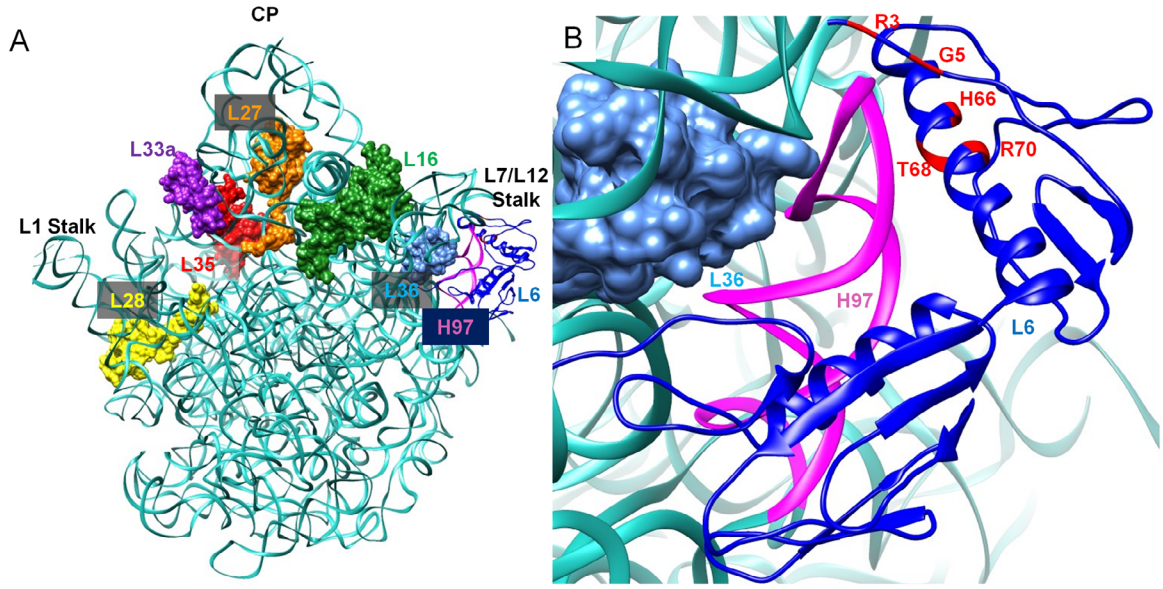

Figure 4.12 Interactions between L6 protein with the 50S ribosomal subunit.

Crystal structure of 50S subunit from *E. coli* (PDB ID :2AW4) with the late binding ribosomal proteins (as indicated in figure) missing from intermediate 45S particles are shown in left panel. Surface representation of all proteins are shown while RNA is shown in ribbon form. L6 binding region including helix 97(colored magenta) is shown in magnified view in right panel. The residues which are mutated in suppressor strains are colored in red at the N terminal of L6 protein.

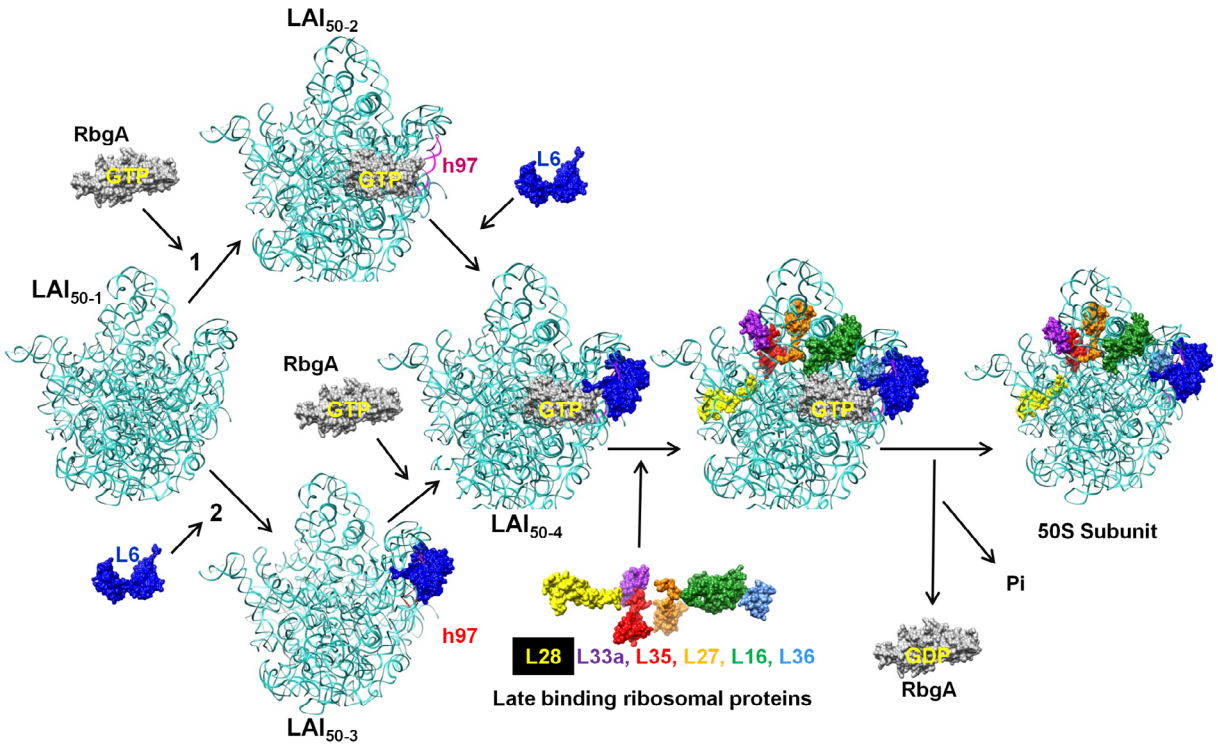

Figure 4.13 Proposed model for the role of RbgA in the mediating productive h97-L6 interactions during the assembly of large ribosomal subunit.

RbgA is an essential protein and play a role in establishing correct L6-helix 97 interactions. An intermediate (depicted as A) first bind to RbgA (depicted as B) that make the correct incorporation site for L6 binding. After RbgA binding L6 joins the complex (C) which prepare the binding site for binding of other late binding ribosomal proteins. Once the complex is complete (D) the mature subunit stimulate the GTP hydrolysis activity of RbgA, that convert GTP bound form of RbgA to GDP bound form which do not have affinity for 50S, as a result RbgA in GDP bound form leaves the complex. In absence of RbgA, L6 binds to the intermediate and forms 45S particle (I), but this complex cannot proceed further without the presence of RbgA probably due to unproductive interactions between RbgA and L6. RbgA binding reverses this interactions and assembly proceeds further as explained. (RbgA binding site is not known the figure shows hypothetical binding site just for imagining)

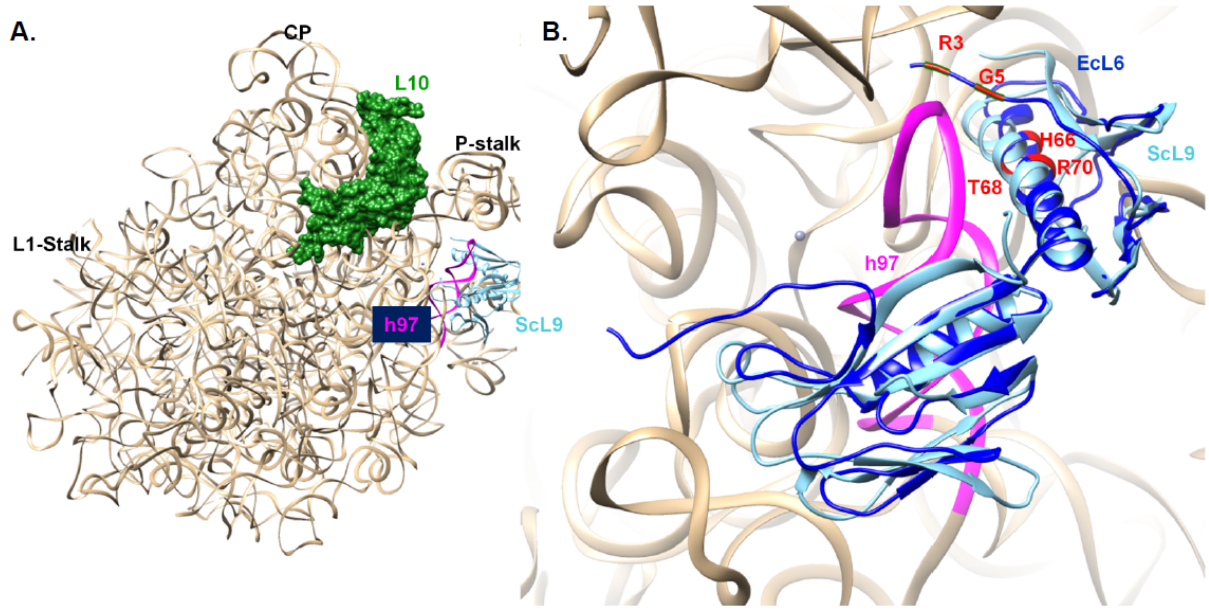

Figure 4.14 Conserved interactions between L6 and helix 97 of 23S rRNA (ScL9-h97)

A. Crystal structure of 60S subunit from *Saccharomyces cerevisiae* (PDB ID: 3U5D and 3U5E) with the positions of ribosomal protein L9 (ScL9, homolog of bacterial ribosomal protein L6, cyan) and ribosomal protein L10 (homolog of bacterial ribosomal protein L16, green) highlighted. B. A magnified view of the interaction between ScL9 (cyan) and h97 (magenta) is shown. Structure of ribosomal protein L6 from *E. coli* (EcL6, blue) from 50S subunit (PDB ID: 2AW4) is superimposed on ScL9 (cyan) and the residues mutated in *B. subtilis* suppressor strains are shown in red.

REFERENCES

REFERENCES

1. Nomura, M. (1970) Bacterial ribosome. *Bacteriological Reviews* 34: 228-77.

2. Wilson, D.N., Nierhaus, K.H. (2007) The weird and wonderful world of bacterial ribosome regulation. *Crit Rev Biochem Mol Biol* 42: 187-219.

3. Nierhaus, K.H. (1991) The assembly of prokaryotic ribosomes. *Biochimie* 73: 739-55.

4. Rohl, R., Nierhaus, K. (1982) Assembly map of the large subunit (50S) of *Escherichia coli* ribosomes. *Proc Natl Acad Sci U S A* 79: 729-33.

5. Nomura, M., Erdmann, V.A. (1970) Reconstitution of 50S ribosomal subunits from dissociated molecular components. *Nature* 228: 744-8.

6. Nomura, M., Fahnestock, S. (1973) Reconstitution of 50S ribosomal subunits and the role of 5S RNA. *Basic Life Sci* 1: 241-50.

7. Shajani, Z., Sykes, M.T., Williamson, J.R. (2011) Assembly of bacterial ribosomes. *Annu Rev Biochem* 80: 501-26.

8. Green, R., Noller, H.F. (1999) Reconstitution of functional 50S ribosomes from *in vitro* transcripts of *Bacillus stearothermophilus* 23S rRNA. *Biochemistry* 38: 1772-9.

9. Mulder, A.M.*, et al.* (2010) Visualizing ribosome biogenesis: Parallel assembly pathways for the 30S subunit. *Science* 330: 673-7.

10. Guo, Q.*, et al.* (2013) Dissecting the *in vivo* assembly of the 30S ribosomal subunit reveals the role of RimM and general features of the assembly process. *Nucleic Acids Res* 41: 2609-20.

11. Sykes, M.T., Shajani, Z., Sperling, E., Beck, A.H., Williamson, J.R. (2010) Quantitative proteomic analysis of ribosome assembly and turnover *in vivo J Mol Biol* 403: 331-45.

12. Britton, R.A. (2009) Role of GTPases in bacterial ribosome assembly. *Annu Rev Microbiol* 63: 155-76.

13. Connolly, K., Culver, G. (2009) Deconstructing ribosome construction. *Trends Biochem Sci* 34: 256-63.

14. Fromont-Racine, M., Senger, B., Saveanu, C., Fasiolo, F. (2003) Ribosome assembly in eukaryotes. *Gene* 313: 17-42.

15. Strunk, B.S., Karbstein, K. (2009) Powering through ribosome assembly. *RNA* 15: 2083-104.

16. Uicker, W.C., Schaefer, L., Britton, R.A. (2006) The essential GTPase RbgA (YlqF) is required for 50S ribosome assembly in *Bacillus subtilis*. *Mol Microbiol* 59: 528-40.

17. Matsuo, Y.*, et al.* (2006) The GTP-binding protein YlqF participates in the late step of 50S ribosomal subunit assembly in *Bacillus subtilis*. *J Biol Chem* 281: 8110-7.

18. Kotani, T., Shiori Akabane, Kunio Takeyasu, Takuya Ueda, Takeuchi., N. (2013) Human G-proteins, OBGH1 and MTG1, associate with the large mitochondrial ribosome subunit and are involved in translation and assembly of respiratory complexes. *Nucleic Acids Res* 41: 3713-22.

19. Kallstrom, G., Hedges, J., Johnson, A. (2003) The putative GTPases NOG1p and LSG1p are required for 60S ribosomal subunit biogenesis and are localized to the nucleus and cytoplasm, respectively. *Mol Cell Biol* 23: 4344-55.

20. Bassler, J., Kallas, M., Hurt, E. (2006) The NUG1 GTPase reveals and N-terminal RNA-binding domain that is essential for association with 60 S pre-ribosomal particles. *J Biol Chem* 281: 24737-44.

21. Im, C.H.*, et al.* (2011) Nuclear/nucleolar GTPase 2 proteins as a subfamily of YlqF/YawG GTPases function in pre-60S ribosomal subunit maturation of mono- and dicotyledonous plants. *J Biol Chem* 286: 8620-32.

22. Jomaa, A.*, et al.* (2014) Functional domains of the 50S subunit mature late in the assembly process. *Nucleic Acids Res* 42: 3419-35.

23. Ban, N. (2000) The complete atomic structure of the large ribosomal subunit at 2.4 A resolution. *Science* 289: 905-20.

24. Nierhaus, K.H., Wilson, D.N. (2006) Peptidyl transfer on the ribosome. *eLS*.

25. Wilson, D.N., Nierhaus, K.H. (2005) Ribosomal proteins in the spotlight. *Crit Rev Biochem Mol Biol* 40: 243-67.

26. Wekselman, I.*, et al.* (2009) Ribosome's mode of function: Myths, facts and recent results. *J Pept Sci* 15: 122-30.

27. Wang, Y., Xiao, M. (2012) Role of the ribosomal protein L27 revealed by single-molecule FRET study. *Protein Sci* 21: 1696-704.

28. Maguire, B.A., Beniaminov, A.D., Ramu, H., Mankin, A.S., Zimmermann, R.A. (2005) A protein component at the heart of an RNA machine: The importance of protein L27 for the function of the bacterial ribosome. *Mol Cell* 20: 427-35.

29. Akanuma, G.*, et al.* (2012) Inactivation of ribosomal protein genes in *Bacillus subtilis* reveals importance of each ribosomal protein for cell proliferation and cell differentiation. *J Bacteriol* 194: 6282-91.

30. Teraoka, H., Nierhaus, K.H. (1978) Protein L16 induces a conformational change when incorporated into a L16-deficient core derived from *Escherichia coli* ribosomes. *FEBS Lett* 88: 223-6.

31. Hedges, J., West, M., Johnson, A.W. (2005) Release of the export adapter, Nmd3p, from the 60s ribosomal subunit requires Rpl10p and the cytoplasmic GTPase Lsg1p. *EMBO J* 24: 567-79.

32. West, M., Hedges, J.B., Chen, A., Johnson, A.W. (2005) Defining the order in which Nmd3p and Rpl10p load onto nascent 60S ribosomal subunits. *Mol Cell Biol* 25: 3802-13.

33. Achila, D., Gulati, M., Jain, N., Britton, R.A. (2012) Biochemical characterization of ribosome assembly GTPase RbgA in *Bacillus subtilis*. *J Biol Chem* 287: 8417-23.

34. Gulati, M., Jain, N., Anand, B., Prakash, B., Britton, R.A. (2013) Mutational analysis of the ribosome assembly GTPase RbgA provides insight into ribosome interaction and ribosome-stimulated GTPase activation. *Nucleic Acids Res* 41: 3217-27.

35. Yang, Z*., et al.* (2011) UCSF chimera, modeller, and imp: An integrated modeling system. *J Struct Biol*.

36. Couch, G.S., Hendrix, D.K., Ferrin, T.E. (2006) Nucleic acid visualization with UCSF chimera. *Nucleic Acids Res* 34: e29.

37. Medigue, C., Rose, M., Viari, A., Danchin, A. (1999) Detecting and analyzing DNA sequencing errors: Toward a higher quality of the bacillus subtilis genome sequence. *Genome Res* 9: 1116-27.

38. Davies, C*., et al.* (1998) Ribosomal proteins S5 and L6: High-resolution crystal structures and roles in protein synthesis and antibiotic resistance. *J Mol Biol* 279: 873-88.

39. Golden, B.L., Ramakrishnan, V., White, S.W. (1993) Ribosomal protein L6: Structural evidence of gene duplication from a primitive RNA binding protein. *EMBO J* 12: 4901-8.

40. Uchiumi, T., Sato, N., Wada, A., Hachimori, A. (1999) Interaction of the sarcin/ricin domain of 23S ribosomal RNA with proteins L3 and L6. *J Biol Chem* 274: 681-6.

41. Stelzl, U., Spahn, C.M., Nierhaus, K.H. (2000) Selecting rRNA binding sites for the ribosomal proteins L4 and L6 from randomly fragmented rRNA: Application of a method called serf. *Proc Natl Acad Sci U S A* 97: 4597-602.

42. Herold, M., Nierhaus, K.H. (1987) Incorporation of six additional proteins to complete the assembly map of the 50S subunit from *Escherichia coli* ribosomes. *J Biol Chem* 262: 8826-33.

43. Lancaster, L., Lambert, N.J., Maklan, E.J., Horan, L.H., Noller, H.F. (2008) The sarcin-ricin loop of 23s rRNA is essential for assembly of the functional core of the 50S ribosomal subunit. *RNA* 14: 1999-2012.

44. Chen, S.S., Williamson, J.R. (2013) Characterization of the ribosome biogenesis landscape in *E. Coli* using quantitative mass spectrometry. *J Mol Biol* 425: 767-79.

45. Clatterbuck Soper, S.F., Dator, R.P., Limbach, P.A., Woodson, S.A. (2013) *In vivo* x-ray footprinting of pre-30S ribosomes reveals chaperone-dependent remodeling of late assembly intermediates. *Mol Cell* 52: 506-16.

CHAPTER 5

Summary and significance

Introduction

While the mechanistic details of ribosome structure and function have been researched extensively, relatively less is known about how ribosomes are assembled *in vivo*[1-4]. For most of the past 40 years research in the field of ribosome assembly has been focused on assembling functional ribosomal subunits from its free purified components *in vitro*[5-8]. This has been tremendously beneficial in uncovering the core rRNA and r-proteins required for optimal ribosome function and the development of assembly maps for both 50S and 30S subunits[9-13]. However, partly due to the success of reconstitution experiments *in vitro,* research on *in vivo* ribosome assembly has lagged behind. Even though the early *in vitro* reconstitution experiments were highly successful in their desired aim of obtaining full functional ribosomal particles from the constituent rRNA and r-proteins *in vitro*, the likely involvement of assembly factors for *in vivo* ribosome assembly was hypothesized. In spite of this early realization, only over the last decade have several assembly factors been identified and only a few of them have been characterized functionally[14-16]. While several proteins from different classes such as helicases, chaperones, modification enzymes, have been implicated in assembly, GTPases feature prominently in the list and are universally required for ribosome assembly with several factors implicated in assembly of bacterial, chloroplast and mitochondrial ribosomes [17-21]. Our current knowledge of different GTPases involved in ribosome assembly in bacteria was discussed in chapter 1. These studies have mostly focused on ribosome assembly defects, growth phenotypes linked to the depletion or mutation of ribosome assembly GTPases and only recently research studies have focused on the direct interaction between these GTPases and few in vivo ribosome assembly intermediates have been identified and characterized. In addition, most of the assembly associated GTPases have not been biochemically characterized and relatively little is

known about their GTPase activity, catalytic mechanism and its role in assembly. The following sections describe the significant results from the thesis and discuss the role of RbgA, an essential GTPase in *B. subtilis* and its role in assembly of the 50S subunit, with an emphasis on its GTPase activity and interaction with ribosomal subunits and intermediate particles.

Role of GTPase activity

Ribosome biogenesis GTPaseA protein, RbgA is an essential GTPase required for the biogenesis of the 50S subunit in *Bacillus subtilis*[22,23]. Depletion of RbgA results in the absence of mature 50S subunits and accumulation of a large complex that migrates at 45S that lacks key ribosomal proteins [22,23]. Research presented in chapter 3 indicated that histidine9 is likely the catalytic residue required for GTPase activation of RbgA in the presence of the 50S subunit. This residue in RbgA, is part of a PGH motif contained within the N-terminus of RbgA contains a stretch of amino acid residues that is highly conserved in RbgA homologs including eukaryotic and human homologs. In addition, the catalytic mechanism of RbgA seems similar to the mechanism of GTPase activation of EF-Tu upon interaction with the 50S subunit and raises an interesting possibility that assembly-associated GTPases interact with the ribosomal subunits similar to translation-associated GTPases.

Biochemical characterization of RbgA and its interaction with the 45S complex and the 50S subunit (Chapter 2) demonstrated that GTPase activity of RbgA is stimulated ~60 fold in the presence of the 50S subunit and initially supported a model in which RbgA utilizes its GTPase activity to exit a mature 50S subunit. Interestingly, strains expressing RbgA mutants with reduced GTPase activity (chapter 3) accumulated a 45S complex similar to RbgA-depleted cells

suggesting that GTPase activity may play a role in maturation of the 50S subunit and may not simply be required to exit a mature subunit. It is possible that L16 (part of the mature 50S subunit but not the 45S complexes) could be the trigger for GTP hydrolysis or a local rRNA structure specific to the mature subunit could be required for hydrolysis.

Interaction with rRNA

We identified a RNA binding domain (the ANTAR domain) in the C-terminal domain of RbgA. The ANTAR domain is utilized by transcription antiterminator proteins to bind to stem-loop structures in mRNA for translational control. This provides an interesting possibility of direct interaction between rRNA and RbgA. While footprinting assays have indicated that RbgA protects specific bases in rRNA there is so far no evidence of a direct interaction between RbgA and rRNA[23]. The structural complexity of 23S rRNA does not allow us to test specific stem-loop structures for association with RbgA. However future experiments utilizing chemical probing might narrow the regions/domains of 23S rRNA that could be tested for interaction with RbgA. It is an interesting possibility to consider that ribosome assembly GTPase interacts directly with rRNA and impacts its secondary and/or tertiary structure. The highly structured and long rRNA molecule likely misfolds and falls into kinetic traps during assembly[24]. Evidence from reconstitution experiments demonstrates that several steps require incubation at high temperatures to form a functional ribosomal subunit. It has been suggested that these incubation steps alter the structure of the rRNA and allow it to escape from the aforementioned kinetic traps. A similar functional role may be performed by assembly factors during *in vivo* assembly. While RNA helicases are the likely candidates for altering rRNA structure due to their RNA-

dependant-ATPase activity evidence of direct interaction between GTPases and rRNA structure would raise the possibility that GTPases could also play a role in rRNA modeling perhaps with the involvement of GTP hydrolysis.

RbgA and assembly of the 50S subunit

Though results from chapter 2 and chapter 3 provided insights into the structure and function of RbgA one question that remains unanswered is how the GTPase activity in the N-terminal domain of RbgA is linked to the C-terminal ANTAR domain in the overall function of RbgA in ribosome assembly. To test the communication between these two domains an RbgA-dependent 50S maturation assay is required. Research on suppressors of RbgA-F6A presented in chapter 4 could potentially aid in the development of an assay that can probe RbgA dependent maturation of the 50S subunit. Our results show that the suppressor strains accumulated a novel large complex that migrates at ~44S and is distinct from the 45S complex. Further, preliminary maturation assays demonstrate the 44S particles from RbgA-F6A suppressor strains can mature into a 50S subunit. Future experiments to achieve RbgA-dependent maturation are underway. The success of such an assay would help elucidate the role of RbgA in assembly of the 50S subunits and for the first time demonstrate GTPase facilitated *in vitro* ribosome assembly. Further, should such an assembly be possible at physiologically relevant temperatures, as opposed to the elevated temperature currently required for *in vitro* reconstitution, this would constitute a particularly compelling demonstration of the role of GTPases in ribosome assembly *in vivo*. Such a factor dependent *in vitro* assembly has previously been shown for the chaperone protein DnaK but conflicting reports exist about its role in ribosome assembly[25,26]. An assay

that tests RbgA function in 50S maturation could also be used to elucidate the interaction between N-terminal domain and ANTAR domain of RbgA during ribosome assembly.

Finally, structural studies of the 44S complex would be another exciting future avenue of research. In particular, the structural differences between the 44S, the 45S and the mature 50S subunit would highlight the difference in local rRNA structure and r-protein positions and provide insight into the events at a late stage of ribosome assembly.

REFERENCES

REFERENCES

1. Ramakrishnan, V. (2002) Ribosome structure and the mechanism of translation. *Cell* 108: 557-72.

2. Ramakrishnan, V. (2008) What we have learned from ribosome structures. *Biochem Soc Trans* 36: 567-74.

3. Schmeing, T.M., Ramakrishnan, V. (2009) What recent ribosome structures have revealed about the mechanism of translation. *Nature* 461: 1234-42.

4. Ogle, J.M., Carter, A.P., Ramakrishnan, V. (2003) Insights into the decoding mechanism from recent ribosome structures. *Trends Biochem Sci* 28: 259-66.

5. Amils, R., Matthews, E.A., Cantor, C.R. (1978) An efficient *in vitro* total reconstitution of the *Escherichia coli* 50S ribosomal subunit. *Nucleic Acids Res* 5: 2455-70.

6. Green, R., Noller, H.F. (1999) Reconstitution of functional 50S ribosomes from *in vitro* transcripts of *Bacillus stearothermophilus* 23S rRNA. *Biochemistry* 38: 1772-9.

7. Nierhaus, K.H. (1991) The assembly of prokaryotic ribosomes. *Biochimie* 73: 739-55.

8. Semrad, K., Green, R. (2002) Osmolytes stimulate the reconstitution of functional 50S ribosomes from in vitro transcripts of *Escherichia coli* 23S rRNA. *RNA* 8: 401-11.

9. Burakovsky, D.E*., et al.* (2011) The structure of helix 89 of 23S rRNA is important for peptidyl transferase function of *Escherichia coli* ribosome. *FEBS Lett* 585: 3073-8.

10. Leung, E.K., Suslov, N., Tuttle, N., Sengupta, R., Piccirilli, J.A. (2011) The mechanism of peptidyl transfer catalysis by the ribosome. *Annu Rev Biochem* 80: 527-55.

11. Rohl, R., Nierhaus, K. (1982) Assembly map of the large subunit (50S) of *Escherichia coli* ribosomes. *Proc Natl Acad Sci U S A* 79: 729-33.

12. Herold, M., Nierhaus, K.H. (1987) Incorporation of six additional proteins to complete the assembly map of the 50 S subunit from *Escherichia coli* ribosomes. *J Biol Chem* 262: 8826-33.

13. Culver, G.M. (2003) Assembly of the 30S ribosomal subunit. *Biopolymers* 68: 234-49.

14. Wilson, D.N., Nierhaus, K.H. (2007) The weird and wonderful world of bacterial ribosome regulation. *Crit Rev Biochem Mol Biol* 42: 187-219.

15. Comartin, D.J., Brown, E.D. (2006) Non-ribosomal factors in ribosome subunit assembly are emerging targets for new antibacterial drugs. *Curr Opin Pharmacol* 6: 453-8.

16. Kaczanowska, M., Ryden-Aulin, M. (2007) Ribosome biogenesis and the translation process in *Escherichia coli*. *Microbiol Mol Biol Rev* 71: 477-94.

17. Britton, R.A. (2009) Role of GTPases in bacterial ribosome assembly. *Annu Rev Microbiol* 63: 155-76.

18. Karbstein, K. (2007) Role of GTPases in ribosome assembly. *Biopolymers* 87: 1-11.

19. Panse, V.G., Johnson, A.W. (2010) Maturation of eukaryotic ribosomes: acquisition of functionality. *Trends Biochem Sci* 35: 260-6.

20. Kotani, T., Akabane, S., Takeyasu, K., Ueda, T., Takeuchi, N. (2013) Human G-proteins, ObgH1 and Mtg1, associate with the large mitochondrial ribosome subunit and are involved in translation and assembly of respiratory complexes. *Nucleic Acids Res* 41: 3713-22.

21. Jeon, Y.*, et al.* (2014) DER containing two consecutive GTP-binding domains plays an essential role in chloroplast ribosomal RNA processing and ribosome biogenesis in higher plants. *J Exp Bot* 65: 117-30.

22. Uicker, W.C., Schaefer, L., Britton, R.A. (2006) The essential GTPase RbgA (YlqF) is required for 50S ribosome assembly in *Bacillus subtilis*. *Mol Microbiol* 59: 528-40.

23. Matsuo, Y.*, et al.* (2006) The GTP-binding protein YlqF participates in the late step of 50 S ribosomal subunit assembly in *Bacillus subtilis*. *J Biol Chem* 281: 8110-7.

24. Woodson, S.A. (2008) RNA folding and ribosome assembly. *Curr Opin Chem Biol* 12: 667-73.

25. Maki, J.A., Southworth, D.R., Culver, G.M. (2003) Demonstration of the role of the DnaK chaperone system in assembly of 30S ribosomal subunits using a purified *in vitro* system. *RNA* 9: 1418-21.

26. Alix, J.H. (2003) DnaK-facilitated ribosome assembly in *Escherichia coli* revisited. *RNA* 9: 787-93.